Berichte des Instituts für Mechanik und Fluiddynamik
Heft 15 (2014)

Generalised continuum approach for modelling quasi-brittle failure

Uwe Mühlich

TECHNISCHE UNIVERSITÄT BERGAKADEMIE FREIBERG

Herausgeber: TU Bergakademie Freiberg
Institut für Mechanik und Fluiddynamik
Prof. Dr.-Ing. A. Ams
Prof. Dr.-Ing. habil C. Brücker
Prof. Dr. rer. nat. habil. M. Kuna
Lampadiusstraße 4
09596 Freiberg

Tel. +49 3731 39-2465
Fax +49 3731 39-3455
E-Mail sekretariat@imfd.tu-freiberg.de
Internet www.imfd.tu-freiberg.de

Vertrieb: Akademische Buchhandlung, Inh. B. Hackel, Merbachstraße, PF 1445, 09599 Freiberg, Telefon 03731/2 21 98, Fax 03731/2 26 44

Bibliografische Information der Deutschen Bibliothek
Die Deutsche Bibliothek verzeichnet diese Publikation in der Deutschen Nationalbibliografie; detaillierte bibliografische Daten sind im Internet über http://dnb.ddb.de abrufbar.

Von der Fakultät für Maschinenbau, Verfahrens- und Energietechnik der TU Bergakademie Freiberg genehmigte Habilitation.
Tag der Verleihung: 4. Februar 2014
Gutachter: Prof. Dr. rer. nat. habil. Meinhard Kuna
Prof. Dr.-Ing. habil. Samuel Forest
Prof. Dr.-Ing. habil. Reinhold Kienzler

Das Werk, einschließlich aller seiner Teile, ist urheberrechtlich geschützt. Jede Verwertung ist ohne die Zustimmung des Verlages außerhalb der engen Grenzen des Urheberrechtsgesetzes unzulässig und strafbar. Das gilt insbesondere für Vervielfältigungen, Übersetzungen, Mikroverfilmungen und die Einspeicherung und Verarbeitung in elektronischen Systemen.

1. Auflage
© Technische Universität Bergakademie Freiberg 2014
Gesamtherstellung: Medienzentrum der TU Bergakademie Freiberg
Printed in Germany

ISBN 978-3-86012-479-6

TECHNISCHE UNIVERSITÄT
BERGAKADEMIE FREIBERG
The University of Resources. Since 1765.

Generalised continuum approach for modelling quasi-brittle failure

By the Faculty of Mechanical, Process and Energy Engineering
of the Technische Universität Bergakademie Freiberg

approved

Habilitation

to attain the academic degree of

Doktor-Ingenieur habil
(Dr.-Ing. habil.)

submitted by **Uwe Mühlich**

born on the 4 April 1964 in Dresden

Assessor: Prof. Dr.rer.nat.habil. Meinhard Kuna
Prof. Dr.Ing.habil. Samuel Forest
Prof. Dr.Ing.habil. Reinhold Kienzler

Date of the award: Freiberg, 4 February 2014

Abstract

A proper description of quasi-brittle failure within the frame of Continuum Mechanics can only be achieved by models based on so-called generalised continua. This thesis focuses on a strain gradient generalised continuum and provides a specific methodology to derive corresponding models which account for the essential features of quasi-brittle failure. This methodology is discussed by means of four peer-reviewed journal articles.

Furthermore, an extensive overview of the state of the art in the field of generalised continua is given at the beginning of the thesis. This overview discusses phenomenological extensions of standard Continuum Mechanics towards generalised continua together with corresponding homogenisation strategies for materials with periodic or random microstructure.

Kurzfassung

Eine geeignete, kontinuumsmechanische Beschreibung quasi-spröden Versagens ist nur unter Verwendung verallgemeinerter Kontinuumstheorien möglich. In dieser Habilitationsschrift stehen sogenannte Gradientenkontinua im Vordergrund. Für diese wird eine Methodik vorgeschlagen, welche die Herleitung von Modellen erlaubt, die in der Lage sind, quasi-sprödes Versagen adäquat abzubilden. Diese Methodik wird anhand von vier Publikationen dargestellt und diskutiert.

Ein umfangreicher Überblick über den Stand der Forschung auf dem Gebiet der veralgemeinerten Kontinuumstheorien wird am Anfang der Habilitationschrift gegeben. Dabei werden neben phänomenologischen Ansätzen zur Ableitung verallgemeinerter Kontinuumstheorien auch die entsprechenden Homogenisierungskonzepte dargestellt. Letztere werden für Materialien mit periodischer Mikrostruktur und für Materialien mit zufälliger Mikrostruktur diskutiert.

Contents

1 Introduction

The primary motivation for this thesis was to properly describe the quasi-brittle failure of porous elastic solids by means of an effective continuum approach. One of the principal characteristics of quasi-brittle rupture is the accumulation of damage prior to final failure. Therefore, the effective continuum approach aimed for has to account for the evolution of damage. This requirement, together with a number of further facts and arguments to be discussed in more detail later, lead to the conclusion that only an effective continuum model derived within the framework of so-called generalised continua has any chance to describe the problem satisfactorily. Due to the variety of generalised continuum theories, the first question to be answered is which particular type of those non-standard continuum approaches should be used. Based on a number of arguments, the decision was taken in favour of the strain gradient elasticity approach as developed by MINDLIN AND ESHEL (1968). Constitutive relations for porous elastic solids which fit into the framework of strain gradient elasticity were derived employing a homogenisation concept. Eventually, this model was used as a basis to develop a continuum damage model for simulating quasi-brittle fracture. All these steps have been reported in four journal articles, and this document aims to discuss those papers in the light of the current knowledge on generalised continua.

The current state of the art of generalised continua is reviewed by discussing a selected part of the vast literature on this subject within the next chapter. Of course, such a selection is partially a matter of taste and equally valuable references could be given with respect to certain topics. Here, particular emphasis is placed on the genuine motivations of different theories and how they can be derived, e.g. by extending familiar concepts of continuum mechanics. The similarities and distinctions between different generalised continuum theories are examined. After this, a synthesis of the four journal articles mentioned above is provided explaining in more detail the reasoning which lead to the methodology used here, presenting the essential results and discussing the achievements.

Print versions of those articles which document the author's contribution on the subject can be found at the end of the document.

2 Generalised Continua - a journey

2.1 Overview

A large number of generalised continuum theories can be derived by focusing on either one of the following basic ingredients of deterministic continuum mechanics: kinematics of the continuum, stress concept and constitutive relations. Extending one of them and working out a consistent theory by using general conservation and / or invariance principles implies consequences for the remaining constituents, which then have to accommodate accordingly. Here, generalised continua are divided into two main classes: polar continua and non-local continua, where the former includes multipolar, micromorphic as well as strain-gradient continua. Of course, every generalised continuum is in some way non-local. However, in the following, the term non-local is strictly used in the sense that the response at some spatial position depends in general on the related information at all other points of the body. Although non-local theories are not of primary interest here, the fundamentals are discussed briefly for the sake of completeness.

According to the statement at the beginning, the same generalised continuum theory can be obtained by choosing different points of departure. Here, these theories are discussed in keeping with the corresponding historical evolution.

Because the continuum concept is always an idealisation of real matter, every continuum theory can be seen as the result of some homogenisation process, even if the continuum description is derived on purely phenomenological grounds. This becomes apparent at the latest when material parameters have to be determined, which requires specimens containing a minimum amount of matter. Nevertheless, such a homogenisation process can be undertaken as well explicitly starting from a material with given micro-structure and replacing the body under consideration by a so-called effective continuum.

Deriving a continuum theory not only in a phenomenological way but also by explicit homogenisation is a rather favourable situation. This, however, is not just because of the deeper theoretical insight which can be gained. An additional practical benefit is that the homogenisation approach reveals information and concepts about how to determine the material parameters for a particular continuum theory.

Apart from the fully generalised continuum theories considered here, somewhat simplified versions of non-standard continua can be derived by starting from the theory of simple materials and focussing exclusively on the internal variables. Those can be replaced by corresponding non-local counterparts. Alternatively, spatial gradients of internal variables can be incorporated into the constitutive equations. Albeit heuristic and rather simplistic at first glance, these models can be sufficiently powerful to solve particular problems with much less theoretical and numerical effort compared to fully-generalised continuum approaches. A unifying scheme which includes both kind of generalised continuum theories has been recently proposed by FOREST (2009). However, the simplified versions of non-standard continua are not within the scope of this work. Therefore, the reader is referred to the review articles of BAŽANT AND JIRASEK (2002) and AIFANTIS (2003) which discuss thoroughly the key aspects of these approaches.

2.2 Principal classes of generalised continua

2.2.1 Polar field theories and their relatives

Multipolar continua

Since the Theory of Mechanics rests upon the fundamental concepts of *material body*, *motion* and *force*, so does continuum mechanics. While the motion of a material body in space is the effect measurable by an observer having a notion of space and time, force, on the other hand is an abstract idea to express what causes this motion or the change of it, respectively. Changes in behaviour of the body are attributed to its interaction with the world. Hence, forces acting upon a body simply reflect this interaction, which is taken into account, e.g. in the energy balance via the power of body forces and the power of tractions at the body's outer surface. Classical continuum mechanics deals only with monopolar body forces and surface tractions, where the corresponding work conjugate quantities are the usual velocities.

Influenced by a discussion about generalised stresses by TRUESDELL C. AND TOUPIN R. (1960), GREEN AND RIVLIN (1964)b developed a continuum theory regarding multipolar body forces and surface tractions of arbitrary order. Multipolar quantities emerge naturally in the theories for beams, plates and shells due to the transition from a three-dimensional problem to a one-dimensional or two-dimensional model, respectively. However, for a three dimensional continuum, multipolar body forces and surface tractions are rather unusual at first glance. Perhaps because of this seeming oddity, the founders of the theory felt obliged to give an illustrative example in the appendix of the paper by GREEN AND RIVLIN (1964)a. The authors associate a mate-

rial point of the continuum with the center of gravity of a set of M rigid particles. The discrete forces per unit mass acting on these particles are computed from the Taylor expansion of a supposed continuous force field around the center of gravity. Associating the specific power of the material point with the power of the corresponding set of discrete particles, n-polar forces related to the nth order term in the series expansion emerge together with corresponding n-polar velocities. An equivalent treatment is discussed focussing on the discrete velocities of the particles. The example indicates that the larger the spatial extension of the associated particle set in the reference configuration, the higher the degree of the multipolar medium has to be in order to derive a suitable continuum approximation.

An energy balance which incorporates multipolar tractions and body forces together with their work-conjugate multipolar velocities was postulated by GREEN AND RIVLIN (1964)b. Furthermore, multipolar stresses were derived by applying this energy balance to a tetrahedron and performing the limit of the tetrahedron's volume towards zero. However, multipolar stresses can be deduced from multipolar tractions in a most natural way by assuming that the tractions depend only linearly on the unit normal vector or, its dual respectively. It turns out that n-polar stresses are, in general, tensors of rank $n+1$. Such quantities are referred to in the following as hyper-stresses in order to distinguish them from the so-called generalised stress tensors to be discussed in section 2.3.2 which are always of order two. The local balance equations were derived by the authors from the energy balance mentioned above demanding its invariance under superimposed rigid motions.

At first glance, one could get the impression that multipolar velocities of arbitrary order can be incorporated without even specifying their particular meaning or origin. However, in order to deduce local balance laws from the invariance of the energy balance, the transformation behaviour of these multipolar velocities under superimposed rigid motion either has to be deduced from their physical meaning or additional assumptions regarding the transformation properties are necessary.

It was shown by GREEN, NAGHDI, AND RIVLIN (1965) and GREEN (1965) that an oriented medium can be regarded as a special case of a multipolar continuum. Oriented media are characterised by the existence of a number of independent vectors, the so-called directors, attached to a material point of the continuum.

Micromorphic continua

The mental picture which led to the theory of mircomorphic continua does not differ much from that used by GREEN AND RIVLIN (1964)b in the context of multipolar continua discussed above. Here, some deformable micro-continuum is attached to every point of the effective continuum. The former would have, in general, an infinite

number of degrees of freedom. However, the motion of this micro-continuum is restricted in order to allow exclusively for homogeneous deformations, which reduces the number of additional degrees of freedom to nine. This in turn allows for an interpretation in terms of so-called deformable directors. It means that a set of three linearly independent vectors is attached to every point of the macro-continuum. In the course of the motion of the macro-continuum, this triad of directors can undergo rigid rotations. In addition, the directors can exhibit individual changes in length, and the mutual angles between these directors may change as well. If the motion of the micro-continuum is restricted to pure rotations, the so-called micro-polar continuum results. The restriction to pure stretch and pure shear lead to the so-called micro-stretch and micro-shear theories respectively. The micro-polar continuum is equivalent to the Cosserat-theory developed long ago by COSSERAT AND COSSERAT (1909). Usually, it is quite helpful and instructive to recall that the Timoshenko-beam is a one-dimensional Cosserat-medium. Direct coupling between the micro-rotation and macro-rotation leads to the so-called couple stress theory or couple-stress solid respectively. The one-dimensional analogue of the latter is the Euler-Bernoulli beam.

A historical review of the contributions prior to the emergence of the theory of micromorphic continua, but certainly decisive for the progress in this field, can be found in TOUPIN (1964). Although, the specific term was coined only later by Eringen, a micromorphic approach for linear elasticity was proposed already by MINDLIN (1964). However, the general framework of micromorphic continua was developed by ERINGEN AND SUHUBI (1964), SUHUBI AND ERINGEN (1964), without imposing restrictions in terms of linear kinematics, linear material behaviour or quasi-static motion. It is interesting to note that the authors based their theory rigorously on volume averaging. The micromorphic continuum is established as a macroscopic description assuming explicitly the existence of an underlying micro-structure. Field variables at a macroscopic point are defined as volume averages of the corresponding quantities with respect to a finite microscopic region, the deformation of which is assumed to be homogeneous. Hence, the interpretation in terms of a micro-continuum attached to every macroscopic point. Furthermore, balance of momentum, angular momentum as well as entropy inequality are derived by averaging, assuming that the micro-continuum is a simple one.

Later on, the local balance laws were obtained by ERINGEN (1995), ERINGEN (1999) from the invariance of the global energy balance for a micromorphic continuum under superimposed rigid body motion.

Classifying the theory developed so far as micromorphic of degree one, not only the governing equations of this theory were derived by GERMAIN (1973) from the Principle of Virtual Power but, in addition, micromorphic continua of arbitrary degree

could be worked out systematically. For further discussion related to the Principle of Virtual Power in the context of generalised continua see as well MAUGIN (2013).

Strain-gradient continua

Assuming, that the thermodynamic state of a material point is completely defined by a set of thermodynamic state functions, the structure of the corresponding continuum theory is determined by the properties of these functions. Standard continuum mechanics uses state functions which depend exclusively on local deformation measures. So-called strain gradient theories result, if in addition gradients of deformation measures of arbitrary order are taken into account. Some authors prefer to call such theories grade-n continua, but care should be taken here because this terminology is also used in the context of materials with memory, see e.g. GURTIN (1968) or TRUESDELL AND NOLL (2004), where it has a different meaning.

Non-linear elastic strain gradient continua were first proposed by TOUPIN (1964). The linear version has been worked out by MINDLIN AND ESHEL (1968), extending the elastic strain energy density by the spatial gradients of the strains. Alternatively, the second gradients of the displacements can be used and even a third possibility exists. However, it can be shown that all three options are completely equivalent and a particular preference is more or less a matter of taste. Constitutive relations are defined by assuming that stresses and hyper-stresses are given by the partial derivatives of the strain energy density with respect to the strains and the strain gradients, respectively. Applying Hamilton's principle, an extended local equilibrium statement together with the corresponding boundary conditions were derived.

For linear materials, the constitutive relations can be expressed by means of respective elasticity tensors. In the most simple case, the stresses and the strains can be related by the usual fourth-order elasticity tensor, whereas hyper-stresses and strain gradients are connected via a sixth-order tensor. Due to the general properties of the latter, an isotropic linear strain gradient solid implies the existence of five independent material parameters in addition to the usual two Lame's constants of classical linear elasticity. Incorporating not only the first but also the second gradients of the strains, a linear second order strain gradient elasticity theory was derived by MINDLIN (1965). Here, even sixteen additional material parameters exist for an isotropic second order strain gradient medium. Hence, the experimental characterisation of a strain gradient solid requires considerable effort even for the most simple case of isotropic behaviour. On the other hand, these parameters should be related somehow to general characteristics of the underlying micro-structure. Reduced material laws have been proposed by various authors, setting certain parameters equal to zero and postulating algebraic relations between the remaining ones. The most com-

mon simplifications, originally proposed by KOITER (1964), KLEINERT (1989), YANG, CHONG, ET AL. (2002), AIFANTIS (2003) and FLECK AND HUTCHINSON (2001), were summarised and classified by ZHANG AND SHARMA (2005).

Based on the linear theory of MINDLIN AND ESHEL (1968), a first order strain gradient plasticity theory was developed by Fleck and co-authors, see FLECK, MULLER, ET AL. (1994), SMYSHLYAEV AND FLECK (1996), FLECK AND HUTCHINSON (1997).

The relation between strain gradient elasticity and the non-local effective medium approach for random elastic composites has been discussed by BERAN AND MCCOY (1970) based on the problem of a concentrated force in an infinite medium, and considering only small statistical fluctuations of the material properties. An analytical solution was obtained for the latter problem which can be split into a Kelvin-type solution and a so-called force layer part. It turns out that the predictions obtained by means of the strain gradient theory within the force layer are of dubious nature.

Relations between the different approaches

Although, a comprehensive and detailed comparison between the different theories discussed within this section is beyond the scope of this work, some remarks on this topic seem appropriate.

The relation between micromorphic continua and the theory of multipolar media was discussed explicitly by GREEN (1965), showing that the latter can be classified as a special case of the former. The resemblance between these two approaches becomes even more obvious, if the global energy balances used by GREEN (1965) and ERINGEN (1995) are compared. On the other hand, a closer look on the boundary terms in MINDLIN (1965) reveals that strain gradient continua of order n are actually n-polar media employing a specific definition of the n-polar surface tractions. Furthermore, it is well known that first order strain gradient theories can be derived from mircomorphic continua by imposing particular constraints. These links have been summarised schematically for the linear theories for example by TEKOGLU (2006).

A unifying viewpoint regarding multipolar, micromorphic and strain gradient continua was sketched by GODDARD (2008). However, to the author's knowledge, a comprehensive classification of the different variants within one single document, discussing and comparing as well the various possibilities to derive these theories, is still missing.

2.2.2 Non-local continua

In contrast to the generalised continua discussed so far, truly non-local continua do not fulfil the Principle of Local Action. They can be derived from at least two equivalent

points of view. Non-local constitutive relations can be assumed. For instance, the stress state at some point of the continuum is given by means of an integral equation. More precisely, the stress tensor is given in terms of an integral over the whole body where the integrand is a product of two objects, a kernel decaying with increasing distance and the usual strain tensor.

Alternatively, global statements, like the usual global energy balance, can be used as a starting point. However, the localisation of such balances must take into account non-local residuals. Furthermore, those residuals must obey certain additional conditions. Since the interaction of the body with the surroundings is already expressed completely by means of fluxes via the body's outer surface and specific body forces, the non-local residuals must not cause any further artificial interactions. Therefore, the integrals of the residuals over the whole configuration of the body must vanish at any time. The latter is known as insulation condition. The argumentation used so far indicate that strain gradient theories that make use of non-local residuals fit into the non-local framework and, therefore, have to be distinguished from the strain gradient continua discussed within the previous section.

There is one exception regarding the localisation argument used above. As stressed by POLIZZOTTO (2003), the entropy inequality is assumed to be valid point-wise, since it is a statement of reversibility or irreversibility, respectively, which in turn is seen as a local property. For instance, as long as a material point undergoes exclusively elastic deformation, its behaviour is reversible no matter how many points of its surroundings deform already inelastically. Hence, the localisation of the global entropy inequality must not involve any non-local residuals.

Since non-local continua are not of primary interest here, the reader is referred to the article by EDELEN, GREEN, AND LAWS (1971) and the textbook by ERINGEN (2002) for further information about this topic.

2.3 Generalised continua by explicit homogenisation

2.3.1 Random micro-structures

Continuum theories dealing explicitly with an underlying random micro-structure are usually subsumed under the term Theory of Effective Media. In most cases, the micro-structure is seen as a simple continuum with randomly-distributed material properties. Thus, the micro-structure is essentially a random field for which, in general, an infinite number of particular realisations exists. Random fields are in general rather complicated entities, primarily because every particular material property such as Young's modulus or thermal conductivity, at every point of the body is a random variable.

Hence, there is in general an infinite number of such variables, and a random field is only specified completely if, for each finite set of spatial positions, the joint distribution function for the corresponding random variables is known.

The coefficients of the differential operator in the associated boundary value problem are directly related to the material properties. If the latter vary randomly with spatial position, then the respective coefficients are random fields and the differential operator becomes stochastic. Now, even more random variables are involved, because the field to which the differential operator applies becomes a random field too. In other words, each physical quantity of the boundary value problem, like temperature or the components of the displacement vector, etc, at some point of the body is one particular random variable. Furthermore, the values of these physical variables at different locations are by no means unrelated, but their mutual dependence is given implicitly by the stochastic boundary value problem mentioned above. Therefore, the micro-structure can be seen as a primary random field of certain complexity from which another, even more complex random field is generated by the boundary value problem. In the following, the term physical random field is used for the latter.

The Theory of Effective Media aims to derive equations for the statistical moments of the considered physical variables from the stochastic boundary value problem. The most simple of these moments is the average of the respective variable, e.g. displacements or temperature, at every point of the continuum over an infinite number of realisations. This first moment is also known as ensemble average or mean field. However, the derivation of an equation for a particular statistical moment always involves the next higher moment. Therefore, an infinite hierarchy of equations results, and some closure argument is needed in order to truncate this sequence of equations. This leads to a finite set of equations for the statistical moments of the relevant unknowns. Of course, the mean field is of primary interest and most of the research focusses almost exclusively on this part. Provided that source terms like volume forces, heat sources, as well as the boundary conditions are deterministic, deriving the equations governing the mean field is equivalent to replacing the essential variable in the boundary value problem, for instance the displacement vector, by its ensemble average and the stochastic differential operator by an effective one. The latter is in general non-local. Strictly speaking it is an integro-differential operator that contains the properties of the primary random field in terms of all-order correlation functions. Usually, the mean field approach is interpreted in terms of scales as follows. The primary random field characterises the microstructure of the problem whereas the effective continuum is seen as the modelling approach valid at the macro-scale.

The fundamentals of the Theory of Effective Media can be found, e.g. in the textbooks by BERAN (1968), SOBCZYK AND KIRKNER (1970), BURYACHENKO (2007) and in

the CISM course material edited by JEULIN AND OSTOJA-STARZEWSKI (2002). A concise overview focussing on continuum mechanics was given by BERAN (1971). Considerable progress in deriving mean field approximations in linear continuum mechanics has been made by employing the concept of polarisation stresses and strains respectively, originated by ESHELBY (1957). What seems to be just an alternative way of formulating the original problem turns out to be a very useful concept to work out a powerful methodology of admirable elegance. This is mainly due to the implied definition of a homogeneous comparison medium, which allows for the use of the standard Green's-function approach. Together with the usual ensemble averaging, the general non-local character of the effective medium can be shown formally in a concise and transparent way, see e.g. KRÖNER AND KOCH (1976). Variational principles like those derived by HASHIN AND SHTRIKMAN (1962) can be used to derive bounds for these non-local operators as well as to construct suitable approximations, see e.g. DIENER, HÜRRICH, AND WEISSBARTH (1984). This method has been developed further and applied successfully to random elastic composites by Willis and co-workers, see e.g. WILLIS (1987), LUCIANO AND WILLIS (2000)a, DRUGAN (2003). Gradient approximations for the non-local effective operator have been derived by DRUGAN AND WILLIS (1996) and DRUGAN (2000) for two-phase composites. The question, how to establish a link to periodic micro-structures as a particular case of fluctuations has been addressed, e.g. by FISHMAN AND MCCOY (1981) and LUCIANO AND WILLIS (2000)b.

The foregoing exposition shows that a simple continuum with random variations of the material properties corresponds in general to a non-local and, therefore, generalised effective continuum. Only if certain conditions are fulfilled, the effective continuum obeys the same structure as the continuum used at the micro-level. The most popular concept which leads to a simple effective continuum relies on the assumption that energetic fluctuations are negligible, see e.g. HUET (1982), HUET (1990), which is termed as non-correlation postulate or macro-homogeneity assumption in the literature. Assuming in addition that the ensemble averages can be replaced by spatial averages, which is referred to as ergodicity hypothesis, the celebrated and widely used concept of the representative volume element (RVE) can be derived. A necessary but not sufficient condition for the existence of an RVE is the statistical uniformity of the primary random field, see SOBCZYK AND KIRKNER (1970). The concept's appeal is that instead of a large number of realisations of the physical random field, just a spatially limited part of one realisation for the primary random field has to be considered. This part, which captures to a certain extent the statistical features of the micro-structure, can be exposed directly to physical boundary conditions, e.g. in terms of surface tractions or boundary displacements. These boundary data must

be in agreement with the macro-homogeneity assumption, expressed by the so-called Hill-Mandel condition, see e.g. HILL (1963). This will be discussed at the beginning of section 2.3.3 in more detail. The constitutive relations are then simply obtained from the solution of the boundary value problem for the RVE. Furthermore, the concept is not limited to linear problems.

There is a vast amount of literature related explicitly to the RVE-approach, including the textbooks by NEMAT-NASSER AND HORI (1999), QU AND CHERKAOUI (2006) and the review article by ZAOUI (2002). The increase of computational power over the last decades has recently caused a revival of the discussion related to the question of how much statistical information of a particular micro-structure should the RVE contain as a minimum, see e.g. OSTOJA-STARZEWSKI (2006), KANIT, FOREST, ET AL. (2003). Nowadays, there are investigations which assume even a generalised continuum with randomly varying coefficients at the micro-level. In OSTOJA-STARZEWSKI (2011) for example, a micro-polar medium has been considered. Obviously, the general methodology of the Theory of Effective Media applies as well, and the mean field approximation would be in general a non-local micro-polar continuum. Furthermore, the conditions can be worked out under which an RVE approach applies. Naturally, the latter will be somewhat more complex than in the case of a simple micro-continuum, but it is not far fetched to anticipate, that the results of such investigations will be particularly useful in the near future, e.g. for granular media with randomly varying particle size.

2.3.2 Periodic micro-structures

Particular solution methods apply if the micro-structure can be idealised as a periodic pattern generated by regular repetition of identical unit cells. The characteristic dimension λ of the unit cell then becomes the essential length property of the micro-structure to be contrasted with the dominant macroscopic length property L, e.g. some length related to the overall dimensions of the considered body, or the wave-length of the macroscopic loading.

If the length-scale ratio $\epsilon = \lambda/L$ is small, solving the corresponding boundary value problem directly becomes laborious or may even prove infeasible. Therefore, it seems to be more efficient to focus on the asymptotic solution for ϵ approaching zero. A common way to attack the problem is to define two scales, together with their respective coordinates; a slowly varying macro-scale and a rapidly varying micro-scale. The rapidly varying coordinates are defined simply by multiplying the slowly varying coordinates with $1/\epsilon$.

The solution of the reformulated boundary value problem is expressed by a two-

scale asymptotic series expansion in the form of an infinite sum of unknown functions, each of them labelled by the summation index, e.g. m with $m = 0, 1, ...\infty$, and multiplied by ϵ^m. Introducing the series expansion into the boundary value problem, sorting and grouping all terms with respect to the powers of the length-scale ratio leads to an infinite sequence of boundary value problems for the unit cell. For instance, in the case of periodic elastic media, the grouping involves the powers ϵ^{-2}, ϵ^{-1}, ..., ϵ^{∞}. Theoretically, all unknown functions in the asymptotic expansion can be determined up to a constant by solving successively the cell problems, starting with the one related to the lowest power of ϵ. Demanding that the boundary value problem is satisfied at each order of the length-scale ratio, a formal representation of the solution has been derived by BAKHVALOV AND PANASENKO (1989). It consists of a slowly varying solution to which an infinite sum of correction terms is superimposed. Every correction term contains a derivative, the order of which coincides with the summation index of the slowly varying solution with respect to the slowly varying coordinates. This derivative is modulated by a periodic field depending only on the rapidly varying coordinates. This formal representation indicates that the solution at the micro-level contains, in general, gradients of the macro-fields of arbitrary order.

If the length-scale ratio approaches zero, only the cell problems up to the order ϵ^0 are taken into account. This, on the other hand, implies truncation of the asymptotic expansion after the three leading terms. Eventually, the homogenised boundary value problem results from averaging the cell problem related to ϵ^0, where the averaging procedure is established quite naturally by the solvability condition for periodic problems, also known as Fredholm's alternative. Hence, an effective medium is defined by means of the homogenised boundary value problem. The latter coincides with the original boundary value problem, except that the material properties are replaced by their homogenised counterparts. A huge amount of literature related to homogenisation based on asymptotic series expansion exists. The fundamentals are presented in detail, for example in the textbooks by BENSOUSSAN, LIONS, AND PAPANICOLAOU (1978), BAKHVALOV AND PANASENKO (1989), PANASENKO (2005) or the review article by SANCHEZ-PALENCIA (1986).

If ϵ is still significantly smaller than one but not likely approaching zero, additional terms of the asymptotic expansion have to be taken into account. Obtaining the corresponding solution at the micro-level, albeit laborious, is still straightforward, at least for linear problems. However, there is no single and unique concept to perform the passage from the micro-field solution to the effective continuum. Therefore, various approaches can be found in the literature. To the authors' knowledge, the first attempt in this direction was undertaken by GAMBIN AND KRÖNER (1989). Here, a macroscopic stress-strain relation containing strain gradients up to infinite order was

derived essentially by averaging the stress-strain relation at the micro-level obtained from the asymptotic expansion. Later, BOUTIN (1996) investigated the problem in a broader sense, focussing on the averaged balance equations at different orders of the length-scale ratio and discussing the meaning of the involved higher order stresses. It should be noted that the latter are second order tensors contrary to the so-called hyper-stresses discussed earlier. Furthermore, it has been shown by BOUTIN (1996) that the higher order stresses cannot be interpreted in terms of force fluxes which demonstrates that these quantities are not stresses in the usual sense. Similar research was performed by TRIANTAFYLLIDIS AND BARDENHAGEN S. (1996), although focussing on the onset of instability in the case of elastic-plastic micro-structures.

Starting from the formal representation of the asymptotic series mentioned above, SMYSHLYAEV AND CHEREDNICHENKO (2000) observed, among other things, that simply cutting off the series at some order of ϵ might cause the loss of ellipticity of the homogenised boundary value problem. In order to avoid this problem, a combination of the asymptotic expansion with a variational approach has been proposed to derive the homogenised boundary value problem. A link to strain-gradient elasticity has been established. Following this idea, PEERLINGS AND FLECK (2004) developed a scheme to compute the homogenised material tensors by numerically solving a sequence of boundary value problems for the unit cell.

Similar to the case of random micro-structures, the two-scale asymptotic approach has been discussed already considering not only simple micro-continua but also periodic generalised micro-continua, see e.g. FOREST (2002).

All contributions mentioned above deal with static situations. First steps towards dynamic problems have been reported by ANDRIANOV, BOLSHAKOV, ET AL. (2012).

2.3.3 Generalised homogenisation based on polynomials

The Hill-Mandel condition, crucial for the RVE-concept discussed at the end of section 2.3.1, requires application of so-called homogeneous boundary conditions to the RVE. Focussing on mechanical problems, the latter can be accomplished by prescribing either boundary displacements, which vary linearly with spatial position, or constant surface tractions. Also certain combinations of these two cases are possible. Furthermore, periodic fluctuations can be superimposed.

Inspired by the RVE-concept, a volume element exposed to displacement or traction boundary conditions respectively is considered. The volume element is supposed to capture the essential features of the micro-structure. However, contrary to the RVE-concept, inhomogeneous boundary conditions are applied. A first step towards inhomogeneous boundary data can be made by adding a term with quadratic spatial

dependence to the usual linear boundary displacements discussed above. A similar extension is possible if surface tractions are prescribed. To the author's knowledge, this concept was used for the first time by GOLOGANU, LEBLOND, ET AL. (1997) in order to derive a continuum model of Mindlin-type for ductile damage, the numerical implementation of which was reported by ENAKOUTSA, LEBLOND, AND PERRIN (2007).

Usually, the volume element is seen as a simple but heterogeneous continuum subjected to prescribed boundary displacements. Even though the concept itself is not limited to this specific type of micro-continuum nor to this kind of boundary data, this is the most common case so far. Therefore, it will be considered here as well, at least to begin with. Furthermore, the straightforward generalisation of the concept will be examined first for linear micro-continua. This rather obvious generalisation consists in expressing the spatial dependence of the boundary displacements by means of a polynomial of order M. The applied boundary conditions generate displacement, strain and stress fields inside the volume element. These fields are interpreted as the micro-fields. The effective strains are defined as usual as the volume averages with respect to the corresponding micro-strains. The coefficients of the linear part of the polynomial can be related to these effective strains, whereas the remaining coefficients correspond to the macroscopic gradients of the effective strains up to the order $M-1$. Effective stresses and hyper-stresses can be defined consistently and averaging rules can be derived for these stress quantities.

The approach coincides with the RVE-concept if only linear displacements are prescribed at the outer surface of the volume element. This, in turn, corresponds to a polynomial of degree one. In this case, the classical Hill-Mandel condition is recovered, which states that the true strain energy density of the volume element, computed by averaging the strain energy density obtained from the micro-fields, equals the scalar product of effective stresses and effective strains, multiplied by one half. For polynomials of higher degree, extended Hill-Mandel relations can be obtained where the computation of the true strain energy density does not change at all. However, the latter is now equal to a sum whose first term is the usual scalar product between effective strains and effective stresses followed by the scalar products of the strain gradients up to the order $M-1$ with their corresponding hyper-stresses.

The constitutive equations which establish relations between the effective stress and strain quantities are obtained from the solution of the boundary value problem for the volume element. Depending on what particular polynomial is used, constitutive equations can be obtained whose structure is compatible with certain generalised continua.

The method has been explored further and developed considerably by Forest and co-workers, see e.g. FOREST (1998), FOREST AND SAB (1998), FOREST (2002). Mo-

tivated by the observation that, seemingly, only effective generalised continua with internal constraints can be deduced by straightforward application of the concept, the proper construction of the polynomials related to the boundary data has been investigated in detail by FOREST AND SAB (1998) and FOREST (2002). For this purpose, the authors adapted a mircomorphic point of view at the macro-level by interpreting the displacements of the effective continuum as some macroscopic displacement vector to which the homogeneous motion of an attached micro-continuum is superimposed. Least square minimisation of the error between the mircomorphic approximation and the micro-displacements (the displacement fields inside the volume element) leads to proper averaging rules. Finally, the construction of the polynomials sought for requires the choice of a particular mircomorphic continuum and the approximation of the micro-displacements within the volume element by polynomials. It has been shown that the coefficients of these polynomials can either be ruled out or that they can be related to the characteristics of the mircomorphic effective continuum as was done for an unconstrained Cosserat medium by the authors.

In order to complete the procedure, a fluctuation field has to be superimposed because the stresses computed from the polynomial micro-displacements do not fulfil in general the equilibrium conditions inside the volume element. As already discussed in TRINH, JÄNICKE, ET AL. (2012), there exist at least three possible choices: (i) the fluctuations vanish at the boundary of the volume element, (ii) the fluctuations are assumed to be periodic at homologous points of the volume element and, (iii) the fluctuations do not obey any constraints but the volume element is embedded into a periodic arrangement of sufficiently many other volume elements as performed by FOREST AND TRINH (2010). It turns out that the homogenisation methodology proposed by GOLOGANU, LEBLOND, ET AL. (1997) is recovered by combining a strain gradient medium at the macro-level with a fluctuation field according to (i). This particular choice for the fluctuation field was used as well by CHEN, LIU, ET AL. (2009) in order to obtain an analytical estimation for the material properties of an unconstrained Cosserat continuum as a homogeneous replacement medium for an elastic two-phase composite.

A strongly related approach has been developed by KOUZNETSOVA (2002) KOUZNETSOVA, GEERS, AND BREKELMANS (2002) for geometrically and physically non-linear problems in terms of a gradient enhanced computational homogenisation procedure. Here, the boundary conditions of a volume element related to a point of the macro-continuum are expressed by means of the first and second gradients of the motion supplemented by periodic fluctuations. The macro-continuum is a non-linear strain gradient continuum, which is why the method can be characterised concisely as an FE^2-method of Mindlin-type.

Unfortunately, the approach discussed so far exhibits a number of drawbacks. First of all, trying to enforce equality between the macroscopic gradient of the mean of a variable and, the mean with respect to the gradient of the very same variable, leads to conflicting boundary conditions at the outer surface of the volume element. Hence, although certain coefficients of the polynomials discussed above can be related to macroscopic gradient of effective variables, for instance the gradient of the mean strain with respect to the macroscopic coordinate, the mean of the gradient of these variables cannot be rigorously prescribed for the volume element, as pointed out for example by TRINH, JÄNICKE, ET AL. (2012). Furthermore, numerical investigations performed by FOREST AND TRINH (2010) indicate that the boundary conditions for the volume element in terms of polynomials with superimposed fluctuations do not necessarily reflect the real situation. In addition, the concept can not be related consistently to periodic nor to random micro-structures because of the following reasons. If the micro-structure is periodic and the heterogeneity at the micro-scale vanishes, it vanishes everywhere. Therefore, in this case the effective continuum should turn into the micro-continuum. However, a closer look at the constitutive relations obtained by higher order homogenisation reveals that the higher order terms do not cancel out automatically for vanishing micro-heterogeneity, see e.g. ZYBELL, MÜHLICH, AND KUNA (2008) or CHEN, LIU, ET AL. (2009). This point has been discussed, e.g. by BIGONI AND DRUGAN (2007) and YUAN, TOMITA, AND ANDOU (2008). In order to remedy this situation, the solution of the asymptotic approach discussed within the previous section was used by TRAN, MONCHIET, AND BONNET (2012) to compute the averaged energy density of the unit cell. The authors derived an extended version of the Hill-Mandel condition which in turn establishes a homogenised elastic potential in the spirit of strain gradient theories.

The situation becomes even more complicated for random micro-structures. The classical Hill-Mandel condition corresponds to the case of vanishing energetic fluctuations. A conceptual difficulty consists in the interpretation of the extended Hill-Mandel condition in terms of statistical information. So far, this question has not yet been investigated. However, reflections on the validity of classical homogenisation schemes such as those by FOREST (1998) suggest that the additional terms in the Hill-Mandel condition are somehow related to the ergodic hypothesis. In fact, replacing the ensemble averages by corresponding volume averages implies that the region over which the volume integration is performed has to be considerably large. If the volume element is too small and the difference between ensemble and volume averages cannot be neglected, the higher order terms might be necessary to correct this difference. Similar to periodic micro-structures, the effective continuum should turn into the micro-continuum if the randomness vanishes everywhere. A concept

which tries to accomplish this has been proposed by JIA L. (2011). Here, an RVE is defined as a collection of a number of volume elements for which the boundary value problem is solved as described at the beginning of this subsection. The strain energy of the RVE is then computed by averaging with respect to this collection of volume elements. Eventually, the computation of the higher order effective elasticity tensor involves two sixth-order tensors. The first one coincides with the higher order elasticity tensor obtained for prescribed higher order boundary conditions. The second one corresponds to the response of the RVE for vanishing material contrast at the micro-level, and hence homogeneous micro-structure. Since the second is subtracted from the first, the strain gradient part cancels out if the micro-structure is homogeneous.

However, if interpreting the concept in the sense of some moving average, then vanishing micro-homogeneity at some point in the effective continuum does not necessarily mean that the micro-homogeneity vanishes everywhere. Furthermore, there is no need for the higher order terms to vanish at some point with vanishing micro-heterogeneity if the latter still exists in the vicinity of that point. How to modify the concept in order to capture the different viewpoints and to resolve the existing problems mentioned above are open questions which are part of an intense ongoing discussion.

Regardless of the number of open problems related to the polynomial approach, the inherent potential of this method should not be underestimated. Although the homogenisation methods discussed within the subsections 2.3.1 and 2.3.2 provide apparently more rigour, their application is rather limited to linear problems. Only a few extensions towards non-linear behaviour exist. The polynomial approach, on the other hand, is by no means limited to linear problems. Furthermore, there is no general objection so far to apply it only to periodic micro-structures although, an accurate treatment with respect to random materials is still missing.

3 Modelling of quasi-brittle failure

3.1 Overview

As already mentioned at the beginning, the primary motivation of this work consists in the modelling of quasi-brittle failure in porous elastic solids by means of a continuum approach. The latter implies replacement of a considered body, whose micro-structure consists of voids surrounded by a linear elastic matrix material, by some effective continuum.

Quasi-brittle rupture is characterised by the evolution of damage prior to final failure and exhibits strong size effects, see e.g. BAŽANT (2005). Hence, the effective continuum must capture deterministic size effects, it must account for damage evolution and last but not least, softening induced by the evolution of damage must not lead to spurious results. These requirements can be accomplished only by models derived from a generalised continuum theory.

The successive development of the effective continuum approach is documented in the following four journal publications:

A ZYBELL, L., MÜHLICH, U., KUNA, M. (2008) "Constitutive equations for porous plane-strain gradient elasticity obtained by homogenization". In: *Archive of Applied Mechanics* 79(4):359-375

B MÜHLICH, ZYBELL, L., KUNA, M. (2009) "Micromechanical modelling of size effects in failure of porous elastic solids using first order plane strain gradient elasticity". In: *Computational Materials Science* 46(3):647-653

C MÜHLICH, ZYBELL, L., KUNA, M. (2012) "Estimation of material properties for linear elastic strain gradient effective media". In: *European Journal of Mechanics, A/Solids*. 31(1):117-130

D MÜHLICH, U., ZYBELL, L., HÜTTER, G., KUNA, M. (2013) "A first order strain gradient damage model for simulating quasi-brittle failure in porous elastic solids". In: *Archive of Applied Mechanics* DOI: 10.1007/s00419-013-0729-6

These articles will be summarised in the remaining part of this chapter, focussing on the general methodology and the primary motivation for certain choices. Fur-

thermore, the main results will be reported and alternative ways of development for future work will be discussed.

3.2 Methodology

The articles mentioned in the previous section cover particular steps or aspects of a general methodology which can be summarised as follows:

1. The strain energy density for the effective generalised continuum has to be provided for the pure elastic response, preferably by some homogenisation scheme;
2. Based on the elastic strain energy density, a damage potential can be derived using the standard continuum thermodynamics scheme with internal variables;
3. The evolution equations for the internal variables have to be specified.

Of course, some generalised continuum framework had to be chosen first. Here, strain gradient elasticity as derived by MINDLIN AND ESHEL (1968) has been favoured as the basis for further development because of the following main reasons. It can be obtained from a straightforward extension of the strain energy density. How constitutive equations which fit into the framework of strain gradient theories can be derived transparently by higher order homogenisation was shown already by GOLOGANU, LEBLOND, ET AL. (1997). Retrospectively, this was probably the most decisive argument. Although the appearance of the second gradient of the displacement field in the governing equations requires additional effort with respect to numerical solution techniques based on the Finite Element Method, suitable strategies to deal with this problem were known already from the theory of plates and shells. Here, a mixed formulation has been used for which suitable finite elements were already developed by SHU, KING, AND FLECK (1999).

3.3 Discussion of main results

In a first step, the constitutive equations for plane porous strain gradient elasticity have been derived by the higher order homogenisation scheme described at the beginning of subsection 2.3.3. In order to obtain a closed form solution, a cylindrical volume element of linear elastic material with a cylindrical void in its center was considered. Plane stress, respectively plane strain conditions were enforced. Quadratic boundary displacements, related to the macroscopic strains and their gradients, were prescribed. Airy's stress function approach together with a Fourier's series representation of the solution was used to derive the corresponding micro-fields. From

the definition of the macroscopic stresses and hyper-stresses, the desired constitutive equations were obtained in closed form. Due to the centro-symmetry of the considered volume element, the constitutive equations admit a rather simple structure. Stresses and strains are related by the usual fourth-order elasticity tensor $\boldsymbol{C}$, whereas the relation between hyper-stresses and strain gradients is given by a sixth-order tensor $\boldsymbol{D}$. While $\boldsymbol{C}$ depends only on the void volume fraction and the elastic constants of the matrix material, $\boldsymbol{D}$ hinges in addition on the outer radius of the volume element R. Hence, the internal length R, related to the mean distance between adjacent voids, enters the model. The solution has been reported in publication [A] together with some numerical studies. Furthermore, a failure criterion was proposed based on the maximum circumferential stress at the micro-void's surface.

The failure criterion mentioned above has been explored in publication [B] by means of an illustrative example. The capability of the model to capture size effects in the elastic response has been shown. At this stage of development, however, the failure criterion could solely be used either to indicate the collapse of the complete structure in the case of weakest-link failure or to predict only the onset of damage evolution. The initial idea to take this criterion as a basis to derive a continuum damage model has been rejected for the following reasons. Since the criterion was derived from an analytical solution, the involved formulas are rather cumbersome. It is limited to plane stress or plane strain respectively, and the transition to three-dimensions would require a different analytical solution which would be even more complicated. On the other hand, it is easier to obtain suitable estimates for the elastic strain energy density, and a continuum damage model based on that quantity provides more flexibility at lower costs.

Estimates for the higher order elasticity tensor were derived in publication [C]. The methodology developed by the authors is not limited to two dimensions nor to porous micro-structures. On the contrary, it can be adapted easily for more general centro-symmetric composites.

Finally, a continuum damage model has been derived in publication [D]. Its basic ingredient is the elastic strain energy density of the effective continuum. Envisaging the damage process as the formation of micro-cracks evolving from the surface of existing micro-voids, a damage potential was derived. The void volume fraction f plays the role of an internal variable and its evolution accounts for the damage process in terms of an effective quantity, the growth of which reflects the decrease in load-bearing capacity at a point in the effective continuum due to the underlying micro-crack evolution.

3.4 Outlook

In order to take full advantage of the approach worked out here, certain problems have to be solved in the future. For instance, as a consequence of the use of rotationally symmetric volume elements in the homogenisation procedure, the higher order elasticity tensors are only positive semi-definite. This may effect uniqueness and stability of the solution of the boundary value problem at the macro-scale. A possible remedy consists in using honeycomb or Kelvin-cell like volume elements.

Even if the macroscopic fields indicate anisotropic damage evolution, the actual continuum damage model predicts exclusively the evolution of the effective void volume fraction, and hence isotropic evolution of damage. In order to account for the evolving anisotropy, estimates for the elastic strain energy density must be provided for volume elements with elliptical voids and arbitrary position of the void's center. It should be noted that the latter leads to the loss of the centro-symmetry of the volume element and more complex constitutive equations will result.

Bibliography

AIFANTIS, E.C. (2003): "Update on a class of gradient theories". In: *Mechanics of Materials* 35. 3-6, pp. 259–280.

ANDRIANOV, I.V., BOLSHAKOV, V.I., ET AL. (2012): "Higher order asymptotic homogenization and wave propagation in periodic composite materials". In: *Proceedings of the Royal Society A* 464. 2093, pp. 1181–1201.

BAKHVALOV, N.S. AND PANASENKO, G. (1989): *Homogenisation: Averaging Processes in Periodic Media: Mathematical Problems in the Mechanics of Composite Materials*. Mathematics and its applications. Soviet series. Springer.

BAŽANT, Z.P. (2005): *Scaling of structural strength*. Elsevier.

BAŽANT, Z.P. AND JIRASEK, M. (2002): "Nonlocal integral formulations of plasticity and damage: survey of progress". In: *Journal of Engineering Mechanics* 128, p. 1119.

BENSOUSSAN, A., LIONS, J.L., AND PAPANICOLAOU, G. (1978): *Asymptotic Analysis for Periodic Structures*. North Holland, Amsterdam.

BERAN, M.J. (1971): "Application of statistical theories to heterogeneous materials". In: *Physica Status Solidi (a)* 6. 2.

– (1968): *Statistical Continuum Theories*. Wiley and Interscience Publishers, New York.

BERAN, M.J. AND MCCOY, J.J. (1970): "The use of strain gradient theory for analysis of random media(Strain gradient theory for random media, considering equations for response to forcing field)". In: *International Journal of Solids and Structures* 6, pp. 1267–1275.

BIGONI, D. AND DRUGAN, W.J. (2007): "Analytical derivation of Cosserat moduli via homogenization of heterogeneous elastic materials". In: *Journal of Applied Mechanics* 74, pp. 741–753.

BOUTIN, C. (1996): "Microstructural effects in elastic composites". In: *International Journal of Solids and Structures* 33. 7, pp. 1023–1051.

BURYACHENKO, V. (2007): *Micromechanics of Heterogeneous Materials*. Springer.

CHEN, H., LIU, X., ET AL. (2009): "Identification of material parameters of micropolar theory for composites by homogenization method". In: *Computational Materials Science* 46, pp. 733–737.

COSSERAT, E. AND COSSERAT, F. (1909): *Theory of deformable bodies*. Translation into English from French by Delphenich, D.H. Hermann and Sons, Paris.

DIENER, G., HÜRRICH, A., AND WEISSBARTH, J. (1984): "Bounds on the nonlocal effective elastic properties of composites". In: *Journal of the Mechanics and Physics of Solids* 32. 1, pp. 21–39.

DRUGAN, W.J. (2000): "Micromechanics-based variational estimates for a higher-order nonlocal constitutive equation and optimal choice of effective moduli for elastic composites". In: *Journal of the Mechanics and Physics of Solids* 48. 6-7, pp. 1359–1387.

– (2003): "Two exact micromechanics-based nonlocal constitutive equations for random linear elastic composite materials". In: *Journal of the Mechanics and Physics of Solids* 51. 9, pp. 1745–1772.

DRUGAN, W.J. AND WILLIS, J.R. (1996): "A micromechanics-based nonlocal constitutive equation and estimates of representative volume element size for elastic composites". In: *Journal of the Mechanics and Physics of Solids* 44. 4, pp. 497–524.

EDELEN, D.G.B., GREEN, A.E., AND LAWS, N. (1971): "Nonlocal continuum mechanics". In: *Archive for Rational Mechanics and Analysis* 43. 1, pp. 36–44.

ENAKOUTSA, K., LEBLOND, J.B., AND PERRIN, G. (2007): "Numerical implementation and assessment of a phenomenological nonlocal model of ductile rupture". In: *Computer Methods in Applied Mechanics and Engineering* 196. 13-16, pp. 1946–1957.

ERINGEN, C. A. AND SUHUBI, E.S. (1964): "Nonlinear theory of simple micro-elastic solids - I". In: *International Journal of Engineering Science* 2. 2, pp. 189–203.

ERINGEN, C.A. (1995): "Balance laws of micromorphic continua revisited". In: *International Journal of Engineering Science* 30. 6, pp. 805–810.

– (1999): *Microcontinuum Field Theories, Vol. I: Foundations and Solids*. Springer Verlag New York.

– (2002): *Nonlocal Continuum Field Theories*. Springer.

ESHELBY, J.D. (1957): "The Determination of the Elastic Field of an Ellipsoidal Inclusion, and Related Problems". In: *Proceedings of the Royal Society of London. Series A. Mathematical and Physical Sciences* 241. 1226, pp. 376–396.

FISHMAN, L. AND MCCOY, J.J. (1981): "A unified view of bulk property theories for stochastic and periodic media". In: *Zeitschrift f"ur Angewandte Mathematik und Physik (ZAMP)* 32. 1, pp. 45–61.

FLECK, N.A. AND HUTCHINSON, J.W. (2001): "A reformulation of strain gradient plasticity". In: *Journal of the Mechanics and Physics of Solids* 49. 10, pp. 2245–2271.

– (1997): "Strain gradient plasticity". In: *Solid Mechanics*, p. 295.

FLECK, N.A., MULLER, G.M., ET AL. (1994): "Strain gradient plasticity: theory and experiment". In: *Acta Metallurgica et Materialia* 42. 2, pp. 475–488.

FOREST, S. (2002): "Homogenization methods and the mechanics of generalized continua-part 2". In: *Theoretical and Applied Mechanics* 28. 29, pp. 113–144.

– (1998): "Mechanics of generalized continua: construction by homogenization". In: *Journal de Physique-Colloques* 8. 4, pp. 39–48.

– (2009): "Micromorphic approach for gradient elasticity, viscoplasticity, and damage". In: *Journal of Engineering Mechanics* 135. 3, pp. 117–131.

FOREST, S. AND SAB, K. (1998): "Cosserat overall modeling of heterogeneous materials". In: *Mechanics Research Communications* 25. 4, pp. 449–454.

FOREST, S. AND TRINH, D. K. (2010): "Generalized and non-homogeneous boundary conditions in homogenization methods". In: *Zeitschrift für Angewandte Mathematik und Mechanik*.

GAMBIN, B. AND KRÖNER, E. (1989): "Higher-order terms in the homogenized stress-strain relation of periodic elastic media". In: *physica status solidi (b)* 151, pp. 513–519.

GERMAIN, P. (1973): "The method of virtual power in continuum mechanics. Part 2: Microstructure". In: *SIAM Jourmnal of Applied Mechanics* 25. 3, pp. 556–575.

GODDARD, J.D. (2008): "From granular matter to generalized continuum". In: *Mathematical models for granular matter*. Ed. by Capriz, Gianfranco, Giovine, Pasquale, and Mariano, Paolo Maria. Vol. 1937. Lecture Notes in Mathematics. Springer, pp. 1–22.

GOLOGANU, M., LEBLOND, J.B., ET AL. (1997): "Continuum micromechanics". In: ed. by Suquet, P. CISM International Centre for Mechanical Sciences 377. Springer. Chap. Recent extensions of Gurson's model for porous ductile metals, pp. 61–130.

GREEN, A. (1965): "Micro-materials and multipolar continuum mechanics". In: *International Journal of Engineering Science* 3. 5, pp. 533–537.

GREEN, A.E., NAGHDI, P.M., AND RIVLIN, R.S. (1965): "Directors and multipolar displacements in continuum mechanics". In: *International Journal of Engineering Science* 2. 6, pp. 611–620.

GREEN, A.E. AND RIVLIN, R.S. (1964): "Multipolar continuum mechanics". In: *Archive for Rational Mechanics and Analysis* 17. 2, pp. 113–147.

– (1964): "Simple force and stress multipoles". In: *Archive for Rational Mechanics and Analysis* 16. 5, pp. 325–353.

GURTIN, M. (1968): "On the thermodynamics of materials with memory". In: *Archive for Rational Mechanics and Analysis* 28. 1, pp. 40–50.

HASHIN, Z. AND SHTRIKMAN, S. (1962): "A variational approach to the theory of the elastic behaviour of polycrystals". In: *Journal of the Mechanics and Physics of Solids* 10, pp. 343–352.

HILL, R. (1963): "Elastic properties of reinforced solids: some theoretical principles". In: *J. Mech. Phys. Solids* 11. 5, pp. 357–372.

HUET, C. (1990): "Application of variational concepts to size effects in elastic heterogeneous bodies". In: *J. Mech. Phys. Solids* 38. 6, pp. 813–841.

– (1982): "Universal conditions for assimilation of heterogeneous material to an effective continuum". In: *Mechanics Research Communications* 9. 3, pp. 165–170.

Jeulin, D. and Ostoja-Starzewski, M., eds. (2002): *Mechanics of Random and Multiscale Microstructures*. CISM Courses and Lectures 430. Springer.

JIA L. (2011): "Establishment of strain gradient constitutive relations by homogenization". In: *Comptes Rendus Mecanique* 339, pp. 235–244.

KANIT, T., FOREST, S., ET AL. (2003): "Determination of the size of the representative volume element for random composites: statistical and numerical approach". In: *International journal of solids and structures* 40. 13-14, pp. 3647–3679.

KLEINERT, H. (1989): *Gauge fields in condensed matter*. Vol. 2 Stresses and defects. Singapore : World Scientific.

KOITER, W.T. (1964): "Couple stresses in the theory of elasticity. I and II." In: *Proceedings of the Koninklijke Nederlandse Akademie Van Wetenschappen*. Vol. 67. B, pp. 17–44.

KOUZNETSOVA, V., GEERS, M.G.D., AND BREKELMANS, W.A.M. (2002): "Multi-scale constitutive modelling of heterogeneous materials with a gradient-enhanced computational homogenization scheme". In: *International Journal of Numerical Methods in Engineering* 54. 8, pp. 1235–1260.

KOUZNETSOVA, V.G. (2002): "Computational homogenization for the multi-scale analysis of multi-phase materials". PhD thesis. Technische Universiteit Eindhoven.

KRÖNER, E. AND KOCH, H. (1976): "Effective properties of disordered materials". In: *Solid Mechanics Archives* 1, pp. 183–238.

LUCIANO, R. AND WILLIS, J.R. (2000): "Bounds on non-local effective relatios for random composites loaded by configuration-dependent body force". In: *Journal of the Mechanics and Physics of Solids* 48, pp. 1827–1849.

– (2000): "Non-local effective relations for fibre reinforced composites loaded by configuration-dependent body forces". In: 49, pp. 2705–2717.

MAUGIN, G.A. (2013): "The principle of virtual power: from eliminating metaphysical forces to providing an efficient modelling tool". In: *Continuum Mechanics and Thermodynamics* 25. 2-4, pp. 127–146.

MINDLIN, R.D. (1964): "Micro-structure in linear elasticity". In: *Archive for Rational Mechanics and Analysis* 16. 1, pp. 51–78.

– (1965): "Second gradient of strain and surface-tension in linear elasticity (Linear deformation of elastic solid in which potential energy-density is function of strain and first and second gradients)". In: *International Journal of Solids and Structures* 1, pp. 417–438.

MINDLIN, R.D. AND ESHEL, N.N. (1968): "On first strain-gradient theories in linear elasticity". In: *International Journal of Solids and Structures* 4, pp. 109–124.

NEMAT-NASSER, S. AND HORI, M. (1999): *Micromechanics: Overall Properties of Heterogeneous Materials*. 2nd ed. North-Holland, Elsevier.

OSTOJA-STARZEWSKI, M. (2011): "Macrohomogeneity condition in dynamics of micropolar media". In: *Archive of Applied Mechanics* 81 (7), pp. 899–906. ISSN: 0939-1533.

– (2006): "Material spatial randomness: from statistical to representative volume element". In: *Probabilistic Engineering Mechanics* 21. 2, pp. 112–132.

PANASENKO, G. (2005): *Multi-scale Modelling for Structures and Composites*. Springer.

PEERLINGS, R.H.J. AND FLECK, N.A. (2004): "Computational evaluation of strain gradient elasticity constants". In: *International Journal for Multiscale Computational Engineering* 2, pp. 599–619.

POLIZZOTTO, C. (2003): "Gradient elasticity and nonstandard boundary conditions". In: *International journal of solids and structures* 40. 26, pp. 7399–7423.

QU, J. AND CHERKAOUI, M. (2006): *Fundamentals of Micromechanics of Solids*. John Wiley & Sons, Inc.

SANCHEZ-PALENCIA, E. (1986): "Homogenization in mechanics. A survey of solved and open problems". In: *Rendiconti del Seminacio Matematico Universita e Politenico di Torino* 44. 145, pp. 1–45.

SHU, J.Y., KING, W.E., AND FLECK, N.A. (1999): "Finite elements for materials with strain gradient effects". In: *International Journal for Numerical Methods in Engineering* 44, pp. 373–391.

SMYSHLYAEV, V.P. AND CHEREDNICHENKO, K.D. (2000): "On rigorous derivation of strain gradient effects in the overall behaviour of periodic heterogeneous media". In: *Journal of the Mechanics and Physics of Solids* 48, pp. 1325–1357.

SMYSHLYAEV, V.P. AND FLECK, N.A. (1996): "The role of strain gradients in the grain size effect for polycrystals". In: *Journal of the Mechanics and Physics of Solids* 44. 4, pp. 465–495.

SOBCZYK, K. AND KIRKNER, D.J. (1970): *Stochastic modeling of Microstructures*. Modeling and Simulation in Science, Engineering and Technology. Birkhäuser.

SUHUBI, E.S. AND ERINGEN, C. A. (1964): "Nonlinear theory of simple micro-elastic solids - II". In: *International Journal of Engineering Science* 2. 4, pp. 389–404.

TEKOGLU, C. (2006): "Size Effects in Cellular Solids". PhD thesis. University of Groningen.

TOUPIN, R.A. (1964): "Theories of elasticity with couple stresses". In: *Archive of Rational Mechanics and Analysis* 17, pp. 85–112.

TRAN, T.-H., MONCHIET, V., AND BONNET, G. (2012): "A micromechanics-based approach for the derivation of constitutive elastic coefficients of strain-gradient media". In: *International Journal of Solids and Structures* 45. 5, pp. 783–792.

TRIANTAFYLLIDIS, N. AND BARDENHAGEN S. (1996): "The influence of scale size on the stability of periodic solutions and the role of associated higher order gradient continuum models". In: *Journal of the Mechanics and Physics of Solids* 44. 1, pp. 1891–1928.

TRINH, D.K., JÄNICKE, R., ET AL. (2012): "Evaluation of generalized continuum substitution models for heterogeneous materials". In: *Journal for Multiscale Computational Engineering* 10. 6, pp. 527–549.

TRUESDELL, C. AND NOLL, W. (2004): *The nonlinear field theories of mechanics*. Ed. by Antman, Stuart S. 3rd ed. Springer.

TRUESDELL C. AND TOUPIN R. (1960): "The Classical Field Theories". In: *Handbuch der Physik*. Vol. III. Springer. Chap. 3, pp. 226–793.

WILLIS, J.R. (1987): "Randomly homogeneous media". In: *Homogenization techniques for composite media*. Ed. by Sanchez-Palencia, E. and Zaoui, A. Vol. 272. Lecture Notes in Physics. Springer. Chap. V, pp. 281–337.

YANG, F., CHONG, A.C.M., ET AL. (2002): "Couple stress based strain gradient theory for elasticity". In: *International Journal of Solids and Structures* 39. 10, pp. 2731 –2743.

YUAN, X., TOMITA, Y., AND ANDOU, T. (2008): "A micromechanical approach of nonlocal modeling for media with periodic microstructures". In: *Mechanics Research Communications* 35. 1-2, pp. 126–133.

ZAOUI, A. (2002): "Continuum micromechanics: survey". In: *Journal of Engineering Mechanics* 128, p. 808.

ZHANG, X. AND SHARMA, P. (2005): "Inclusions and inhomogeneities in strain gradient elasticity with couple stresses and related problems". In: *International Journal of Solids and Structures* 42. 13, pp. 3833–3851.

ZYBELL, L., MÜHLICH, U., AND KUNA, M. (2008): "Constitutive equations for porous plane-strain gradient elasticity obtained by homogenization". In: *Archive of Applied Mechanics* 79. 4, pp. 359–375.

4 Collection of articles reflecting the author's contribution

Constitutive equations for porous plane-strain gradient elasticity obtained by homogenization. In: *Archive of Applied Mechanics* 79(4):359-375

Constitutive equations for porous plane strain gradient elasticity obtained by homogenization

Lutz Zybell Uwe Mühlich Meinhard Kuna

The paper addresses the problem of plane strain gradient elasticity models derived by higher order homogenization. A microstructure which consists of cylindrical voids surrounded by a linear elastic matrix material is considered. Both plane stress or plane strain conditions are assumed and the homogenization is performed by means of a cylindrical RVE subjected to quadratic boundary displacements. The constitutive equations for the equivalent medium at the macro-scale are obtained analytically by means of Airy's Stress Function in conjunction with Fourier-Series. Furthermore, a failure criterion based on the maximum hoop stress on the void surface is formulated. A mixed finite element formulation has been implemented into the commercial finite-element program Abaqus. Using the constitutive relations derived above, numerical simulations were performed in order to compute the stress concentration at a hole with varying parameters of the constitutive equations. The results predicted by the model are discussed in comparison with the results of the theory of simple materials.

1. Introduction

Because of the discontinuous and heterogeneous nature of real materials, continuum mechanics can always be interpreted as the result of a certain kind of homogenization. The homogenization process may pass through various levels, each one related to a different material length scale.

Most of existing homogenization methods in literature are based on the concept of the representative volume element (RVE). In this context, a theory of simple materials

on the microscale implies a theory of simple materials on the macroscale if the classical form of the Principle of Macrohomogeneity applies. The latter can be directly derived from the so-called Hill-Mandel Lemma if linear displacements or constant surface tractions are assumed on the outer boundary of the RVE. The constitutive relations for the effective material at the macro-scale are determined by solving the boundary value problem for the RVE. For a detailed exposition of this topic the reader is referred to Nemat-Nasser and Hori [20]. The continuum models derived by the homogenization approach outlined above account, to a certain extent, for the influence of the micro-structure on the macroscopic material properties. However, only specific values enter into these models. Therefore, experimentally observed size effects cannot be reflected. Furthermore, that approach is no longer justified if strong gradients appear in the macroscopic fields since the classical form of the Principle of Macrohomogeneity does not apply in this case.

On the other hand, the serious drawbacks of continuum damage models derived within the framework of simple materials have caused a growing interest in higher order continuum theories, like gradient enhanced theories, micropolar theories or nonlocal theories. The spurious mesh dependence of the numerical results which is characteristic for continuum models including softening can be avoided or at least reduced by applying higher order continuum theories as shown e.g. by De Borst et al. [7]. Furthermore, size effects can be reflected because additional length parameters always emerge. In general higher order continuum theories are more complex and imply considerable effort in the theoretical treatment, the numerical implementation and parameter identification. On the other hand, the mesh dependence can be avoided even if only the damage variable is treated as nonlocal. For an extensive discussion of nonlocal continuum damage models the reader is referred to Bažant [4]. Although this heuristic approach is capable to regularize the numerical results with much less effort, the comparison of different models performed by Engelen et al. [9] revealed that size effects can not correctly be predicted in contrast to the strain gradient models included in the analysis recorded in [9].

A strain gradient elasticity theory was derived by Mindlin [18] based on reasoning about micro-structure and homogenization. This approach which also covers the linear Cosserat elasticity was further developed in [19]. This is referred as Mindlin-type theory in the sequel and has been extended towards strain gradient plasticity by Fleck and Hutchinson [11]. Subsequently, the latter was simplified in order to reduce complexity in [12] which, however, corrupts the capability of regularization as shown by Engelen et al. [9].

An advantage of continuum models of Mindlin-type is that they can be transparently obtained from higher order homogenization, i.e. homogenization with more complex conditions prescribed at the boundary of the RVE. A comprehensive treatise about higher order homogenization related to elasticity problems is given by Forest [13], including the discussion of different kinds of boundary conditions. In general, an extension of the Principle of Macrohomogeneity is derived. Similar to the theory of simple materials, the constitutive equations have to be determined by solving the boundary problem for the RVE, which has been numerically performed considering Cosserat elasticity e.g. by Kruch and Forest [16]. Quadratic boundary displace-

ments were applied by Gologanu et al. [14] in the context of ductile damage and a semi-analytical model was derived. A numerical homogenization approach based on higher order deformation gradients has been developed by Kouznetsova et al. [15].

The use of Mindlin-type models in conjunction with the finite-element method requires in general $C^{(1)}$-continuous elements. In order to overcome this difficulty, so-called mixed-type formulations might be used. According to [19], strain gradient elasticity can be formulated in three different but equivalent ways. A mixed-type formulation based on one of these models was derived by Shu et al. [21] and various finite elements were developed and tested. Mixed finite elements for Mindlin-type gradient elasticity were developed as well by Amanatidou et al. [2] [3], although a different formulation was chosen.

In our model the simplest case of homogenization with only two different scales, a continuous macro-scale and one underlying discontinuous and heterogeneous microscale, is considered. It is assumed that the mechanical behavior at the microscale can be completely described by means of a continuum theory of simple materials. The microstructure consists of cylindrical voids surrounded by a linear elastic matrix material. Corresponding macroscopic constitutive equations are derived within the framework of strain gradient elasticity by means of a homogenization procedure using a cylindrical representative volume element (RVE) under plane strain conditions and assuming quadratic displacements on the outer boundary of the RVE. The model has been implemented into the commercial finite element program Abaqus using a mixed-type formulation in order to deal with the continuity requirements due to the presence of the macroscopic strain gradients. Finally, numerical studies were performed with varying the parameters of the constitutive equations. The results are discussed with respect to length scales and are compared with the theory of simple materials.

This paper is organized as follows: In the first part the homogenization is performed and the constitutive relations are derived analytically. The second part deals with the numerical validation of the model and the simulation results of the stress concentration due to a hole are compared with analytical ones. Finally, the paper is summarized and possible extensions and applications of the model are discussed.

In the following, symbolic notation is used. Vectors and second order tensors are indicated by boldface letters. The rank of higher order tensors is indicated by the corresponding number, for example ${}^{4}\mathbf{a}$. The dyadic product of two vectors $\boldsymbol{a}$ and $\boldsymbol{b}$ is expressed by $\boldsymbol{a} \otimes \boldsymbol{b}$ and the scalar product by $\boldsymbol{a} \cdot \boldsymbol{b}$. If the symbolic notation becomes ambiguous, then index notation [5] together with the summation convention is used. Macroscopic field variables refer to the macroscopic point $\mathbf{X}$ unless otherwise indicated.

2. Representative Volume Element (RVE)

2.1. Preliminary considerations

In the following, two different scales are considered: a heterogeneous and discontinuous microscale and a continuous macroscale. The geometrical and mechanical

properties at the microscale are known and we look for an equivalent formulation of the problem at the macroscale where the real material is replaced by a so-called effective medium. Every macroscopic point $\mathbf{X}$ is associated with a surrounding volume at the microscale. Furthermore, it is assumed that a volume element at the microscale can be chosen which fully represents the microstructural properties at least in a statistical sense. This volume is referred to as representative volume element (RVE) in the following. The RVE considered here is supposed to be of cylindrical shape and consists of a cylindrical void surrounded by an isotropic linear elastic matrix material as indicated in Figure 1. The macroscopic stresses and strains at a point $\mathbf{X}$ are defined

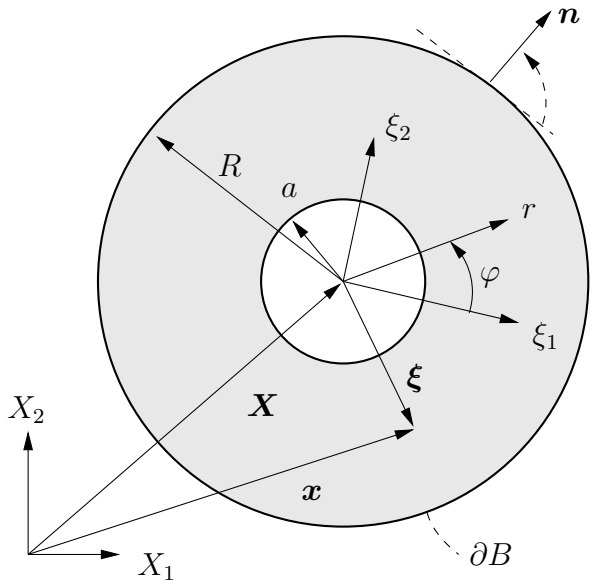

Fig. 1: Cross section of the representative volume element (RVE).

as mean values with respect to the corresponding microscopic quantities

$$\boldsymbol{\Sigma} = \frac{1}{B}\int\limits_{B_m} \boldsymbol{\sigma}\, dV\,, \tag{1}$$

$$\boldsymbol{E} = \frac{1}{2B}\int\limits_{\partial B} [\boldsymbol{u}\otimes\boldsymbol{n} + \boldsymbol{n}\otimes\boldsymbol{u}]\, dA\,, \tag{2}$$

where B denotes the total volume of the RVE and B_m is the volume of the matrix material. Furthermore, $\boldsymbol{n}$ is the outward normal unit vector of the outer boundary ∂B. Assuming linear elastic matrix material the Hill-Mandel Lemma reads

$$\frac{1}{2B}\int\limits_{B_m} \boldsymbol{\sigma} : \boldsymbol{\varepsilon}\, dV = \frac{1}{2}\boldsymbol{\Sigma} : \boldsymbol{E} + \frac{1}{2B}\int\limits_{\partial B} [\boldsymbol{n}\cdot(\boldsymbol{\Sigma}-\boldsymbol{\sigma})]\cdot[\boldsymbol{x}\cdot\boldsymbol{E}-\boldsymbol{u}]\, dA\,. \tag{3}$$

In the sequel, prescribed displacements at the outer boundary of the volume element are considered. The boundary displacements are split into a linear and an oscillating residual term

$$\boldsymbol{u}|_{\partial B} = \bar{\boldsymbol{u}}|_{\partial B} + \hat{\boldsymbol{u}}|_{\partial B} \tag{4}$$

with

$$\bar{\boldsymbol{u}}|_{\partial B} = \boldsymbol{x} \cdot \boldsymbol{E} \tag{5}$$

and

$$\hat{\boldsymbol{u}} = \boldsymbol{u}|_{\partial B} - \boldsymbol{x} \cdot \boldsymbol{E}\,. \tag{6}$$

Since the matrix material is linear elastic, all microscopic fields can be written as the sum of two superimposed fields

$$\boldsymbol{\sigma} = \bar{\boldsymbol{\sigma}} + \hat{\boldsymbol{\sigma}} \tag{7}$$

$$\boldsymbol{\varepsilon} = \bar{\boldsymbol{\varepsilon}} + \hat{\boldsymbol{\varepsilon}} \tag{8}$$

This applies as well to the corresponding mean values

$$\boldsymbol{\Sigma} = \bar{\boldsymbol{\Sigma}} + \hat{\boldsymbol{\Sigma}} \tag{9}$$

$$\boldsymbol{E} = \bar{\boldsymbol{E}} + \hat{\boldsymbol{E}}\,. \tag{10}$$

However, it follows from (6), (2) and (1) that $\hat{\boldsymbol{\Sigma}}$ and $\hat{\boldsymbol{E}}$, which are associated with the boundary displacements $\hat{\boldsymbol{u}}$, vanish because of their mean-value property, as already discussed in [13]. Therefore, the stress tensor $\boldsymbol{\Sigma}$ corresponds to the stress tensor of the theory of simple materials

$$\boldsymbol{\Sigma} = {}^4\bar{\boldsymbol{C}} : \boldsymbol{E} \tag{11}$$

where ${}^4\bar{\boldsymbol{C}}$ is the overall elasticity tensor of the theory of simple materials. Based on the results obtained above, the strain energy density of the RVE can be written as

$$\frac{1}{2B}\int\limits_{B_m} \boldsymbol{\sigma} : \boldsymbol{\varepsilon}\, dV = \frac{1}{2}\boldsymbol{\Sigma} : \boldsymbol{E} + \frac{1}{2B}\int\limits_{B_m} \hat{\boldsymbol{\sigma}} : \hat{\boldsymbol{\varepsilon}}\, dV\,. \tag{12}$$

Summarizing so far, the boundary displacements $\hat{\boldsymbol{u}}$ oscillate around the mean boundary displacements $\bar{\boldsymbol{u}}$ and the strain energy density increases due to the presence of $\hat{\boldsymbol{u}}$ as it was expected. The objective of the following steps is to express the second term of the right hand side of (12) by macroscopic quantities.

2.2. General Solution by means of Airy's Stress Function and Fourier-Series

The concept of Airy's Stress Function is applied in order to derive the general solution for the microscopic fields. Polar coordinates are used because of the geometry of the RVE. The stress function $F(r, \varphi)$ must satisfy the biharmonic equation

$$\Delta\Delta F(r, \varphi) = 0\,, \tag{13}$$

where the Laplace operator Δ is given by

$$\Delta() = \frac{\partial^2()}{\partial r^2} + \frac{1}{r}\frac{\partial()}{\partial r} + \frac{1}{r^2}\frac{\partial^2()}{\partial \varphi^2}\,. \tag{14}$$

The stresses are calculated from the solution of (13) by

$$\sigma_{rr} = \frac{1}{r}\frac{\partial F}{\partial r} + \frac{1}{r^2}\frac{\partial^2 F}{\partial \varphi^2}\,,\ \sigma_{\varphi\varphi} = \frac{\partial^2 F}{\partial r^2} \tag{15}$$

$$\sigma_{r\varphi} = -\frac{\partial}{\partial r}\left(\frac{1}{r}\frac{\partial F}{\partial \varphi}\right) \tag{16}$$

and the corresponding strains can be obtained from the constitutive relations. A general solution of (13) based on Fourier-series was derived by Mitchel (see e.g. [22]). This solution is split into two parts

$$F = \bar{F} + \hat{F}\,, \tag{17}$$

where $\bar{F}$ and $\hat{F}$ correspond to the linear (5) and oscillating boundary displacements (6), respectively. Here, only the stress and strain fields corresponding to $\hat{F}$ are of interest, because $\bar{F}$ represents the solution of the theory of simple materials from which ${}^4\bar{\boldsymbol{C}}$ is determined in general. The determination of ${}^4\bar{\boldsymbol{C}}$ is meanwhile standard (see e.g. [20]) and, therefore, omitted here. The final result is given in Appendix C.

$\breve{m}^{(1)}_{ijk}$	ij = 11	22	12	$\breve{m}^{(2)}_{ijk}$	ij = 11	22	12
k = 1	g_1	$3g_1$	0	k = 1	0	0	-g_1
2	0	0	-g_1	2	$3g_1$	g_1	0
$\breve{m}^{(3)}_{ijk}$	ij = 11	22	12	$\breve{m}^{(4)}_{ijk}$	ij = 11	22	12
k = 1	-g_3	g_3	0	k = 1	0	0	-g_3
2	0	0	g_3	2	-g_3	g_3	0

Tab. 1: Components of the couple stress tensors ${}^3\breve{\boldsymbol{m}}^{(s)}$.

The tractions at the surface of the cylindrical void must vanish which implies that the stress fields given by $\hat{F}$ must satisfy the conditions

$$\sigma_{rr}(r=a,\varphi) = 0 \tag{18}$$

$$\sigma_{r\varphi}(r=a,\varphi) = 0\,, \tag{19}$$

where a denotes the void radius as indicated in Figure 1. The final result for stress function which corresponds to the oscillating boundary displacements reads

$$\hat{F} = \left(r^3 + \frac{a^4}{r}\right)(B_1\cos\varphi + D_1\sin\varphi) + \left(\frac{a^2}{2r} + r\ln r\right)(b_1\cos\varphi + d_1\sin\varphi) + \sum_{n=3}^{\infty}\left\{\left[f_n^{(1)}(r)B_n + f_n^{(2)}(r)b_n\right]\cos(n\varphi) + \left[f_n^{(1)}(r)D_n + f_n^{(2)}(r)d_n\right]\sin(n\varphi)\right\}\,, \tag{20}$$

where $f_n^{(1)}(r)$ and $f_n^{(2)}(r)$ are given by

$$f_n^{(1)}(r) = r^{n+2} - \frac{a^{2n}}{r^{n-2}} + n\frac{a^{2(n+1)}}{r^n} - n\frac{a^{2n}}{r^{n-2}} \tag{21}$$

$$f_n^{(2)}(r) = r^n - \frac{a^{2n}}{r^n} - n\frac{a^{2(n-1)}}{r^{n-2}} + n\frac{a^{2n}}{r^n}\,. \tag{22}$$

The coefficients B_1, b_1, D_1, d_1, B_n, b_n, D_n and d_n are determined from the boundary conditions of the RVE.

2.3. Solution for quadratic boundary displacements

Following the argumentation of Gologanu [14], the boundary displacements

$$\hat{u}_i|_{\partial B} = \frac{1}{2} K_{ijk} x_j x_k - \frac{1}{2} \left[K_{ijk} + K_{jki} \right] X_k x_j \,, \tag{23}$$

are considered. The third order tensor ${}^3\boldsymbol{K}$ can be expressed by means of the gradients of the macroscopic strains

$$K_{ijk} = E_{ij,k} - E_{jk,i} + E_{ki,j} \,, \tag{24}$$

where $()_{,k}$ denotes the partial derivative of () with respect to the macroscopic coordinate X_k. It should be noticed that (24) holds only for moderate macroscopic strain gradients. Furthermore, ${}^3\boldsymbol{K}$ is symmetric with respect to its second and third indexes

$$K_{ijk} = U_{i,jk} = U_{i,kj} = K_{ikj} \tag{25}$$

since $\boldsymbol{E}$ is symmetric and the order of differentiation is commutable. As shown in [14], the standard definition of macroscopic strains

$$E_{ij} = \frac{1}{2} \left[U_{i,j} + U_{j,i} \right] \tag{26}$$

holds if an arbitrary extension of the microscopic displacement fields over the voids is permitted. Due to the boundary conditions (23), the coefficients b_1 and d_1 in (20) can be expressed by means of B_1 and D_1

$$b_1 = \omega B_1 \tag{27}$$

$$d_1 = \omega D_1 \,. \tag{28}$$

Furthermore, owing to the boundary conditions all coefficients vanish for $n > 3$ which shows that the derived solution is exact and

$$b_3 = \omega^* B_3 \tag{29}$$

$$d_3 = \omega^* D_3 \tag{30}$$

holds, where ω and ω_n^* are given together with the corresponding calculations in Appendix A and Appendix B, respectively. Using (27) and (28), the stress function which corresponds to the oscillating boundary displacements can be formally written as

$$\hat{F} = \sum_{k=1}^{4} A_k \tilde{F}_k(r, \varphi) \,, \tag{31}$$

where the remaining coefficients $A_1 \ldots A_4$ are related to those used in (20) by $A_1 = B_1$, $A_2 = D_1$, $A_3 = B_3$ and $A_4 = D_3$. However, no particular order exists and the choice made here is arbitrary and just a matter of convenience.

	111	221	112	222	121	211	122	212
111	h_1	h_2	0	0	0	0	$-h_1$	$-h_1$
221	h_2	h_3	0	0	0	0	$-h_2$	$-h_2$
112	0	0	h_3	h_2	$-h_2$	$-h_2$	0	0
222	0	0	h_2	h_1	$-h_1$	$-h_1$	0	0
121	0	0	$-h_2$	$-h_1$	h_1	h_1	0	0
211	0	0	$-h_2$	$-h_1$	h_1	h_1	0	0
122	$-h_1$	$-h_2$	0	0	0	0	h_1	h_1
212	$-h_1$	$-h_2$	0	0	0	0	h_1	h_1

$h_1 = a_1 + a_2$
$h_2 = 3a_1 - a_2$
$h_3 = 9a_1 + a_2$

Tab. 2: Components of the material tensor ${}^6\check{\boldsymbol{D}}$ written in matrix form ($\left[\check{D}\right]_{(ijk)(lmn)}$).

Because of the linearity of the considered problem, the microscopic stresses and strains as well as the boundary displacements $\hat{\boldsymbol{u}}$ and surface tractions $\hat{\boldsymbol{t}}$ can be written analogously as

$$\begin{aligned} \hat{\boldsymbol{\sigma}} &= \sum_{k=1}^{4} A_k \, \tilde{\boldsymbol{\sigma}}^{(k)} , \quad \hat{\boldsymbol{\varepsilon}} = \sum_{k=1}^{4} A_k \, \tilde{\boldsymbol{\varepsilon}}^{(k)} \\ \hat{\boldsymbol{t}} &= \sum_{k=1}^{4} A_k \, \tilde{\boldsymbol{t}}^{(k)} , \quad \hat{\boldsymbol{u}} = \sum_{k=1}^{4} A_k \, \tilde{\boldsymbol{u}}^{(k)} \end{aligned} \tag{32}$$

It follows from the orthogonality properties of the trigonometric functions that

$$\frac{1}{B} \int_{B_m} \tilde{\boldsymbol{\sigma}}^{(k)} : \tilde{\boldsymbol{\varepsilon}}^{(l)} dV = \begin{cases} \kappa_k & k = l \\ 0 & k \neq l \end{cases} \tag{33}$$

and therefore

$$\frac{1}{2B} \int_{B_m} \hat{\boldsymbol{\sigma}} : \hat{\boldsymbol{\varepsilon}} \, dV = \frac{1}{2} \sum_{k=1}^{4} A_k^2 \kappa_k \, . \tag{34}$$

The coefficients κ_k are given by [1]

$$\begin{aligned}\kappa_1 = \kappa_2 =& R^2\frac{4}{E}\left[(3-\nu)-(1+\nu)f^4-2(1-\nu)f^2\right]-\frac{\omega^2}{R^2}\frac{1}{E}\left[(1+\nu)(1-f)^2+2\ln(f)\right]\\ &+4\omega\frac{1}{E}\left[(f^2-f^3)(1+\nu)+(1-f)(3-\nu)\right]\end{aligned} \tag{35}$$

$$\begin{aligned}\kappa_3 = \kappa_4 =& 4\,\frac{R^6}{E}\Bigg[18(1+\nu)(16f^7-9f^8)+4(1-\nu)(16f^3-9f^4)+2(11+7\nu)(1-8f^6)\\ &+24\frac{\omega^*}{R^2}\left\{(1+\nu)(16f^6-9f^7+1)-(11+7\nu)f^5+2(1-\nu)f^2\right\}\\ &+9\frac{(\omega^*)^2}{R^4}\left\{(1+\nu)(16f^5-8f^6+1)-(11+7\nu)f^4+2(1-\nu)f^2\right\}\Bigg]\,.\end{aligned} \tag{36}$$

where $f=\frac{a^2}{R^2}$ is the void volume fraction.

The determination of the coefficients A_k is the objective of the following steps. The sought solution must obey the boundary conditions (23). Using (32) we can express this in the following way:

$$\hat{u}_i|_{\partial B}=\sum_{r=1}^{4}A_r\;\tilde{u}_i^{(r)}|_{\partial B}=\frac{1}{2}K_{ijk}x_jx_k-\frac{1}{2}\left[K_{ijk}+K_{jki}\right]X_kx_j\,, \tag{37}$$

and the coefficients A_k can be determined directly from (37). Calculating the scalar product of both sides of equation (37) with the surface tractions $\tilde{\boldsymbol{t}}^{(s)}$ and integration over the outer boundary ∂B leads to

$$A_s\kappa_s=\frac{1}{2}K_{ijk}\frac{1}{B}\int\limits_{\partial B}x_jx_k\tilde{t}_i^{(s)}dA-\frac{1}{2}\left[K_{ijk}+K_{jki}\right]\frac{1}{B}\int\limits_{\partial B}X_kx_j\tilde{t}_i^{(s)}dA\;\;\text{(no sum over } s\text{!)}\,, \tag{38}$$

where (33) was taken into account and the identities from Appendix D were used. Further algebraic manipulations yield

$$A_s\kappa_s=\frac{1}{2}K_{ijk}\left[\frac{1}{B}\int\limits_{B}x_k\tilde{\sigma}_{ij}^{(s)}dV+\frac{1}{B}\int\limits_{B}x_j\tilde{\sigma}_{ik}^{(s)}dV\right]-\frac{1}{2}\left[K_{ijk}+K_{jki}\right]\frac{1}{B}\int\limits_{B}X_k\tilde{\sigma}_{ij}^{(s)}dV \tag{39}$$

Due to the symmetry properties of $\boldsymbol{\sigma}$ and ${}^3\boldsymbol{K}$ equation (39) can be written as

$$A_s\;\;=\;\;\frac{1}{\kappa_s}K_{ijk}\frac{1}{B}\int\limits_{B}\left(x_k-X_k\right)\tilde{\sigma}_{ij}^{(s)}dV=\frac{1}{\kappa_s}K_{ijk}m_{ijk}^{(s)} \tag{40}$$

[1] Unfortunately, there were some mistakes regarding this results in the article originally published. For the correct values, please see the appendix in: Micromechanical modelling of size effects in failure of porous elastic solids using first order plane strain gradient elasticity. In: *Computational Materials Science* 46(3):647-653

if the definitions

$$m_{ijk}^{(s)} = \frac{1}{B}\int\limits_B \xi_k \tilde{\sigma}_{ij}^{(s)} dV \tag{41}$$

and $\xi_k = x_k - X_k$ are used (see Figure 1). Using (25)

$$\check{H}_{ijk} := \frac{1}{2}\left[U_{i,jk} + U_{j,ik}\right] \tag{42}$$

equation (40) can be rewritten as

$$A_s = \frac{1}{\kappa_s} m_{ijk}^{(s)} \check{H}_{ijk} \quad \text{(no sum over s!)} \tag{43}$$

The third order tensors ${}^3\boldsymbol{m}^{(s)}$ (41) are interpreted as couple stresses which result from

	111	221	112	222	121	211	122	212
111	h_1	$-h_1$	0	0	0	0	h	h
221	$-h_1$	h_1	0	0	0	0	$-h$	$-h$
112	0	0	h_1	$-h_1$	$-h$	$-h$	0	0
222	0	0	$-h_1$	h_1	h	h	0	0
121	0	0	$-h$	h	h_1	h_1	0	0
211	0	0	$-h$	h	h_1	h_1	0	0
122	h	$-h$	0	0	0	0	h_1	h_1
212	h	$-h$	0	0	0	0	h_1	h_1

$$\begin{aligned} h &= a_1 - a_2 \\ h_1 &= a_1 + a_2 \end{aligned}$$

Tab. 3: Components of the material tensor ${}^6\boldsymbol{D}$ written in matrix form ($[D]_{(ijk)(lmn)}$).

the stress fields $\tilde{\boldsymbol{\sigma}}^{(s)}$; the components are given in Table 1 with with

$$g_1 = g_2 = \frac{R^2}{4}\left[2(1-f^2) + \frac{\omega}{R^2}(1-f)\right] \tag{44}$$

$$g_3 = g_4 = \frac{R^4}{2}\left[4(1-f^3) + \frac{3\omega^*}{R^2}(1-f^2)\right] \tag{45}$$

Using (34) and (41), the second term of the right hand side of (12) gives

$$\frac{1}{2B}\int\limits_B \hat{\sigma}_{ij}\hat{\varepsilon}_{ij} dV = \frac{1}{2}\sum_{r=1}^{4} \kappa_r A_r^2 = \frac{1}{2}\check{M}_{ijk}\,\check{H}_{ijk}\,, \tag{46}$$

where the third order couple stress tensor ${}^3\check{\boldsymbol{M}}$ is defined by

$$\check{M}_{ijk} = \check{D}_{ijklmn}\check{H}_{lmn}\,. \tag{47}$$

The sixth order tensor ${}^6\check{\boldsymbol{D}}$ can be calculated by

$$\check{D}_{ijklmn} = \sum_{r=1}^{4} \frac{1}{\kappa_r} m_{ijk}^{(r)} m_{lmn}^{(r)}\,. \tag{48}$$

and possesses the symmetries

$$\check{D}_{ijklmn} = \check{D}_{jiklmn} = \check{D}_{ijkmln} \tag{49}$$

and

$$\check{D}_{ijklmn} = \check{D}_{lmnijk} \tag{50}$$

which can be immediately read from (41) and (48). The Hill-Mandel Lemma (3) for the considered case can now be written as

$$\frac{1}{2B}\int_B \sigma_{ij}\varepsilon_{ij}\,dV = \frac{1}{2}\Sigma_{ij}E_{ij} + \frac{1}{2}\check{M}_{ijk}\check{H}_{ijk}\,, \tag{51}$$

which is in accordance with the results given in [14]. Equation (51) constitutes an extension of the classical Principle of Macrohomogeneity which allows for gradients of macroscopic strains $\boldsymbol{E}$. Further consequences of (51) in terms of equilibrium conditions, boundary conditions, etc. are discussed e.g. in [19]. The macroscopic couple stress tensor ${}^3\check{\boldsymbol{M}}$ (47) can be obtained as well from

$$\check{M}_{ijk} = \frac{1}{B}\int_{B_m} \hat{\sigma}_{ij}\xi_k dV \tag{52}$$

if (32) and (43) are taken into account. The components of ${}^6\check{\boldsymbol{D}}$ are given in Table 2. For the case of plane stress, the basic coefficients a_1 and a_2 of this tensor are defined by

$$a_1 \;=\; \frac{g_1^2}{\kappa_1}\,,\; a_3 = \frac{g_2^2}{\kappa_2} \tag{53}$$

As the void volume fraction f diminishes, the coefficients a_1 and a_2 achieve the limits

$$\lim_{f\to 0} a_1 \;=\; \frac{ER^2}{16(3-\nu)} \tag{54}$$

$$\lim_{f\to 0} a_3 \;=\; \frac{ER^2}{16(1+\nu)}\,. \tag{55}$$

The normalized coefficients of ${}^4\bar{\boldsymbol{C}}$ are plotted together with the normalized coefficients a_1 and a_2 in Figure 2. In order to obtain the corresponding coefficients for plane strain, E and ν must be replaced by $E/(1-\nu^2)$ and $\nu/(1-\nu)$, respectively. From the material tensor ${}^6\check{\boldsymbol{D}}$ given in Table 2 and (47) it can be seen that the couple stresses obey the condition

$$\check{M}_{ijj} = 0_i\,. \tag{56}$$

It follows from (56) that rigid body motions are excluded from the constitutive equations. For a more detailed discussion on this topic the reader is referred to [14].

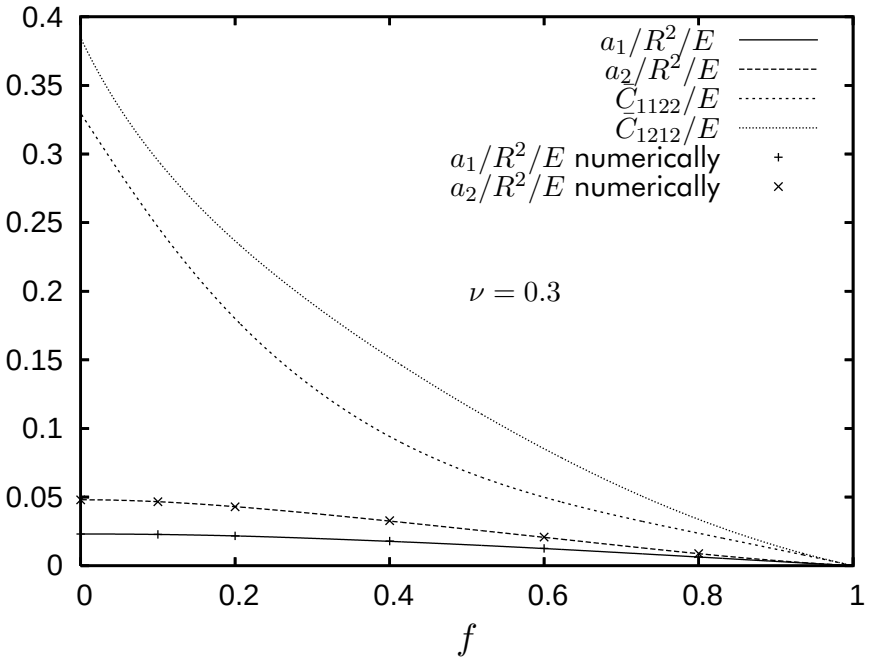

Fig. 2: Normalized material coefficients related to ${}^4\bar{\boldsymbol{C}}$ and normalized coefficients a_1, a_2 plotted as functions of the void volume fraction f for $\nu = 0.3$.

2.4. Strength criterion

The maximum hoop stress at the void, $\sigma_{\varphi\varphi}^{\max}(r=a)$ may serve as a possible strength criterion. If the macroscopic strains $\boldsymbol{E}$ and the strain gradients ${}^3\check{\boldsymbol{H}}$ are known, the hoop stress at $r=a$ is given by

$$\sigma_{\varphi\varphi}(r=a,\varphi) \;=\; \bar{\sigma}_{\varphi\varphi}(r=a,\varphi) + \left[\sum_{s=1}^{4} \tilde{\sigma}_{\varphi\varphi}^{(s)}(r=a,\varphi)\frac{1}{\kappa_s} m_{ijk}^{(s)}\right] \check{H}_{ijk}\,, \tag{57}$$

where (32) and (40) are taken into account. The κ_s are given by (35) and (36), whereat $\kappa_2 = \kappa_1$ and $\kappa_4 = \kappa_3$ hold. The hoop stress from the theory of simple materials reads

$$\begin{aligned}\bar{\sigma}_{\varphi\varphi}(r=a,\varphi) = k_{A_0}(E_{11}+E_{22}) \;&+\; 2(6k_{B_2}f + k_{A_2})\cos(2\varphi)(E_{11}-E_{22}) \\ &+\; 4(8k_{B_2}f + k_{A_2})\sin(2\varphi)E_{12}\end{aligned} \tag{58}$$

with the coefficients k_{A_0}, k_{A_2} and k_{B_2} given in Appendix C. The stresses $\tilde{\sigma}_{\varphi\varphi}^{(s)}$ are obtained from

$$\tilde{\sigma}_{\varphi\varphi}^{(1)}(r=a,\varphi) \;=\; 2R(4\sqrt{f} + \frac{\omega}{\sqrt{f}})\cos(\varphi) \tag{59}$$

$$\tilde{\sigma}_{\varphi\varphi}^{(2)}(r=a,\varphi) \;=\; 2R(4\sqrt{f} + \frac{\omega}{\sqrt{f}})\sin(\varphi) \tag{60}$$

$$\tilde{\sigma}_{\varphi\varphi}^{(3)}(r=a,\varphi) \;=\; 24R\sqrt{f}(2R^2 f + \omega^*)\cos(3\varphi) \tag{61}$$

$$\tilde{\sigma}_{\varphi\varphi}^{(4)}(r=a,\varphi) \;=\; 24R\sqrt{f}(2R^2 f + \omega^*)\sin(3\varphi)\,. \tag{62}$$

It has been checked that

$$\lim_{f\to 0} \tilde{\sigma}^{(s)}_{\varphi\varphi} \frac{1}{\kappa_s} m^{(s)}_{ijk} = 0 \tag{63}$$

holds, which means that the hoop stress $\hat{\sigma}_{\varphi\varphi}(r=a,\varphi)$ vanishes as f tends to zero. The angle $\varphi = \varphi^*$ were the hoop stress reaches its maximum value depends on ${}^3\check{\boldsymbol{H}}$ via (57) and has to be determined numerically at a macroscopic point $\boldsymbol{X}$ by solving the corresponding extrem value problem. A failure criterion can be formulated assuming that failure at a macroscopic point occurs if the condition

$$\sigma^{\max}_{\varphi\varphi}(r=a) = \sigma_{\varphi\varphi}(r=a,\varphi^*) \geq \sigma_c \tag{64}$$

is fulfilled, where the material parameter σ_c has to be identified by experiments. Such a failure criterion which is able to predict size effects due to the presence of the microstructural length R can be applied to strength analysis of components made of porous ceramics or aircrete. This will be the objective of future work.

2.5. Alternative representation

In order to simplify the numerical implementation it is useful to express the internal strain energy by means of the second displacement gradients instead of the strain gradients. Different representations of the internal strain energy density were already discussed by Mindlin [19] for the case of an isotropic linear elastic material. However, due to the geometry of the RVE, ${}^6\check{\boldsymbol{D}}$ is only transversely isotropic (see Figure 1) and the results given in [19] do not apply here. Following the general idea outlined in [19], we define the third order tensor ${}^3\boldsymbol{H}$

$$H_{ijk} := U_{k,ij} \tag{65}$$

and a material tensor ${}^6\boldsymbol{D}$ demanding that

$$D_{ijklmn} H_{ijk} H_{lmn} = \check{D}_{ijklmn} \check{H}_{ijk} \check{H}_{lmn} \,. \tag{66}$$

Furthermore,

$$M_{ijk} = \frac{\partial \hat{W}}{\partial H_{ijk}} = M_{jik} \tag{67}$$

must hold because of the symmetry properties of ${}^3\boldsymbol{H}$, with $\hat{W} = {}^3\boldsymbol{H} \vdots {}^6\boldsymbol{D} \vdots {}^3\boldsymbol{H}$. It can be shown that ${}^6\boldsymbol{D}$ given by

$$D_{ijklmn} = \frac{1}{4}\left[\check{D}_{jkimnl} + \check{D}_{jkinlm} + \check{D}_{kijmnl} + \check{D}_{kijnlm}\right] \tag{68}$$

fulfills the requirements discussed above and the components of ${}^6\boldsymbol{D}$ are given in Table 3.

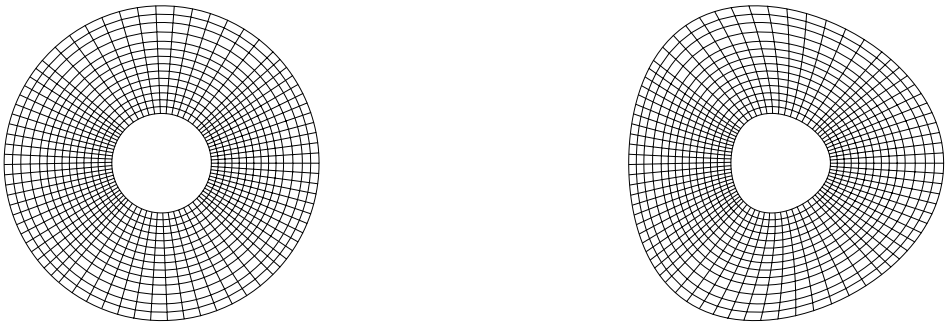

Fig. 3: Undeformed mesh of the RVE used for the validation of the model together with an example of a deformed mesh.

3. Numerical studies

3.1. Numerical validation of the model

In order to validate the model, the response of the RVE has been simulated using finite-element calculations and the coefficients a_1 and a_2 were determined numerically for $f = 0, 0.1, 0.2, 0.4, 0.6$ and $f = 0.8$. The boundary displacements were prescribed according to (23) and the higher order stresses were calculated by means of (52). The undeformed finite element mesh for $f = 0.2$ is shown in Figure 3 together with the deformed mesh which corresponds to the case where only $\check{H}_{111}$ differs from zero. The numerically determined coefficients are depicted together with the analytical solution for $\nu = 0.3$ in Figure 2. The analytical solution is in excellent accordance with the numerical results.

3.2. Stress concentration at a hole

In the following, the macroscopic boundary value problem of a stress concentration at a cylindrical hole in an infinite plane subjected to uni-axial remote tension σ_0 is investigated. Plane strain conditions are assumed and a quadratic domain of length $L = 20\rho$ is considered. Since L is large compared to ρ, the solution will be sufficiently close to that of an infinite domain. Owing to symmetry only a quarter of the problem had to be modeled. Following [21], strain gradient elasticity was implemented into the commercial finite-element program Abaqus [1] for plane strain conditions. The implementation is described comprehensively in [23].

Finite element calculations were performed using the strain gradient elasticity model derived within the previous section. The finite element mesh is shown in Figure 5. The stress concentration factor T is defined by the maximum hoop stress divided by the remote stress

$$T = \frac{\Sigma_{11}(X_1 = 0, X_2 = \rho)}{\sigma_0} \,. \tag{69}$$

The values of T predicted by the strain gradient model are shown in Figure 4 whereat

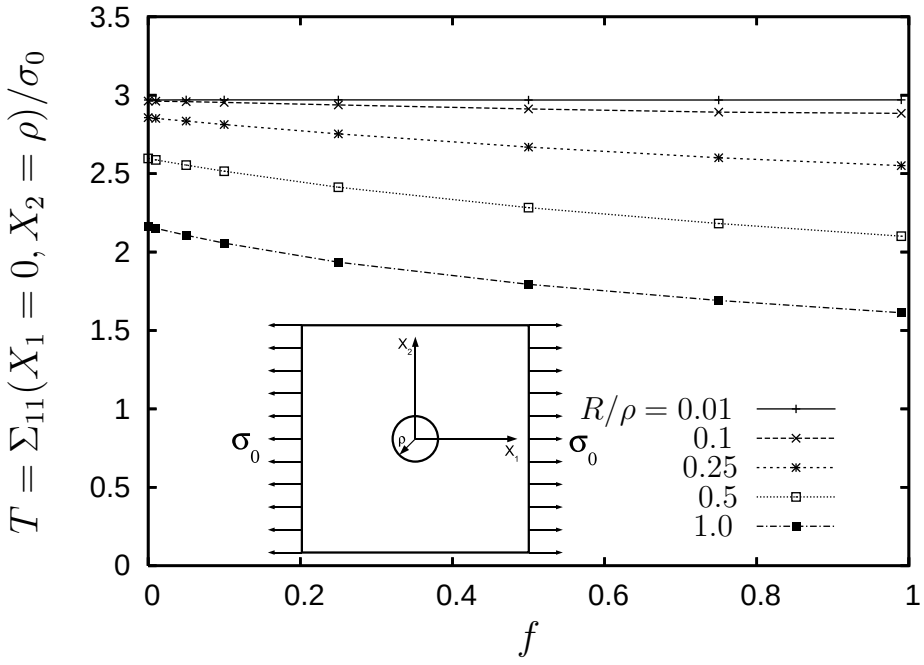

Fig. 4: Stress concentration at a hole under uni-axial tension.

the ratio R/ρ and the specific void volume fraction f have been varied. As R/ρ tends to zero, T matches the classical solution with $T = 3$. For finite values R/ρ however, the strain gradient model predicts a size effect manifested by a stress concentration always lower than three.

The problem of stress concentration was solved analytically for isotropic strain gradient elasticity by Eshel and Rosenfield [10]. Due to the general representation of isotropic tensors of sixth order and additional symmetry properties, the higher order constitutive behavior of an isotropic strain gradient solid is completely characterized by five independent material parameters. These parameters do not have a clear micro-mechanical interpretation in terms of void spacing or grain size, etc. Because of the anisotropy included in present the model, the predictions are not exactly comparable. But our results are qualitatively in accordance with those obtained in [10]. Furthermore, the predictions of our model are reasonable for certain combinations of R/ρ and f. However, the model predicts an unreasonable large size effect also for $R/\rho = 1$ and very small void volume fractions f. These parameters correspond to micro-structures with very small voids far away from each other and one would expect a result closer to the theory of simple materials.

Furthermore, zero void volume fraction implies in any case classical linear elasticity but the higher order material parameters take a finite value which prevents the higher order terms from vanishing as long as macroscopic strain gradients appear. However, the result is formally correct and can be explained by the fact that if a RVE with radius R is subjected to higher order boundary displacements then higher order stresses must emerge even if there is no void at all. Of course, for $f = 0$ the limit process $R \to 0$ can be performed from which classical elasticity would result but this case

is not a priori included in the model which is a quite unsatisfactory circumstance. Because of the explicit meaning of the micro-structural parameters R and f, these problems arise. It is to be expected that they reflect a more general difficulty of models obtained by higher order homogenization techniques. For example, a closer look at the ductile damage model derived in [14] reveals that this model suffers from the same problems. On the other hand, the strain gradient elasticity model obtained by Drugan and Willis [8] using statistical mechanics in conjunction with homogenization based on eigenstrains approaches classical elasticity if the void volume fraction tends to zero. Furthermore, increasing stress concentration has been predicted by Cowin [6] by means of a different approach, whereas strain gradient elasticity predicts in the most cases lower stress concentrations. In addition, couple stress elasticity which can be interpreted as a special case of the strain gradient theory always predicts stress concentrations lower or equal to three [17]. Therefore, it is not clear whether strain gradient elasticity is able to predict the actual stress concentration at a hole. Numerical simulations taking into account the corresponding micro-structure could help to enlighten this problem by contrasting the results with the predictions obtained by using strain gradient elasticity.

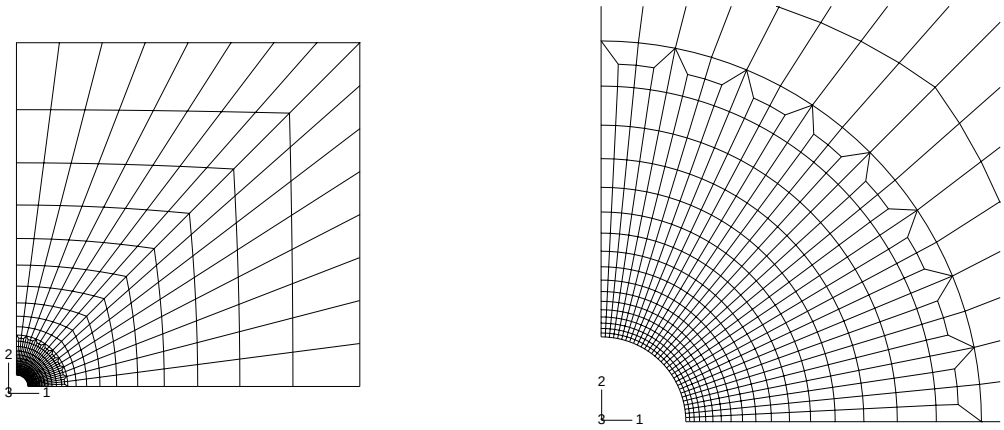

Fig. 5: Finite-element mesh used for the stress concentration problem.

4. Summary and Outlook

Based on the concept of the representative volume element (RVE) higher order homogenization was performed for materials, whose micro-structure consists of cylindrical voids surrounded by a linear elastic matrix material. Effective constitutive equations were derived analytically within the framework of plain strain gradient elasticity. Furthermore, a simple failure criterion for porous brittle materials has been developed which is able to predict size effects. The method developed here is based on Fourier-Series approximation. It can be applied to more complex micro-structures, e.g. voids with elliptic cross section, inclusions, etc.

The predicted stress concentrations due to a hole in an infinite domain subjected to uniaxial tension indicate some general problems of strain gradient models obtained

by higher order homogenization. These problems become obvious due to the explicit meaning of the micro-structural parameters.

The solution strategy applied here is limited to two dimensional problems. The derived constitutive equations are based on simplifications with respect to the geometry of the RVE and the character of the macroscopic strain gradients. The model can be used for strength analysis and also for the validation of numerical homogenization schemes.

References

[1] ABAQUS. *Version 6.6 Documentation*. Hibbit, Karlsson and Sorensen (HKS) Inc., Pawtuchek, 2005.

[2] E. Amanatidou and N. Aravas. Mixed finite element formulations of strain-gradient elasticity problems. *Computer Methods in Applied Mechanics and Engineering*, 191:1723–1751, 2002.

[3] E. Amanatidou, A. Giannakopoulos, and N. Aravas. Finite element models of strain-gradient elasticity: accuracy and error estimates. In *5th GRACM International Congress on Computational Mechanics*, Limassol, 2005.

[4] Z.P. Bazant and M. Jirasek. Nonlocal integral formulations of plasticity and damage: Survey of progress. *Journal of Engineering Mechanics*, 128(11):1119–1149, 2002.

[5] J. Betten. *Tensorrechnung für Ingenieure*. Teubner, Stuttgart, 1987.

[6] S.C. Cowin. The stresses around a hole in a linear elastic material with voids. *The Quarterly Journal of Mechanics and Applied Mathematics*, 37(3):441–465, 1984.

[7] R. De Borst, L.J. Sluys, H.-B. Mühlhaus, and J. Pamin. Fundamental issues in finite element analysis of localization of deformation. *Engineering Computations*, 10:99–121, 1993.

[8] W.J. Drugan and J.R. Willis. A micromechanics-based nonlocal constitutive equation and estimates of representative volume element size for elastic composites. *Journal of the Mechanics and Physics of Solids*, 44(4):497–524, 1996.

[9] R.A.B. Engelen, N.A. Fleck, R.H.J. Peerlings, and M.G.D. Geers. An evaluation of higher-order plasticity theories for predicting size-effects and localisation. *International Journal of Solids and Structures*, 43:1857–1877, 2006.

[10] N.N. Eshel and G. Rosenfield. Effects of strain-gradient on the stress-concentration at a cylindrical hole in a field of uniaxial tension. *Journal of Engineering Mathematics*, 4(2):97–111, 1970.

[11] N. A. Fleck and J. W. Hutchinson. Strain gradient plasticity. *Advances in Applied Mechanics*, 33:295–361, 1997.

[12] N.A. Fleck and J.W. Hutchinson. A reformulation of strain gradient plasticity. *Journal of the Mechanics and Physics of Solids*, 49:2245–2271, 2001.

[13] S. Forest. Homogenization methods and the mechanics of generalized continua. In G. Maugin, editor, *Geometry, Continua and Microstructure*, pages 35–48. Hermann, Paris, 1999.

[14] M. Gologanu, J.B. Leblond, G. Perrin, and J. Devaux. Recent extensions of Gurson's model for porous ductile metals. *Springer-Verlag Cism Courses And Lectures: International Centre For Mechanical Sciences Series*, pages 61–130, 1997.

[15] V. Kouznetsova, M.G.D. Geers, and W.A.M. Brekelmans. Multi-scale constitutive modelling of heterogeneous materials with a gradient-enhanced computational homogenization scheme. *International Journal for Numerical Methods in Engineering*, 54:1235–1260, 2002.

[16] S. Kruch and S. Forest. Computation of coarse grain structures using a homogeneous equivalent medium. *Journal de physique. IV*, 8(8):197–205, 1998.

[17] R. D. Mindlin. Influence of couple stresses on stress concentrations. *Experimental Mechanics*, 3:1–7, 1963.

[18] R. D. Mindlin. Micro-structure in linear elasticity. *Archive for Rational Mechanics and Analysis*, 16:51–78, 1964.

[19] R. D. Mindlin and N. N. Eshel. On first strain-gradient theories in linear elasticity. *International Journal of Solids and Structures*, 4(1):109–124, 1968.

[20] S. Nemat-Nasser and M. Hori. *Micromechanics: Overall Properties of Heterogeneous Materials*. Elsevier, Amsterdam, 1993.

[21] J. Y. Shu, W. E. King, and N. A. Fleck. Finite elements for materials with strain gradient effects. *International Journal for Numerical Methods in Engineering*, 44:373–391, 1999.

[22] S. P. Timoshenko and J. N. Goodier. *Theory of Elasticity*. McGraw-Hill, New York, 1970.

[23] L. Zybell. Implementation of a User-Element considering strain gradient effects into the FE-program Abaqus. Master's thesis, TU-Bergakademie Freiberg, 2007.

Appendix

A. Calculation of ω in equations (27), (28)

The boundary displacements $\hat{\boldsymbol{u}}|_{\partial B}$ which result from (20) can be formally written as

$$\begin{aligned}\hat{\boldsymbol{u}}|_{\partial B} \;=\;& B_1\tilde{\boldsymbol{u}}^{(B_1)}|_{\partial B} + b_1\tilde{\boldsymbol{u}}^{(b_1)}|_{\partial B} + D_1\tilde{\boldsymbol{u}}^{(D_1)}|_{\partial B} + d_1\tilde{\boldsymbol{u}}^{(d_1)}|_{\partial B} \\ &+ \sum_{n=3}^{\infty}\left[B_n\tilde{\boldsymbol{u}}^{(B_n)}|_{\partial B} + b_n\tilde{\boldsymbol{u}}^{(b_n)}|_{\partial B} + D_n\tilde{\boldsymbol{u}}^{(D_n)}|_{\partial B} + d_n\tilde{\boldsymbol{u}}^{(d_n)}|_{\partial B}\right]. \qquad \text{(A.1)}\end{aligned}$$

Taking into account (A.1), multiplying both sides of (23) with the surface tractions $\tilde{\boldsymbol{t}}^{(B_1)}|_{\partial B}$ and executing the integration with respect to the outer surface of the volume element finally gives

$$B_1\breve{\kappa}_{11} + b_1\breve{\kappa}_{12} = \frac{1}{2}K_{ijk}\breve{m}_{ijk}^{(B_1)} \qquad \text{(A.2)}$$

after dividing by the total volume of the volume element B. The simple structure of (A.2) results from the orthogonality relations of the trigonometric functions. Performing the same calculation using $\tilde{\boldsymbol{t}}^{(b_1)}|_{\partial B}$, $\tilde{\boldsymbol{t}}^{(D_1)}|_{\partial B}$, and $\tilde{\boldsymbol{t}}^{(d_1)}|_{\partial B}$, respectively, instead of $\tilde{\boldsymbol{t}}^{(B_1)}|_{\partial B}$ leads to

$$\begin{aligned} B_1\breve{\kappa}_{12} + b_1\breve{\kappa}_{22} &= \frac{1}{2}K_{ijk}\breve{m}_{ijk}^{(b_1)} && \text{(A.3)}\\ D_1\breve{\kappa}_{11} + d_1\breve{\kappa}_{12} &= \frac{1}{2}K_{ijk}\breve{m}_{ijk}^{(D_1)} && \text{(A.4)}\\ D_1\breve{\kappa}_{12} + d_1\breve{\kappa}_{22} &= \frac{1}{2}K_{ijk}\breve{m}_{ijk}^{(d_1)}, && \text{(A.5)}\end{aligned}$$

where the coefficients $\breve{\kappa}_{11}$, $\breve{\kappa}_{12}$, $\breve{\kappa}_{22}$ are given by

$$\begin{aligned} \breve{\kappa}_{11} &= R^2\frac{4}{E}\left[(3-\nu) - 2f^2(1-\nu) - (1+\nu)f^4\right] && \text{(A.6)}\\ \breve{\kappa}_{22} &= -\frac{1}{R^2}\frac{1}{E}\left[2\ln(f) + (1+\nu)(1+f)^2\right] && \text{(A.7)}\\ \breve{\kappa}_{12} &= \frac{2}{E}\left[(3-\nu)(1-f) - (1-\nu)f^2 - (1+\nu)f^3\right]. && \text{(A.8)}\end{aligned}$$

The components of the third order tensor ${}^3\breve{\boldsymbol{m}}^{(B_1)}$ are calculated by means of

$$\breve{m}_{ijk}^{(B_1)} = \frac{1}{B}\int_B \xi_k\tilde{\sigma}_{ij}^{(B_1)}dV \qquad \text{(A.9)}$$

and the components of the other tensors ${}^3\breve{\boldsymbol{m}}^{(b_1)}$, ${}^3\breve{\boldsymbol{m}}^{(D_1)}$, ${}^3\breve{\boldsymbol{m}}^{(d_1)}$ are computed analogously using the corresponding stress fields. The results given in matrix form in Table 4 reveal that the right hand sides of the equations (A.2) and (A.3) differ only by the factors G_1 and G_2

$$\begin{aligned} G_1 &= \frac{R^2}{2}(1-f^2) && \text{(A.10)}\\ G_2 &= \frac{1}{4}(1-f). && \text{(A.11)}\end{aligned}$$

The same argumentation applies for the equations (A.4) and (A.5) and therefore,

$$b_1 = \omega B_1 \tag{A.12}$$
$$d_1 = \omega D_1 \tag{A.13}$$

with

$$\omega = \frac{G_1 \breve{\kappa}_{12} - G_2 \breve{\kappa}_{11}}{G_2 \breve{\kappa}_{12} - G_1 \breve{\kappa}_{22}} \,. \tag{A.14}$$

$\breve{m}^{(B_1)}_{ijk}$	ij = 11	22	12	$\breve{m}^{(b_1)}_{ijk}$	ij = 11	22	12
k = 1	G_1	$3G_1$	0	k = 1	G_2	$3G_2$	0
2	0	0	-G_1	2	0	0	-G_2
$\breve{m}^{(D_1)}_{ijk}$	ij = 11	22	12	$\breve{m}^{(d_1)}_{ijk}$	ij = 11	22	12
k = 1	0	0	$-G_1$	k = 1	0	0	$-G_1$
2	$3G_1$	G_1	0	2	$3G_1$	G_1	0

Tab. 4: Components of the third order tensors ${}^3\breve{\boldsymbol{m}}^{(B_1)}$, ${}^3\breve{\boldsymbol{m}}^{(b_1)}$, ${}^3\breve{\boldsymbol{m}}^{(D_1)}$, ${}^3\breve{\boldsymbol{m}}^{(d_1)}$.

B. Result for ω^* in equations (29), (30)

Similar calculation can be performed with respect to the coefficients b_n, B_n and d_n and D_n. Furthermore, it turns out that the higher order stresses ${}^3\breve{\boldsymbol{m}}^{(B_n)}$, ${}^3\breve{\boldsymbol{m}}^{(b_n)}$, ${}^3\breve{\boldsymbol{m}}^{(D_n)}$ and ${}^3\breve{\boldsymbol{m}}^{(d_n)}$ vanish for $n > 3$ from which follows that the corresponding coefficients vanish, too. The result for $n = 3$ reads

$$b_3 = \omega^* B_3 \tag{B.1}$$
$$d_3 = \omega^* D_3 \tag{B.2}$$

with

$$\omega_3^* = \frac{G_1^* \kappa_{12}^* - G_2^* \kappa_{11}^*}{G_2^* \kappa_{12}^* - G_1^* \kappa_{22}^*} \,. \tag{B.3}$$

The coefficients G_1^* and G_2^* are given by

$$G_1^* = 2R^4(1 - f^3) \tag{B.4}$$
$$G_2^* = \frac{3}{2} R^2 (1 - f^2) \,. \tag{B.5}$$

Finally, the coefficients κ_{11}^*, κ_{22}^* and κ_{12}^* result in

$$\kappa_{11}^* = 8\frac{R^6}{E}\left[9(1+\nu)(16f^7 - 9f^8) + (11+7\nu)(1-8f^6) + 2(1-\nu)(16f^3 - 9f^4)\right] \tag{B.6}$$

$$\kappa_{22}^* = 36\frac{R^2}{E}\left[(1+\nu)(1+16f^5-8f^6) - (11+7\nu)f^4 + 2(1-\nu)f^2\right] \tag{B.7}$$

$$\kappa_{12}^* = 48\frac{R^4}{E}\left[(1+\nu)(1+17f^6-9f^7) + 2(1-\nu)f^2 - (11+7\nu)f^5\right] \,. \tag{B.8}$$

C. Effective elasticity matrix ${}^4\bar{C}$

The macroscopic stresses are given by

$$\Sigma_{11} = \bar{C}_{1111}E_{11} + \bar{C}_{1122}E_{22} \quad \text{(C.1)}$$
$$\Sigma_{22} = \bar{C}_{2211}E_{11} + \bar{C}_{2222}E_{22} \quad \text{(C.2)}$$
$$\Sigma_{12} = 2\bar{C}_{1212}E_{12} \quad \text{(C.3)}$$

with

$$\bar{C}_{1111} = +\frac{1}{2}(1-f)\left[(k_{A_0} - k_{A_2} - 3k_{B_2}(1+f)\right] = \bar{C}_{2222} \quad \text{(C.4)}$$
$$\bar{C}_{1122} = +\frac{1}{2}(1-f)\left[(k_{A_0} + k_{A_2} + 3k_{B_2}(1+f)\right] = \bar{C}_{2211} \quad \text{(C.5)}$$
$$\bar{C}_{1212} = -\frac{1}{2}(1-f)\left[k_{A_2} + 3k_{B_2}(1+f)\right] . \quad \text{(C.6)}$$

For the case of plane stress, the coefficients k_{A_0}, k_{A_2}, k_{B_2} and g_{11} read

$$k_{A_0} = \frac{E}{1-\nu+f(1+\nu)} \quad \text{(C.7)}$$
$$k_{A_2} = \frac{E}{g_{11}}\left[(1+\nu)(4f^3-3f^2)+3-\nu\right] \quad \text{(C.8)}$$
$$k_{B_2} = \frac{E}{g_{11}}f(1-f)(1+\nu) \quad \text{(C.9)}$$
$$g_{11} = (\nu^2-2\nu-3)(1+f^4)+2(1+\nu)^2(3f^2-2f^3)-4f(\nu^2+3)\,. \quad \text{(C.10)}$$

D. Useful identities

In the following, some useful identities needed for the calculation of the A_k (40) are given.

$$\int_{\partial B} x_k \tilde{t}_i^{(s)} dA = \int_{\partial B} x_k \tilde{\sigma}_{ip}^{(s)} n_p dA = \int_B (x_k \tilde{\sigma}_{ip}^{(s)})_{,p} dV = \int_B \tilde{\sigma}_{ik}^{(s)} dV = \tilde{\Sigma}_{ik}^{s} = 0_{ik} \quad \text{(D.1)}$$

$$\int_{\partial B} x_j x_k \tilde{t}_i^{(s)} dA = \int_{\partial B} x_j x_k \tilde{\sigma}_{ip}^{(s)} n_p dA = \int_B (x_j x_k \tilde{\sigma}_{ip}^{(s)})_{,p} dV = \int_B x_k \tilde{\sigma}_{ij}^{(s)} dV + \int_B x_j \tilde{\sigma}_{ik}^{(s)} dV \quad \text{(D.2)}$$

Micromechanical modelling of size effects in failure of porous elastic solids using first order plane strain gradient elasticity. In: *Computational Materials Science* 46(3):647-653

Micromechanical modelling of size effects in failure of porous elastic solids using first order plane strain gradient elasticity

Uwe Mühlich Lutz Zybell Meinhard Kuna

In this paper a first order porous strain gradient elasticity model is presented. The constitutive equations have been obtained by higher order homogenization and the model is used with a failure criterion in order to discuss size effects in failure of porous elastic solids. The model contains two microstructural parameters namely the void volume fraction and the half void spacing. After an extended numerical validation of the porous strain gradient elasticity model, the boundary value problem of a plate with a hole under bi- and uniaxial remote tension is investigated. The numerical simulations have been performed varying both microstructural parameters in order to study the influence of different microstructural dimensions on the onset of macroscopic failure. The numerical results show that the presented model is able to predict size effects and that size effects in failure do not only depend on the microstructural properties but also on the macroscopic geometry, loading conditions, and the failure mechanism.

1. Introduction

Size effects have been reported in failure of parts made of porous elastic material as e.g. porous concrete [1, 2] and various porous ceramics [3, 4]. Within this paper, the size effect is understood as the influence of the ratio between the macroscopic dimensions and the microstructural length properties on the failure strength of a considered part or structural component, provided that geometrically similar parts are

compared. This is a slightly modified version of the definition given in [5] for parts or structures made of brittle or quasi-brittle materials. Microstructural length properties are material properties such as void spacing and grain size. As pointed out e.g. in [6], size effects are in general the result of an interplay of statistical and deterministic effects. However, only deterministic size effects are considered here.

Continuum models formulated within the theory of simple materials are not able to account for these size effects, because the influence of the microstructure on the macroscopic behaviour can only be incorporated by means of specific values like void volume fraction, microcrack density, etc., as extensively discussed in the literature. With respect to the class of materials considered here, this means that the aforementioned models cannot distinguish between a material whose microstructure consists of many small voids surrounded by linear elastic matrix material and another material with less but bigger voids as long as the void volume fraction is the same in both cases. The obvious need to incorporate additional length parameters into the continuum models led to an increasing interest in so-called higher order continuum theories over the past decades. Here, we focus on first order strain gradient elasticity developed in [7]. Within this framework, additional parameters which are related somehow to microstructural length properties appear almost naturally due to the incorporation of higher order displacement gradients into the formulation of the macroscopic strain energy density. The major challenge, however, is the determination of these additional parameters. There are homogenization schemes based on higher order boundary conditions for a single representative volume element (RVE) [8, 9] and procedures regarding interaction between RVEs arranged in clusters [10] developed more recently. Here we focus on the first approach, where the constitutive equations do not only fit into the framework of strain gradient elasticity / plasticity, depending on the underlying microstructural behaviour, but also the additional material parameters can be linked transparently to measurable microstructural quantities like the mean spacing of the microvoids. Based on this approach, constitutive equations for plane porous strain gradient elasticity were obtained in [11] and a failure criterion has been formulated, which will be explored in more detail within this paper.

The paper is organized as follows: In the first section the fundamental equations of strain gradient elasticity are reviewed, the higher order homogenization procedure is discussed and two failure criteria based directly on the homogenization are briefly outlined. Next, an extended validation of the analytical model is presented and numerical results of the failure criteria are described in detail. Finally, the numerical results are discussed and an outlook on the porous strain gradient elasticity model is given.

In this paper index notation together with the summation convention is used and capital letters are related to macroscopic variables. Macroscopic and microscopic variables depend on the macroscopic coordinates $\boldsymbol{X}$ and the microscopic coordinates $\boldsymbol{x}$, respectively. The abbreviation $()_{,i}$ indicates the partial derivative of the considered quantity () with respect to the corresponding spatial coordinate and δ_{ij} are the components of the identity tensor.

2. First order porous strain gradient elasticity

2.1. Fundamental equations of strain gradient elasticity

Strain gradient elasticity was first introduced by Mindlin [7] based on an earlier work of Toupin [12]. He extended the strain energy density W, which depends in the case of linear elasticity only on the strains E_{ij}, by the strain gradients $\breve{H}_{ijk}$. There exist two other possibilities to express W resulting in equivalent formulations, what is briefly outlined in [13].

Based on the extended strain energy density the following set of equations holds for the variables on the macrolevel $\boldsymbol{X}$:

Equilibrium equation:

$$\left(\Sigma_{ij} - \breve{M}_{kij,k}\right)_{,j} = 0_i \tag{1}$$

Kinematic relations:

$$E_{ij} = \frac{1}{2}\left[U_{i,j} + U_{j,i}\right] \ , \quad \breve{H}_{ijk} = E_{ij,k} \tag{2}$$

Constitutive relations:

$$\Sigma_{ij} = \bar{C}_{ijkl} E_{kl} \ , \quad \breve{M}_{ijk} = \breve{D}_{ijklmn} \breve{H}_{lmn} \ . \tag{3}$$

In (2) U_i are the components of the displacement vector. The macroscopic stress tensor $\boldsymbol{\Sigma}$ and the higher order stress tensor $\breve{\boldsymbol{M}}$ are related to their work conjugate kinematic variables, namely the strain tensor $\boldsymbol{E}$ and the strain gradient tensor $\breve{\boldsymbol{H}}$, by the fourth and sixth order material tensors $\bar{\boldsymbol{C}}$ and $\breve{\boldsymbol{D}}$, respectively.

The boundary value problem at the macrolevel is completely defined, if in addition to (1)–(3) the following natural boundary conditions related to the surface tractions T_i and the higher order surface tractions R_i are taken into account

$$T_i = N_j(\Sigma_{ij} - \breve{M}_{kji,k}) - D_j(N_k \breve{M}_{kji}) + (D_p N_p) N_j N_k \breve{M}_{kji} = T_i^* \qquad \boldsymbol{X} \in \partial B_{\mathrm{T}} \tag{4}$$

$$R_i = N_k N_j \breve{M}_{kji} = R_i^* \qquad \boldsymbol{X} \in \partial B_{\mathrm{R}} \tag{5}$$

as well as the essential boundary conditions

$$U_i = U_i^* \qquad \boldsymbol{X} \in \partial B_U \tag{6}$$

$$N_p U_{i,p} = V_i^* \qquad \boldsymbol{X} \in \partial B_V \ . \tag{7}$$

In (4)–(7) N_i are the components of the unit normal vector,

$$D_j(.) = (\delta_{jp} - N_p N_j)(.)_{,p} \tag{8}$$

are the components of the surface gradient and variables marked with an asterisk (*) indicate prescribed values. In order to apply strain gradient elasticity to real problems the main difficulties arise from the determination of the material parameters included in (3). Since the determination of all these material parameters implies considerable effort we used higher order homogenization to derive the constitutive relations.

The strain gradient elasticity model was implemented as a User Element (UEL) in the commercial finite element software Abaqus [14]. We used a mixed-type formulation by Shu et. al [15] based on the second gradients of the displacements. Details of the implementation are given in [16].

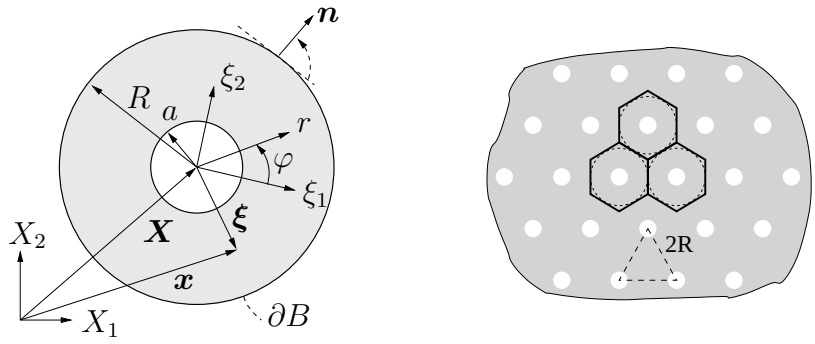

Fig. 1: Cylindrical volume element (VE) containing a cylindrical void used for the homogenization and macroscopic interpretation of a periodic assembly of VEs

2.2. Constitutive relations obtained by higher order homogenization

The homogenization was performed using a cylindrical volume element (VE) consisting of a cylindrical void surrounded by linear elastic matrix material as shown on the left of Fig. 1.

We assume that the VE represents the main features of the microstructure. In the context of random media the overall behaviour of the VE depends on its size as well as on the boundary data and it can no longer be interpreted as representative in a statistical sense. Therefore, the VE might be seen as a volume which does not capture all statistical information of the microstructure. In the context of materials with periodic microstructure one may still interpret the VE as the unit cell defining the geometry of the microstructure. Thus, regarding the cylindrical VEs as idealized honeycombs results in a periodic assembly of VEs on the macrolevel which is depicted on the right of Fig. 1.

We distinguish between macroscopic coordinates $\boldsymbol{X}$ and microscopic coordinate $\boldsymbol{x}$, whose meanings are shown on the left of Fig. 1. Following the general idea of homogenization, we assume that every macroscopic point $\boldsymbol{X}$ is related to a corresponding VE. Plane stress and plane strain conditions are assumed and quadratic boundary displacements according to Gologanu et. al [8] which are related to the macroscopic strains and strain gradients are prescribed on the outer boundary of the VE

$$u_i|_{\partial B} = E_{ij}x_j + \frac{1}{2}K_{ijk}x_jx_k - \frac{1}{2}[K_{ijk} - K_{jki}]X_kx_j \tag{9}$$

with

$$K_{ijk} = \breve{H}_{ijk} + \breve{H}_{kij} - \breve{H}_{jki}\,. \tag{10}$$

Due to considerable gradients in the macroscopic fields, the microscopic stresses and strains are no longer periodic and the quadratic terms in (9) reflect the deviation of the microscopic fields from periodicity.

At the inner boundary of the VE zero tractions are prescribed. The macroscopic stresses and higher order stresses are defined as mean values with respect to the

corresponding microscopic fields

$$\Sigma_{ij} = \frac{1}{B}\int_B \sigma_{ij}\, dV \tag{11}$$

$$\breve{M}_{ijk} = \frac{1}{B}\int_B \sigma_{ij}(x_k - X_k)\, dV \tag{12}$$

and solving the boundary value problem for the VE leads to the material tensors $\bar{\boldsymbol{C}}$ and $\bar{\boldsymbol{D}}$. The solution has been derived analytically and detailed information is given in [11]. The material tensor $\bar{\boldsymbol{C}}$ depends on the void volume fraction $f = a^2/R^2$ and the properties of the matrix material, whereas the material tensor $\bar{\boldsymbol{D}}$ hinges, in addition, on the outer radius R of the VE, where R is interpreted as the half mean spacing between the microvoids. Due to the choice of the VE transverse isotropy is included on the microscale and the material tensor $\bar{\boldsymbol{D}}$ cannot be rewritten in the general isotropic representation by Mindlin [17] containing five independent material parameters.

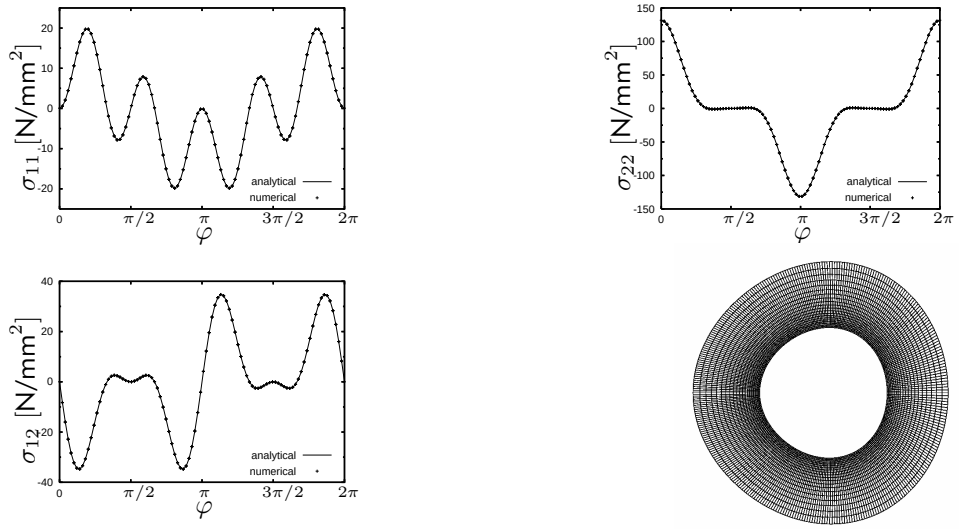

Fig. 2: Numerical validation of the analytical model: Comparison of the stress results σ_{ij} between unit cell calculation and the analytical solution at the inner boundary of the VE and corresponding deformed mesh for case 4

2.3. Discussion of the failure criteria

After solving the boundary value problem at the macrolevel, the macroscopic strains and strain gradients are known for every macroscopic point $\boldsymbol{X}$. Furthermore, the microscopic stress and strain fields inside the corresponding VE are known. In order to obtain a failure criterion, it is postulated that failure occurs if the hoop stress $\sigma_{\varphi\varphi}(r = a, \varphi)$ at the microvoid reaches a critical value σ_{cr}. The hoop stress given in [11] can

be split into

$$\sigma_{\varphi\varphi}(r=a,\varphi) = \left[\sum_{s=1}^{3} \bar{\sigma}^{(s)}_{\varphi\varphi}(r=a,\varphi)\alpha^{(s)}_{ij}\right] E_{ij} + \left[\sum_{s=1}^{4} \tilde{\sigma}^{(s)}_{\varphi\varphi}(r=a,\varphi)\frac{1}{\kappa_s} m^{(s)}_{ijk}\right] \check{H}_{ijk} \quad (13)$$

where the first part with the coefficients

$$\alpha^{(1)}_{ij} = \begin{bmatrix} 1 & 0 \\ 0 & 1 \end{bmatrix}\ ,\ \alpha^{(2)}_{ij} = \begin{bmatrix} 1 & 0 \\ 0 & -1 \end{bmatrix}\ ,\ \alpha^{(3)}_{ij} = \frac{1}{2}\begin{bmatrix} 0 & 1 \\ 1 & 0 \end{bmatrix} \quad (14)$$

is related to theory of simple materials and the second part is related to higher order theory. In order to evaluate the extremum problem (34) more easily equation (13) is rewritten as a truncated Fourier series

$$\sigma_{\varphi\varphi}(r=a,\varphi) = A_0 + \sum_{i=1}^{3} A_i \sin(i\varphi) + B_i \cos(i\varphi) \quad (15)$$

with the coefficients

case	1	2	3	4	5	6	7
E_{11}	0.1	0.1	0	0	0	0	0
E_{22}	0.1	–0.1	0	0	0	0	0
E_{12}	0	0	0.1	0	0	0	0
$\check{H}_{111}$	0	0	0	0.2	0.1	0	0
$\check{H}_{221}$	0	0	0	0.1	0.1	0	0
$\check{H}_{122}$	0	0	0	0.1	0.4	0	0
$\check{H}_{112}$	0	0	0	0	0	0.1	0.1
$\check{H}_{222}$	0	0	0	0	0	0.2	0.1
$\check{H}_{121}$	0	0	0	0	0	0.1	0.4

Tab. 1: Components of strains E_{ij} and strain gradients $\check{H}_{ijk}$ for the seven cases investigated for the numerical validation of the coefficients A_i and B_i in Eq. (15).

$$A_0 = k_{\mathrm{A}_0}(E_{11}+E_{22}) \quad (16)$$

$$A_1 = 2R\left(4\sqrt{f} + \frac{\omega}{R^2}\frac{1}{\sqrt{f}}\right)\frac{1}{\kappa_2} m^{(2)}_{ijk}\check{H}_{ijk} \quad (17)$$

$$B_1 = 2R\left(4\sqrt{f} + \frac{\omega}{R^2}\frac{1}{\sqrt{f}}\right)\frac{1}{\kappa_1} m^{(1)}_{ijk}\check{H}_{ijk} \quad (18)$$

$$A_2 = 4(6k_{\mathrm{B}_2}f + k_{\mathrm{A}_2})E_{12} \quad (19)$$

$$B_2 = 2(6k_{\mathrm{B}_2}f + k_{\mathrm{A}_2})(E_{11}-E_{22}) \quad (20)$$

$$A_3 = 24R^3\sqrt{f}\left(2f + \frac{\omega^*}{R^2}\right)\frac{1}{\kappa_4} m^{(4)}_{ijk}\check{H}_{ijk} \quad (21)$$

$$B_3 = 24R^3\sqrt{f}\left(2f + \frac{\omega^*}{R^2}\right)\frac{1}{\kappa_3} m^{(3)}_{ijk}\check{H}_{ijk}\ . \quad (22)$$

The coefficients k_{A_0}, k_{A_2}, k_{B_2} read

$$k_{\mathrm{A}_0} = \frac{E'}{1-\nu'+f(1+\nu')} \tag{23}$$

$$k_{\mathrm{A}_2} = E'\left[(1+\nu')(4f^3-3f^2)+3-\nu'\right] / g_{11} \tag{24}$$

$$k_{\mathrm{B}_2} = E'\, f\,(1-f)\,(1+\nu') / g_{11} \tag{25}$$

and

$$g_{11} = (\nu'^2-2\nu'-3)(1+f^4)+2(1+\nu')^2(3f^2-2f^3)-4f(\nu'^2+3)\;, \tag{26}$$

where the elastic parameters E' and ν' have to be chosen according to

$$E' = \begin{cases} E \\ E/(1-\nu^2) \end{cases}\;,\quad \nu' = \begin{cases} \nu & \text{plane stress} \\ \nu/(1-\nu) & \text{plane strain} \end{cases}\;. \tag{27}$$

and the calculation of the coefficients κ_k (k=1...4) can be found in Appendix A. Finally, the products $m^{(s)}_{ijk}\check{H}_{ijk}$ read

$$\boldsymbol{m}^{(1)}\vdots\check{\boldsymbol{H}} = g_1\left[\check{H}_{111}+3\,\check{H}_{221}-2\,\check{H}_{122}\right] \tag{28}$$

$$\boldsymbol{m}^{(2)}\vdots\check{\boldsymbol{H}} = g_2\left[3\,\check{H}_{112}+\check{H}_{222}-2\,\check{H}_{121}\right] \tag{29}$$

$$\boldsymbol{m}^{(3)}\vdots\check{\boldsymbol{H}} = g_3\left[-\check{H}_{111}+\check{H}_{221}+2\,\check{H}_{122}\right] \tag{30}$$

$$\boldsymbol{m}^{(4)}\vdots\check{\boldsymbol{H}} = g_4\left[-\check{H}_{112}+\check{H}_{222}-2\,\check{H}_{121}\right] \tag{31}$$

with

$$g_1 = g_2 = G_1+\omega G_2 \tag{32}$$

$$g_3 = g_4 = G_1^*+\omega^* G_2^* \tag{33}$$

and the coefficients G_i and G_i^* from Appendix A. Hence all coefficients within (15) are known.

The assumption that failure occurs if the hoop stress at the inner boundary of the microvoid $\sigma_{\varphi\varphi}(r=a,\varphi)$ reaches a critical value includes actually two failure criteria. Failure by tension occurs if the maximum positive hoop stress $\sigma_{\varphi\varphi}^{\mathsf{max}+}$ reaches a critical value σ_{cr}^{+} and failure by compression takes place if the minimum negative hoop stress $\sigma_{\varphi\varphi}^{\mathsf{max}-}$ becomes smaller than or equal to a critical value σ_{cr}^{-}. Both criteria are used in the following in order to predict the onset of failure of the considered body.

In order to calculate the maximum positive and negative hoop stresses from (13) the extremum problem

$$\frac{\mathrm{d}\sigma_{\varphi\varphi}(a,\varphi)}{\mathrm{d}\varphi} = 0 \tag{34}$$

has to be solved at all integration points. Then the absolute extreme values $\sigma_{\varphi\varphi}^{\mathsf{max}+}$ and $\sigma_{\varphi\varphi}^{\mathsf{max}-}$ have to be found within the structural component in order to be able to evaluate the failure criteria

$$\sigma_{\varphi\varphi}^{\mathsf{max}+} > \sigma_{\mathsf{cr}}^{+}\;,\quad \sigma_{\varphi\varphi}^{\mathsf{max}-} < \sigma_{\mathsf{cr}}^{-}\;. \tag{35}$$

An analytical solution of (34) can be obtained only in a few special cases. Therefore, the problem is solved numerically in general within a postprocessing routine.

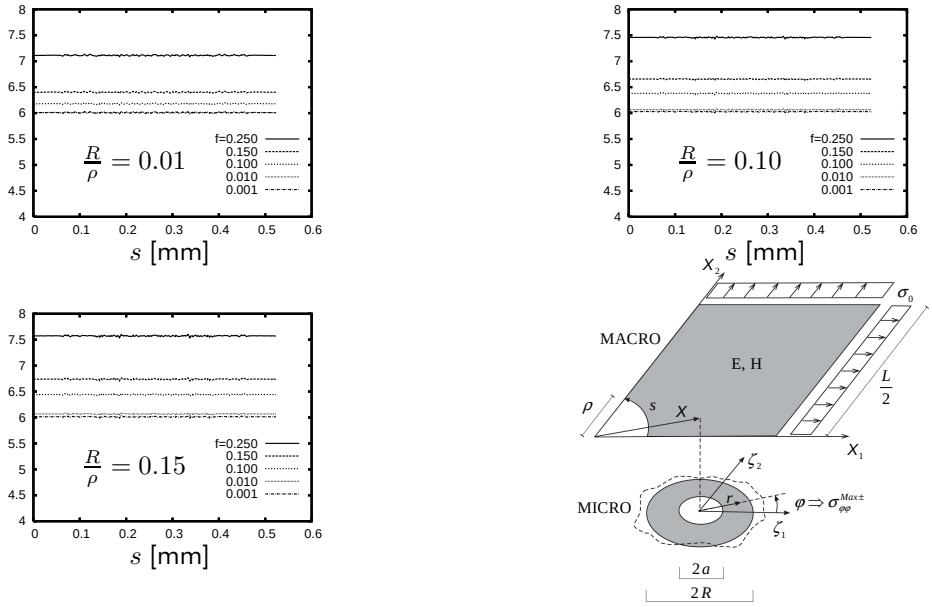

Fig. 3: Failure criterion by tension $\sigma^{\max+}_{\varphi\varphi}/\sigma_0$ along boundary s of a circular hole under biaxial remote tension for different void volume fractions f and ratios R/ρ and geometry of the macroscopic boundary value problem

3. Numerical results

3.1. Extended validation of the constitutive equations

The validation of the model was extended beyond the verification of the coefficients a_1 and a_3 which were already investigated in [11]. In order to check the analytical results, e.g. the definitions of the coefficients in (13), numerical simulations of the cylindrical volume element (VE) containing a void (see Fig. 2 on the bottom right) were performed and the stresses σ_{ij} at the inner boundary were analyzed. The seven cases defined in Table 1 were investigated in order to isolate the effects of the terms related to the A_i and B_i in (13).

The displacements on the outer boundary of the VE were prescribed in terms of the strain gradient $\check{\boldsymbol{H}}$

$$u_1(r=R,\varphi) \;=\; E_{11}x_1 + E_{12}x_2 + \frac{1}{2}\left[\check{H}_{111}x_1x_1 + 2\check{H}_{112}x_1x_2 + (2\check{H}_{122} - \check{H}_{221})x_2x_2\right] \tag{36}$$

$$u_2(r=R,\varphi) \;=\; E_{21}x_1 + E_{22}x_2 + \frac{1}{2}\left[(2\check{H}_{121} - \check{H}_{112})x_1x_1 + 2\check{H}_{221}x_1x_2 + \check{H}_{222}x_2x_2\right]. \tag{37}$$

Investigations of all seven cases unveiled incorrect definitions of the coefficients κ_k in [11]. Finally, all deviations between analytical and numerical solution for the stresses at the inner boundary of the VE could be removed. The comparison between analytical and numerical results is exemplarily depicted for the study case 4 in Fig. 2.

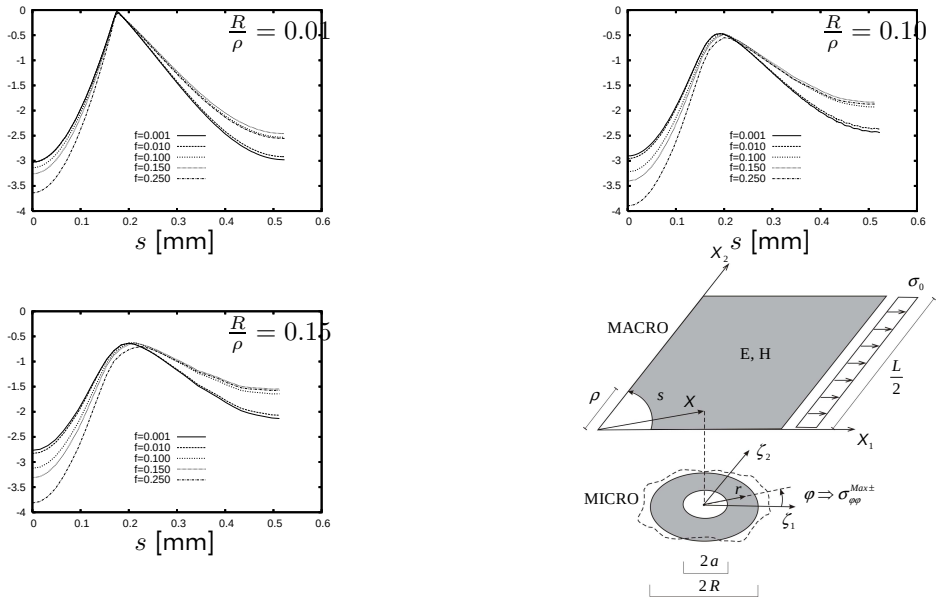

Fig. 4: Failure criterion by compression $\sigma_{\varphi\varphi}^{\max-}/\sigma_0$ along boundary s of a circular hole under uniaxial remote tension with different void volume fractions f and ratios R/ρ and geometry of the macroscopic boundary value problem

3.2. Application of the failure criteria

The failure criteria $\sigma_{\varphi\varphi}^{\max+}$ and $\sigma_{\varphi\varphi}^{\max-}$ proposed in [11] were investigated at a cylindrical hole surrounded by linear elastic strain gradient material under bi- and uniaxial remote tension. Due to symmetry only a quarter of the problem had to be modeled as shown on the bottom right of Fig. 3.

The geometry is given by a quadratic domain of length L containing a macroscopic hole with the constant radius $\rho = L/20$. Plane strain conditions were assumed and the elasticity constants $E = 1000$ MPa and $\nu = 0.3$ were used for all calculations. The microstructure of the material was characterized by the void volume fraction $f = a^2/R^2$ and the half void spacing R. Different microstructures were realized by varying the void volume fraction f between 0.001 and 0.25 and setting the ratio of half void spacing R divided by the radius of the macroscopic hole ρ equal to 0.01, 0.1 and 0.15. For a fixed void volume fraction f this results either in a microstructure with many small voids characterized by small values of R/ρ or in a microstructure with less but bigger voids for large values of R/ρ.

First the cylindrical hole surrounded by linear elastic strain gradient material was loaded in biaxial remote tension. The numerical results of the failure criterion $\sigma_{\varphi\varphi}^{\max+}$ along the boundary s of the macroscopic hole are depicted for the biaxial loading case in Fig. 3. The numerical values of $\sigma_{\varphi\varphi}^{\max+}$ are constant along the boundary s, what is consistent with the analytical solution of Eshel and Rosenfield [18], who showed that for a rotational symmetric problem the solution including higher order terms is independent of the angle. Furthermore, it can be seen that for high porosities f the failure $\sigma_{\varphi\varphi}^{\max+}$ increases as R/ρ grows, whereas there is almost no size effect for low porosities. Therefore, the failure criterion of maximum hoop stress in tension $\sigma_{\varphi\varphi}^{\max+}$

predicts that the onset of failure occurs for higher porosities at lower applied loads if the material has a coarse microstructure (R/ρ large), compared with the case of a dense microstructure (R/ρ small).

Next, the boundary value problem discussed above was investigated in the loading case of uniaxial remote tension, while geometry and material parameters were kept constant. The results of the failure criterion by compression $\sigma_{\varphi\varphi}^{\max-}/\sigma_0$ are shown in Fig. 4. Obviously, the critical stress $\sigma_{\varphi\varphi}^{\max-}$ is no longer constant along the boundary s since the macroscopic problem lost its rotational symmetry. All maximum values of $\sigma_{\varphi\varphi}^{\max-}$ are located at approximately $0.2\,s$ and there is a regularization effect for increasing ratios R/ρ, i.e. the curve of $\sigma_{\varphi\varphi}^{\max-}$ becomes smoother.

The maximum values of the failure criteria by tension $\sigma_{\varphi\varphi}^{\max+}/\sigma_0$ and compression $\sigma_{\varphi\varphi}^{\max-}/\sigma_0$ are compared for all simulations of the biaxial loading case in Fig. 5. Obviously, the results for $\sigma_{\varphi\varphi}^{\max+}$ increase for growing void volume fraction as well as for growing ratios R/ρ, i.e. microstructures with a larger ratio R/ρ fail earlier than microstructures with small R/ρ.

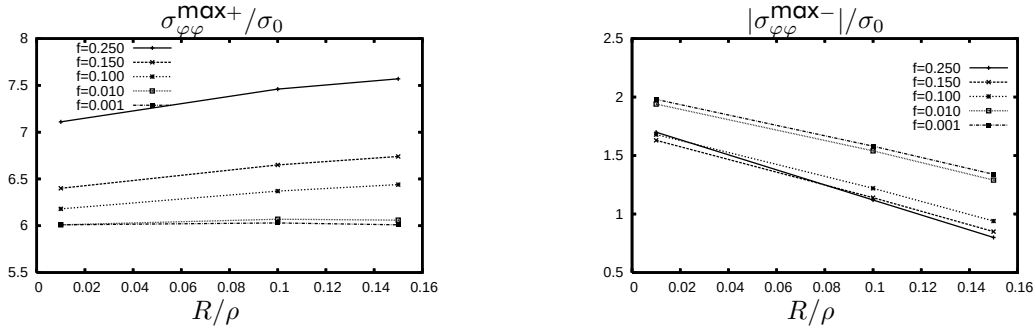

Fig. 5: Failure criterion by tension $\sigma_{\varphi\varphi}^{\max+}/\sigma_0$ and failure criterion by compression $|\sigma_{\varphi\varphi}^{\max-}|/\sigma_0$ for circular hole under biaxial remote tension for all realized variations of void volume fraction f and ratio R/ρ

The numerical results for $\sigma_{\varphi\varphi}^{\max-}$ show a total different behavior by decreasing values for growing ratios R/ρ. Furthermore, for small void volume fraction f combined with negligible ratios R/ρ, the results of $\sigma_{\varphi\varphi}^{\max-}$ are astonishingly larger than for larger values of f. If $R/\rho \to 0$ the higher order terms in (13) are negligible resulting in a failure criterion for theory of simple materials. It has been proved for theory of simple materials in the biaxial loading case, that the analytical solution for $\sigma_{\varphi\varphi}^{\max-}$ corresponds to the numerical values for small R/ρ, i.e. the values of $\sigma_{\varphi\varphi}^{\max-}$ for very small f are greater than those for larger f.

Figure 6 shows the maximum values of the failure criteria by tension $\sigma_{\varphi\varphi}^{\max+}/\sigma_0$ and compression $\sigma_{\varphi\varphi}^{\max-}/\sigma_0$ for all simulations of the uniaxial loading case. Both figures show a trend of decreasing values of $\sigma_{\varphi\varphi}^{\max+}$ and $\sigma_{\varphi\varphi}^{\max-}$, resp., with increasing ratios R/ρ after a certain maximum value. This trend was further investigated for a wider range of R/ρ at a fixed void volume fraction f and it turns out that there is such a global maximum of $\sigma_{\varphi\varphi}^{\max-}$ at a certain R/ρ for any void volume fraction f. This implies that both failure criteria by tension $\sigma_{\varphi\varphi}^{\max-}$ and by compression $\sigma_{\varphi\varphi}^{\max-}$ predict

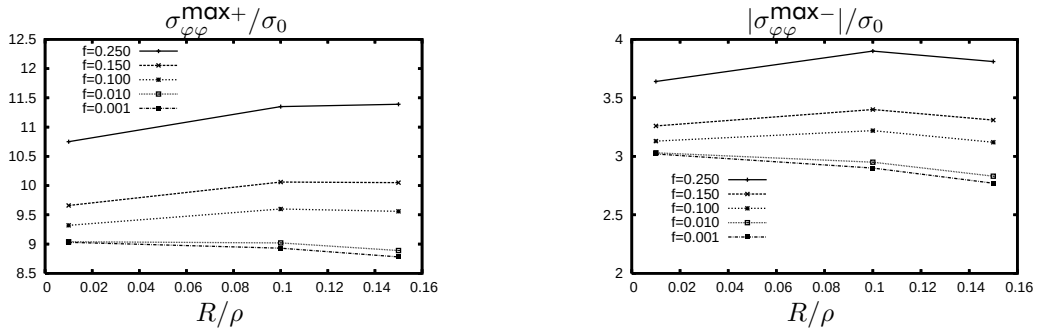

Fig. 6: Failure criterion by tension $\sigma^{max+}_{\varphi\varphi}/\sigma_0$ and failure criterion by compression $|\sigma^{max-}_{\varphi\varphi}|/\sigma_0$ for circular hole under uniaxial remote tension for all realized variations of void volume fraction f and ratio R/ρ

that there is a microstructure with a certain ratio of R/ρ which is most endangered in the uniaxial loading case.

4. Conclusions

Strain gradient elasticity has been applied in order to simulate size effects in the failure of structures consisting of porous elastic material. The numerical results for the considered examples indicate that size effects in failure do not only depend on the microstructural properties but also on the macroscopic geometry, loading conditions, and the failure mechanism.

It has been shown that the presented strain gradient elasticity model obtained by higher order homogenization is able to predict size effects. However, the failure criteria used herein have been chosen more or less arbitrarily without any experimental background. Thus, other failure criteria e.g. based on maximum shear stress inside the VE or energetic criteria will be investigated in conjunction with corresponding experiments to validate the approach. In order to simulate real porous materials a combination of the strain gradient elasticity model with a statistical approach is currently under preparation.

A. Calculation of the coefficients κ_k

Due to some unexpected results the calculation of the coefficients κ_k in [11] was reviewed and existing errors were fixed. Therefore, a reformulated version of the calculation of the κ_k is given in the following.

The coefficients κ_k needed in equations (16)–(22) can be calculated in a more convenient way than in [11] as follows

$$\kappa_1 = \kappa_2 = \breve{\kappa}_{11} + 2\,\breve{\kappa}_{12}\,\omega + \breve{\kappa}_{22}\,\omega^2 \tag{A.1}$$

$$\kappa_3 = \kappa_4 = \kappa^*_{11} + 2\,\kappa^*_{12}\,\omega^* + \kappa^*_{22}\,(\omega^*)^2\ . \tag{A.2}$$

The term ω is given by

$$\omega = (G_1 \breve{\kappa}_{12} - G_2 \breve{\kappa}_{11}) \,/\, (G_2 \breve{\kappa}_{12} - G_1 \breve{\kappa}_{22}) \tag{A.3}$$

and the corrected coefficients $\breve{\kappa}_{ij}$ read

$$\breve{\kappa}_{11} = 4\,R^2 \left[(3-\nu') - 2f^2(1-\nu') - (1+\nu')f^4\right] / E' \tag{A.4}$$

$$\breve{\kappa}_{22} = -\left[2\ln(f) + (1+\nu')\,(1-f)^2\right] / (R^2 E') \tag{A.5}$$

$$\breve{\kappa}_{12} = 2\left[(3-\nu')\,(1-f) + (1+\nu')\,(f^2-f^3)\right] / E' \,. \tag{A.6}$$

The factors G_1 and G_2 can be calculated by

$$G_1 = R^2\,(1-f^2)\,/\,2\,, \quad G_2 = (1-f)\,/\,4\,. \tag{A.7}$$

The terms appearing in (A.2) are given by

$$\omega^* = (G_1^* \kappa_{12}^* - G_2^* \kappa_{11}^*) \,/\, (G_2^* \kappa_{12}^* - G_1^* \kappa_{22}^*) \tag{A.8}$$

and

$$\begin{aligned}\kappa_{11}^* = 8\,R^6 \big[&9(1+\nu')\,(16f^7 - 9f^8) + (11+7\nu')\,(1-8f^6) \\ &+ 2(1-\nu')\,(16f^3 - 9f^4)\big] / E'\end{aligned} \tag{A.9}$$

$$\begin{aligned}\kappa_{22}^* = 36\,R^2 \big[&(1+\nu')\,(1+16f^5-8f^6) \\ &- (11+7\nu')f^4 + 2(1-\nu')f^2\big] / E'\end{aligned} \tag{A.10}$$

$$\begin{aligned}\kappa_{12}^* = 48\,R^4 \big[&(1+\nu')\,(1+17f^6-9f^7) \\ &+ 2(1-\nu')f^2 - (11+7\nu')f^5\big] / E'\end{aligned} \tag{A.11}$$

and the coefficients G_1^* and G_2^* read

$$G_1^* = 2\,R^4(1-f^3)\,, \quad G_2^* = 3\,R^2(1-f^2)/2\,. \tag{A.12}$$

References

[1] T. Schneider, P. Greil, G. Schober, Strength modeling of brittle materials with two- and three-dimensional pore structures, Computational Materials Science 16 (1999) 98–103.

[2] E. Kunhanandan Nambier, K. Ramamurthy, Air-void characterization of foam concrete, Cement and Concrete Research 37 (2007) 221–230.

[3] C. Lu, R. Danzer, F. Fischer, Scaling effect of fracture strength in ZnO: Effects of pore/grain-size interaction and porosity, Journal of the European Ceramics Society 24 (2004) 3643–3651.

[4] T. Isobe, Y. Kameshima, A. Nakajima, K. Okada, Hotta Y., Gas permeability and mechanical roperties of porous alumina ceramics with unidirectionally aligned pores, Journal of the European Ceramics Society 29 (2007) 53–59.

[5] Z. Bazant, Handbook of Materials Behaviour Models, Academic Press, 2001, Ch. Size Effect on Structural Strength, pp. 30–68.

[6] M. van Vliet, J. van Mier, Experimental investigation of size effect in concrete and sandstone under uniaxial tension, Engineering Fracture Mechanics 65 (2000) 165–188.

[7] R. Mindlin, Micro-structure in linear elasticity, Archive for Rational Mechanics and Analysis 16 (1964) 51–78.

[8] M. Gologanu, J. Leblond, G. Perrin, A micromechanically based approach gurson-type model for ductile porous metals including strain gradient effects, in: K. S. (Ed.), Net Shape Processing of Powder Materials, Vol. 216 of AMD, 1995.

[9] S. Forest, Homogenization methods and the mechanics of generalized continua, in: G. Maugin (Ed.), Geometry, Continua and Microstructure, Hermann, Paris, 1999, pp. 35–48.

[10] P. Neff, J. Jeong, H. Ramezani, Subgrid interaction and micro-randomness - novel invariance requirements in infinitesimal gradient elasticity, Preprint 2568, http://www3.mathematik.tu-darmstadt.de/fb/mathe/bibliothek/preprints.html, submitted to Journal of the Mechanics and Physics of Solids.

[11] L. Zybell, U. Mühlich, M. Kuna, Constitutive equations for porous plane-strain gradient elasticity obtained by homogenization, Archive of Applied Mechanics (2008) DOI 10.1007/s00419–008–0238–1.

[12] R. Toupin, Elastic materials with couple-stresses, Archive for Rational Mechanics and Analysis 11 (1962) 385–414.

[13] E. Amanatidou, N. Aravas, Mixed finite element formulations of strain-gradient elasticity problems, Computer Methods in Applied Mechanics and Engineering 191 (2002) 1723–1751.

[14] Simulia, Abaqus Version 6.7 Documentation, Dassault systèmes (2008).

[15] J. Shu, W. King, N. Fleck, Finite elements for materials with strain gradient effects, International Journal for Numerical Methods in Engineering 44 (1999) 373–391.

[16] L. Zybell, Implementation of a User-Element considering strain gradient effects into the FE-program Abaqus, Master's thesis, TU Bergakademie Freiberg (2007).

[17] R. Mindlin, N. Eshel, On first strain-gradient theories in linear elasticity, International Journal of Solids and Structures 4 (1968) 109–124.

[18] N. Eshel, G. Rosenfield, Effects of strain-gradient on the stress-concentration at a cylindrical hole in a field of uniaxial tension, Journal of Engineering Mathematics 4 (1970) 97–111.

Estimation of material properties for linear elastic strain gradient effective media. In: *European Journal of Mechanics, A/Solids*. 31(1):117-130

Estimation of material properties for linear elastic strain gradient effective media

Uwe Mühlich Lutz Zybell Meinhard Kuna

In this paper materials with microstructures, composed of linear elastic constituents are considered. Spherical volume elements with spherical inclusions are used to obtain Voigt and Reuss bounds for the material properties of a corresponding strain gradient effective continuum. The bounds are derived following the general line of argumentation well established for simple effective continua presenting in detail the major differences arising in the case of a strain gradient continuum. Furthermore, an alternative method for the approximation of the material properties is developed, where the volume element is exposed entirely to a kinematically admissible quadratic displacement field. Since the resulting stresses do not fulfil the equilibrium conditions, a second strain field is superimposed which is approximated by a third order polynomial. The coefficients of this polynomial are determined from an energy principle together with a constraint equation in order to fulfil the equilibrium conditions in an integral sense and to assure that the resulting effective constitutive relations are insensitive to rigid body motions. Based on this approximate solution, the components of the sixth order material tensor which relates the gradients of the macroscopic strain with the corresponding higher order stresses can be approximated analytically. In spite of the fact that these estimations are no bounds in general, useful results for the effective material parameters can be derived. This is shown by comparing the obtained approximations with the corresponding numerical results from finite element solutions of the boundary value problem for a spherical volume element considering different void volume fractions.

1. Introduction

Since generalized continuum theories have been shown to be very useful for the theoretical description of size effects and because of their regularization properties, a growing interest in these theories has been developed over the past decades. Nowadays, a great variety of such theories exists, among them nonlocal continuum theories motivated by the aim to capture interactions at length scales in the range of atomic spacing (see e.g. A. C. ERINGEN (2002)) or those nonlocal theories developed for the description of random composites by means of effective continuous media e.g. in BERAN (1971), WILLIS (1987) and DRUGAN AND WILLIS (1996), just to mention a few. Furthermore, the so-called micromorphic continua as laid out e.g. in C. ERINGEN (1999) and the strain gradient continua as developed in MINDLIN AND ESHEL (1968) and MINDLIN (1965) do belong as well to the class of generalized continuum theories. A feature common to all these theories is the incorporation of length parameters which are related somehow to genuine material length properties like defect spacing, grain size etc.. This fact distinguishes them from theories like conventional linear elasticity, plasticity etc., which belong to a class of materials denominated simultaneously by simple continua, Boltzmann continua or Cauchy continua in the literature.

Here, we focus exclusively on strain gradient elasticity. Nevertheless, in some cases micromorphic continua and strain gradient continua are closely related as pointed out already in TRUESDELL AND NOLL (2004) or e.g. in TEKOĞLU AND ONCK (2008) for the corresponding linearized theories. Linear strain gradient elasticity can be derived by extending the strain energy density, which in the case of simple continua depends only on a local deformation meassure, by additional kinematic variables related to the gradient of the local deformation. The general structure of the resulting theory is well known. For instance, for an isotropic linear strain gradient material, five material parameters appear in addition to the usual Young's modulus and Poisson's ratio.

On the other hand, constitutive relations which fit into the framework of strain gradient continua or micromorphic continua, respectively, can be derived by extending homogenization concepts known from the theory of simple continua. Considering a volume element which captures the important micro-structural information, these constitutive relations can be obtained from the solution of the boundary value problem for such a volume element under generalized boundary conditions, provided that the mean quantites are defined properly. To the authors knowledge, this concept was used for the first time in GOLOGANU, LEBLOND, ET AL. (1997) in order to obtain an extension of the Gurson-model within the framework of strain gradient plasticity. Furthermore, in FOREST AND SAB (1998) and FOREST (1998) it has been investigated which type of displacement boundary conditions corresponds to which kind of generalized continuum.

The boundary value problem for the volume element can be solved analytically or numerically. While numerical schemes are more flexible with respect to the microstructure at hand, analytical solutions provide a better insight with respect to general tendencies. Furthermore, analytical estimates and bounds allow e.g. for the formulation of energetically based fracture and yield criteria in closed form which are simple enough to be manageable while still capturing the most important mechanisms.

Numerical schemes for the extraction of the additional material parameters of generalized continua have been developed and applied e.g. in FOREST, DENDIEVEL, AND CANOVA (1999), FOREST AND SAB (1998), PEERLINGS AND FLECK (2004), KOUZNETSOVA (2002), KACZMARCYK, PEARCE, AND BICANIC (2008) and BACIGALUPO AND GAMBAROTTA L. (2010). Analytical solutions were derived only for two-dimensional problems e.g. in ZYBELL, MÜHLICH, AND KUNA (2008), CHEN, LIU, ET AL. (2009), BIGONI AND DRUGAN (2007). Although the numerical schemes mentioned above have been employed in general only for two-dimensional examples, their application to three-dimensional situations seems to be straight forward. This is different for the analytical solutions. Analytical solutions of the corresponding three-dimensional boundary value problems are difficult to derive because the calculations involved become very lengthy even for significantly simplified problems restricting the outcome e.g. to small fractions of second phase particels etc., or employing simple rules of mixture as e.g. in MAYE (1969). Therefore, it seems more promising to adopt methods well established for simple continua like those of Voigt and Reuss estimates which in addition provide bounds of the effective material properties.

The strategy to obtain Voigt and Reuss estimates is extended here for linear strain gradient effective continua. Furthermore, an alternative approximation scheme is presented which does not provide bounds. Nevertheless, it provides useful approximations of the effective material parameters. This is shown by comparing the obtained approximations with the corresponding results from the numerical solution of the boundary value problem for the volume element.

In order to keep the calculations as simple as possible, a volume element of spherical shape has been chosen. Unfortunately, the choice of an isotropic geometry for the VE leads to higher order material tensors which are only positive semi-definite. This has been discussed aleady for the two-dimensional case and cylindrical volume elements in AUFFRAY, BOUCHET, AND BRECHET (2010). Here, this fact is proven analytically for three dimensions.

The paper is organized as follows. First, the problem envisaged here is summarized in section 2. Section 3 sketches the general idea of Voigt and Reuss estimates for simple effective continua. This idea is adopted for strain gradient effective continua considering a completely isotropic volume element in section 4. The geometrical moments appearing in the subsequent calculations are presented at the beginning of this section for volume elements of isotropic geometry. The discussion of some general aspects related to the averaging scheme for strain gradient elasticity is followed by a close examination of the general properties of the higher order elasticity tensor before deriving its Voigt and Reuss bounds. An alternative method for the approximation of the effective material properties is developed in section 5. In order to present the calculations as transparent as possible, we focus on linear strain gradient effective media for porous linear elastic materials. Finally, the analytical results are compared with the numerical solution of the boundary value problem for a spherical volume element with a spherical void in its centre.

2. Formulation of the problem

In the sequel, a global cartesian coordinate system is used together with the index notation and the summation convention. The variables x_k are used to denote the spatial coordinates, where the index k can take the values 1, 2 and 3. The derivative of some term "$()$" with respect to the spatial coordinate x_k is written as follows

$$()_{,k} := \frac{\partial()}{\partial x_k} \,. \tag{1}$$

(2)

Bold face symbols indicate tensors whose rank is given by the context.

We consider a body which consists of a linear composite material and occupies the region $\mathcal{B}^*$ with boundary $\partial\mathcal{B}^*$. The body is exposed to some mechanical loading and the governing equations of the corresponding boundary value problem are given as follows for all $\boldsymbol{x} \in \mathcal{B}^*$

$$\sigma_{ij,j} + f_i = 0_i \tag{3}$$

$$\varepsilon_{ij} = \frac{1}{2}\left[u_{i,j} + u_{j,i}\right] \tag{4}$$

$$\sigma_{ij} = L_{ijkl}\varepsilon_{kl} \tag{5}$$

together with the corresponding boundary conditions. The σ_{ij}, ε_{ij}, u_i and f_i are the components of the stress and strain tensors, the displacements and the volume loads, respectively. The fourth order material tensor $\boldsymbol{L}$ reflects the microstructure of the material and may vary rapidly with spatial position. This makes it difficult to solve the boundary value problem outlined above. Therefore, we wish to replace the original material by an effective macro-continuum defining that way a corresponding boundary value problem, calling it e.g. macro-problem, which is much simpler to solve.

In order to distinguish between the two levels mentioned above, a slowly varying coordinate $\boldsymbol{X}$ is introduced in addition to the fast varying coordinate $\boldsymbol{x}$, see Figure 1. For the derivatives with respect to the coordinates $\boldsymbol{X}$ the following notation is used

$$\partial_k() := \frac{\partial()}{\partial X_k} \,. \tag{6}$$

As usual, the field variables at a point $\boldsymbol{X}$ of the effective macro-continuum are defined as averages of the corresponding micro-fields over a certain surroundings of the considered point which occupies the region $\mathcal{B}$ with volume B and boundary $\partial\mathcal{B}$, using the operator

$$<\diamond>:= \frac{1}{B}\int_{\mathcal{B}} \diamond \,\mathrm{d}V \,. \tag{7}$$

These surroundings are termed as volume element (VE) and an example for a spherical volume element is depicted in Figure 1. Then, the stresses and strains in the

macro-continuum are given as follows

$$\Sigma_{ij} = < \sigma_{ij} > \tag{8}$$

$$E_{ij} = < \varepsilon_{ij} > \ . \tag{9}$$

According to the definition above, the micro-fields have to be known in order to determine the corresponding macro-fields. However, the objective is just to avoid the solution of the problem at the micro-level. Therefore, the volume element which corresponds to a point $\boldsymbol{X}$ is considered together with proper boundary conditions in terms of prescribed displacements or tractions on $\partial\mathcal{B}$. From the solution of this boundary value problem the constitutive relations for the macro-level are derived.

Furthermore, the question arises which kind of theory applies at the macro-level. It turns out that in the case of prescribed linear displacements or constant tractions the macro-continuum corresponds to a simple continuum, whereas for quadratic boundary displacements or linear tractions a strain gradient continuum results as discussed e.g. in FOREST (2002) and GOLOGANU, LEBLOND, ET AL. (1997).

As mentioned above, a boundary value problem for the VE has to be solved in order to obtain the constitutive relations at the macro-level. If an analytical solution cannot be obtained, estimates are a favoured alternative to numerical solutions. This is because estimates may provide bounds on material parameters and the influence of certain variables on the constitutive behaviour can be seen more clearly. Therefore, within the next section the principles of this method will be revised briefly for simple effective continua. Then, this concept will be extended for strain gradient effective continua.

3. Classical estimates of the material properties for the effective medium

Nowadays, estimates for simple effective continua are well established and the theoretical fundamentals can be found already in many textbooks. Therefore, only the informations needed within this paper are outlined briefly. More detailed expositions of this topic can be found e.g. in NEMAT-NASSER AND HORI (1999) or QU AND CHERKAOUI (2006).

If the Hill-condition

$$\frac{1}{2} < \sigma_{ij}\varepsilon_{ij} > = \frac{1}{2}\Sigma_{ij}E_{ij} \tag{10}$$

is fulfilled, a simple continuum approach is justified at the macro-level. For this kind of problem we are dealing with, this means that we can apply linear elasticity at the macrolevel and we are looking for the constitutive equations of the effective medium in the form

$$\Sigma_{ij} = C_{ijkl}E_{kl}\,. \tag{11}$$

Defining the strain energy density $\mathcal{W}$ of the volume element by

$$\mathcal{W} = \frac{1}{2} < L_{ijkl}\varepsilon_{ij}\varepsilon_{kl} > \tag{12}$$

it can be seen from (5) that the left hand side of the Hill-condition (10) equals $\mathcal{W}$. Incorporating (11), the Hill-condition finally reads

$$\mathcal{W} = \frac{1}{2} E_{ij} C_{ijkl} E_{kl} \,. \tag{13}$$

The fourth order tensor $\boldsymbol{C}$ has to be determined in general by solving the boundary value problem for the considered volume element for given boundary data so that the Hill-condition (10) is fulfilled. There are various kinds of possible boundary conditions. Two of them are

$$\left.\begin{array}{rcll} u_i &=& E_{ij} x_j & \\ t_i &=& \Sigma_{ij} n_j & \end{array}\right\} \qquad \boldsymbol{x} \in \partial\mathcal{B} \tag{14}$$

which means that either linear displacements or constant tractions are prescribed at the outer boundary of the volume element. Furthermore, mixed boundary conditions or periodic boundary conditions are also possible. Here, we focus on prescribed displacements. The boundary problem for the volume element can be quite complex. Therefore, various methods have been established to approximate $\boldsymbol{C}$ and its inverse $\boldsymbol{C}^{-1}$, respectively, see e.g QU AND CHERKAOUI (2006). The simplest estimates for $\boldsymbol{C}$ and $\boldsymbol{C}^{-1}$ can be derived by combining the minimum potential energy principle or the minimum complementary potential energy principle respectively, with either prescribed displacements or prescribed surface tractions. The potential energy and the complementary energy of the volume element are given by

$$\Pi = \frac{1}{2} \int\limits_{\mathcal{B}} L_{ijkl} \varepsilon_{ij} \varepsilon_{kl} \, \mathrm{d}V - \int\limits_{\partial\mathcal{B}_t} \bar{t}_i u_i \, \mathrm{dA} \tag{15}$$

and

$$\Pi^{\mathrm{c}} = \frac{1}{2} \int\limits_{\mathcal{B}} L^{-1}_{ijkl} \sigma_{ij} \sigma_{kl} \, \mathrm{d}V - \int\limits_{\partial\mathcal{B}_u} t_i \bar{u}_i \, \mathrm{dA} \tag{16}$$

respectively, where $\bar{t}_i$ and $\bar{u}_i$ are prescribed values. The corresponding extremum principles read

$$\Pi(\boldsymbol{u}) \leq \Pi(\hat{\boldsymbol{u}}) \tag{17}$$

$$u_i = \bar{u}_i \qquad \boldsymbol{x} \in \partial\mathcal{B}_u \tag{18}$$

and

$$\Pi^{\mathrm{c}}(\boldsymbol{\sigma}) \leq \Pi^{\mathrm{c}}(\hat{\boldsymbol{\sigma}}) \tag{19}$$

$$t_i = \bar{t}_i \qquad \boldsymbol{x} \in \partial\mathcal{B}_t \,, \tag{20}$$

which means that among all kinematically admissible displacement fields $\hat{\boldsymbol{u}}$ the true field $\boldsymbol{u}$ renders the potential energy an absolute minimum and that among all statically admissible fields $\hat{\boldsymbol{\sigma}}$ the true stress field $\boldsymbol{\sigma}$ renders the complementary potential energy an absolute minimum.

For prescribed displacements according to (14 a) $\partial\mathcal{B} = \partial\mathcal{B}_u$ which implies $\partial\mathcal{B}_t = \emptyset$ holds. The energy and the complementary energy read

$$\Pi = \frac{1}{2}\int\limits_{\mathcal{B}} L_{ijkl}\varepsilon_{ij}\varepsilon_{kl}\,\mathrm{d}V \qquad = \quad \mathcal{W}\,B \tag{21}$$

$$\Pi^{\mathrm{c}} = \frac{1}{2}\int\limits_{\mathcal{B}} L^{-1}_{ijkl}\sigma_{ij}\sigma_{kl}\,\mathrm{d}V - \int\limits_{\partial\mathcal{B}} t_i x_j\,\mathrm{d}A\,E_{ij} \qquad = \; -\mathcal{W}\,B \tag{22}$$

if (12) and (7) are taken into account. The Voigt-estimate consists in evaluating Π for a constant strain field which in addition has to fulfill the boundary conditions (14 a). Therefore,

$$\hat{u}_i = E_{ij}x_j \qquad\qquad \boldsymbol{x} \in \mathcal{B} \tag{23}$$

is used. Regarding the complementary energy (22), the boundary conditions (14 a) are already incorporated explicitely in the surface integral. According to the Reuss-approach, Π^{c} is evaluated for a constant stress field $\boldsymbol{S}$

$$\hat{\sigma}_{ij} = S_{ij} \qquad\qquad \boldsymbol{x} \in \mathcal{B} \tag{24}$$

which is the simplest choice for a statically admissible stress field. This results in

$$\Pi(\hat{\boldsymbol{u}}) = \frac{1}{2}E_{ij} < L_{ijkl} > E_{kl} \tag{25}$$

and

$$\Pi^{\mathrm{c}}(\hat{\boldsymbol{\sigma}}) = \frac{1}{2}S_{ij} < L^{-1}_{ijkl} > S_{kl} - S_{ij}E_{ij}\,, \tag{26}$$

respectively. Obviously, $\Pi^{\mathrm{c}}(\boldsymbol{\sigma}) \leq \Pi^{\mathrm{c}}(\hat{\boldsymbol{\sigma}})$ holds but the question arises which would be the best choice for $\boldsymbol{S}$ in order to minimize $\Pi^{\mathrm{c}}(\hat{\boldsymbol{\sigma}})$. The first variation of $\hat{\Pi}^{\mathrm{c}}$ reveals that the optimal choice is

$$S_{ij} = < L^{-1}_{ijkl} >^{-1} E_{kl} \tag{27}$$

and $\Pi^{\mathrm{c}}(\hat{\boldsymbol{\sigma}})$ then reads

$$\Pi^{\mathrm{c}}(\hat{\boldsymbol{\sigma}}) = -\frac{1}{2}E_{ij} < L_{ijkl} >^{-1} E_{kl}\,. \tag{28}$$

It follows from (17), (19), (21) and (22) that

$$E_{ij} < L^{-1}_{ijkl} >^{-1} E_{kl} \quad \leq \quad E_{ij}C_{ijkl}E_{kl} \quad \leq \quad E_{ij} < L_{ijkl} > E_{kl}\,. \tag{29}$$

Analogously, the compliance tensor $\boldsymbol{C}^{-1}$ can be estimated considering constant surface tractions instead of linear displacements at the outer boundary of the volume element.

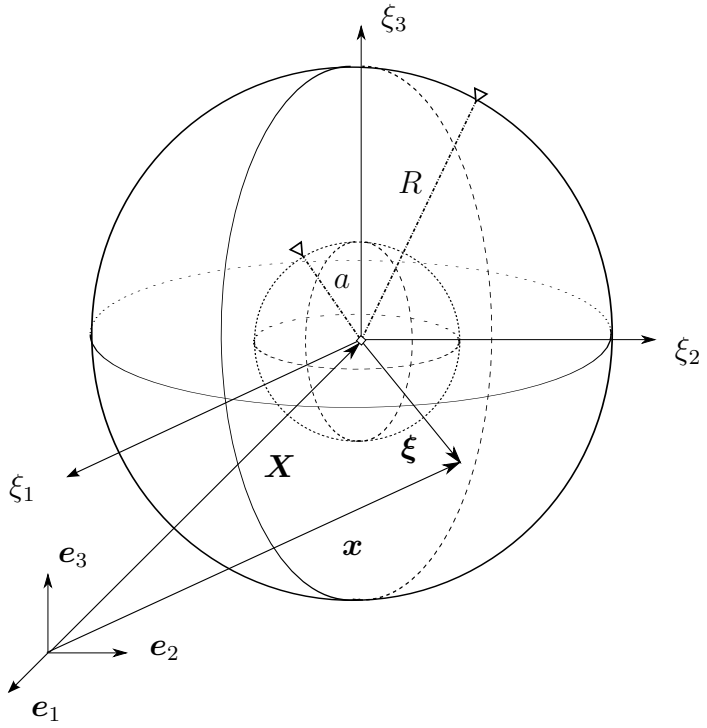

Fig. 1: Spherical volume element with radius R containing an inclusion or void, respectively, with radius a, together with the different coordinate systems.

4. Voigt and Reuss estimates for strain gradient effective continua

4.1. Geometrical moments due to averaging for fully isotropic volume elements

In the following, the geometrical quantities

$$\Xi_{ij...z} := < \xi_i \xi_j ... \xi_z > \qquad \text{with} \quad i,j,...,z = 1,2,3 \tag{30}$$

will be needed up to order six. The ξ_k are the spatial coordinates referring to a cartesian coordinate system in the center of the volume element as shown in Figure 1. Here, we limit ourself to isotropic volume elements like spheres. Then, all geometrical tensors of even order are fully isotropic and symmetric, whereas all tensors of odd order vanish. We recieve for the tensors up to order six

$$< \xi_i > \;=\; 0_i \tag{31}$$

$$< \xi_i \xi_j > \;=\; \kappa\, \delta_{ij} \tag{32}$$

$$< \xi_i \xi_j \xi_k > \;=\; 0_{ijk} \tag{33}$$

$$A_{ijkl} = < \xi_i \xi_j \xi_k \xi_l > \;=\; \phi(\delta_{ij}\delta_{kl} + \delta_{ik}\delta_{jl} + \delta_{il}\delta_{jk}) \tag{34}$$

$$< \xi_i \xi_j \xi_k \xi_l \xi_m > \;=\; 0_{ijklm} \tag{35}$$

$$B_{ijklmn} = < \xi_i \xi_j \xi_k \xi_l \xi_m \xi_n > \;=\; \chi(J_{ijklmn} + K_{ijklmn} + P_{ijklmn}) \tag{36}$$

where $\boldsymbol{J}$, $\boldsymbol{K}$ and $\boldsymbol{P}$ are given in C.

In the following, the components of the contracted tensor B_{ijkkmm}

$$B_{ijkkmm} = \theta\delta_{ij} \tag{37}$$

will be needed, where $\theta = 35\chi$ in the case of an isotropic VE . The values of the different coefficients depend on the considered geometry and are given for the sphere with Radius R in Table 1.

For microstructures which consist of voids or inclusions with constant elastic properties surrounded by a matrix material whose elastic properties are constant as well, the averaging operator can be splitted as follows

$$<>= f <>_{\mathcal{B}^{\mathrm{I}}} +(1-f) <>_{\mathcal{B}^{\mathrm{M}}} \tag{38}$$

where the volume fraction of the inclusion or void, respectively, is given by

$$f = \frac{B^{\mathrm{I}}}{B} \tag{39}$$

and the indices I and M stand for inclusion and matrix, respectively. With respect to the spherical volume element depicted in Figure 1, the volume fraction f is given by $f = a^3/R^3$. The averaging operators $<>_{\mathcal{B}^{\mathrm{I}}}$ and $<>_{\mathcal{B}^{\mathrm{M}}}$ are defined as follows

$$<>_{\mathcal{B}^{\mathrm{I}}}= \frac{1}{B^{\mathrm{I}}} \int\limits_{\mathcal{B}^{\mathrm{I}}} \mathrm{d}V \qquad , \qquad <>_{\mathcal{B}^{\mathrm{M}}}= \frac{1}{B^{\mathrm{M}}} \int\limits_{\mathcal{B}^{\mathrm{M}}} \mathrm{d}V \ . \tag{40}$$

Applying (38) with respect to the geometrical moment (32), it follows that

$$\kappa = f\kappa^{\mathrm{I}} + (1-f)\kappa^{\mathrm{M}} \tag{41}$$

with

$$\kappa^{\mathrm{M}} = \frac{1}{1-f}[\kappa - f\kappa^{\mathrm{I}}] \tag{42}$$

and analogously for ϕ^{M}, χ^{M} and θ^{M}. The values of these constants are also given in Table 1 for a spherical volume element containing a spherical inclusion or void with radius a in its center.

κ	κ^{I}	κ^{M}	ϕ	ϕ^{I}	ϕ^{M}	χ	χ^{I}	χ^{M}	θ	θ^{I}	θ^{M}
$\frac{R^2}{5}$	$\frac{a^2}{5}$	$\kappa\frac{1-\sqrt[3]{f^5}}{1-f}$	$\frac{R^4}{35}$	$\frac{a^4}{35}$	$\phi\frac{1-\sqrt[3]{f^7}}{1-f}$	$\frac{R^6}{315}$	$\frac{a^6}{315}$	$\chi\frac{1-f^3}{1-f}$	$\frac{R^6}{9}$	$\frac{a^6}{9}$	$\theta\frac{1-f^3}{1-f}$

Tab. 1: Coefficients of the geometrical moment tensors for the sphere with radius R containing a spherical void or inclusion of radius a in its center. The volume fraction f equals a^3/R^3.

4.2. Averaging scheme for strain gradient elasticity

According to GOLOGANU, LEBLOND, ET AL. (1997), the follwing boundary conditions for the volume element

$$u_i = E_{ij}x_j + \frac{1}{2}\left[H_{ijk} - H_{jki} + H_{kij}\right]x_j x_k - H_{ijk}X_k x_j \qquad \boldsymbol{x} \in \partial\mathcal{B}\,, \tag{43}$$

are considered. These boundary conditions constitute a straight forward extension from linear boundary displacements (14 a), resulting in a simple effective continuum, to quadratic ones. The H_{ijk} in (43) are the gradients of the macroscopic strains

$$H_{ijk} = \partial_k E_{ij} \tag{44}$$

with respect to the slowly varying coordinate $\boldsymbol{X}$. The meaning of the coordinates $\boldsymbol{x}$, $\boldsymbol{X}$ and $\boldsymbol{\xi}$ is depicted in Figure 1. Regarding only centro-symmetric volume elements, it can be shown that the extended Hill-condition reads for this case

$$\frac{1}{2} < \sigma_{ij}\varepsilon_{ij} >= \frac{1}{2}\Sigma_{ij}E_{ij} + \frac{1}{2}M_{ijk}H_{ijk} \tag{45}$$

with the higher order stresses

$$M_{ijk} =< \sigma_{ij}\xi_k > \tag{46}$$

which can be obtained also from the boundary data as sketched in B. It can be seen from (45) that due to the limitation to centro-symmetry the effects related to the strain gradients are completely decoupled from the strains.

Comparision of (43) with (14) motivates the attempt to formulate as well corresponding traction boundary conditions. A straight forward extension of the boundary conditions (43) consists in the formulation of prescribed linear tractions at the outer boundary of the volume element which finally leads to

$$t_i = \Sigma_{ij}n_j + \widetilde{M}_{ijk}n_j(x_k - X_k) \qquad \boldsymbol{x} \in \partial\mathcal{B} \tag{47}$$

where the corresponding calculation is outlined in A. The $\widetilde{M}_{ijk}$ are the gradients of the macroscopic stresses

$$\widetilde{M}_{ijk} = \partial_k \Sigma_{ij}\,, \tag{48}$$

with respect to the slowly varying coordinate $\boldsymbol{X}$. The n_i are the components of the outward normal vector on $\partial\mathcal{B}$. The corresponding work conjugate kinematic variables $\widetilde{H}_{ijk}$ is given by

$$\widetilde{H}_{ijk} =< \varepsilon_{ij}\xi_k > \tag{49}$$

as outlined in A. It turns out that the higher order tensors $\boldsymbol{H}$ and $\widetilde{\boldsymbol{H}}$ are not compatible. Therefore, the boundary conditions (47) may be better suited for a stress gradient theory. This is different from the theory of simple effective continua, where

the work conjugate variables are always $\boldsymbol{\Sigma}$ and $\boldsymbol{E}$ no matter if linear displacements or constant surface tractions are prescribed at the outer surface of the volume element.

In the following, we focus on prescribed displacements. The constitutive equations relating the higher order stresses $\boldsymbol{M}$ and the strain gradients $\boldsymbol{H}$ have the general form

$$M_{ijk} = D_{ijklmn} H_{lmn} \tag{50}$$

with the sixth order tensor $\boldsymbol{D}$. Using (5) and (50), the extended Hill-condition (45) can be written as

$$\mathcal{W} = \frac{1}{2} E_{ij} C_{ijkl} E_{kl} + \frac{1}{2} H_{ijk} D_{ijklmn} H_{lmn} \,. \tag{51}$$

Furthermore, using (51) it can be shown that

$$\Pi = \mathcal{W} \tag{52}$$

and

$$\Pi^{\mathrm{c}} = -\mathcal{W} \tag{53}$$

hold as well for the boundary displacements (43). This, on the other hand, indicates that estimates for the strain gradient effective media can be obtained by a strategy similar to those discussed above for simple effective media. However, there are some significant differences. For instance, considering a completely homogeneous volume element and applying the displacement field given by (43) not only at the boundary but for the entire volume element leads to the following stress response

$$\sigma_{ij} = L_{ijkl} H_{klp} \xi_p \tag{54}$$

whose divergence

$$\sigma_{ij,j} = L_{ijkl} H_{klj} \tag{55}$$

does not vanish in general. This indicates that, contrary to the situation for simple effective continua, the exact solution for a homogeneous material is not just given by the field (43) for the entire volume element. Other differences will be discussed within the next section.

4.3. General discussion of the higher order elasticity tensor $\boldsymbol{D}$

For an isotropic material, $\boldsymbol{D}$ is an isotropic sixth-order tensor. Every isotropic sixth-order tensor is fully determined by fifteen independent coefficients as discussed eg. in MOAKHER (2007). Due to the symmetries

$$D_{ijouvw} = D_{iojuvw} = D_{ijouwv} = D_{uvwijo} \tag{56}$$

the number of independent coefficient reduces to five and $\boldsymbol{D}$ can be written as

$$\begin{aligned} D_{ijouvw} = \quad & \eta_1 \delta_{ij}\delta_{uv}\delta_{ow} + \eta_2(\delta_{iu}\delta_{jv} + \delta_{iv}\delta_{ju})\delta_{ow} \\ & + \eta_3[\delta_{ij}(\delta_{ou}\delta_{vw} + \delta_{ov}\delta_{uw}) + \delta_{uv}(\delta_{iw}\delta_{jo} + \delta_{io}\delta_{jw})] \\ & + \eta_4[\delta_{io}(\delta_{ju}\delta_{vw} + \delta_{jv}\delta_{uw}) + \delta_{jo}(\delta_{iu}\delta_{vw} + \delta_{iv}\delta_{uw})] \\ & + \eta_5[\delta_{ov}(\delta_{iu}\delta_{jw} + \delta_{iw}\delta_{ju}) + \delta_{ou}(\delta_{iv}\delta_{jw} + \delta_{iw}\delta_{jv})] \,. \end{aligned} \tag{57}$$

In order to ensure the strain energy density being always positive, $\boldsymbol{D}$ must be positive definite which means that for all eigenvalues ω_k of $\boldsymbol{D}$

$$\omega_k > 0 \tag{58}$$

must hold. In the following, the eigenvalues of $\boldsymbol{D}$ are determined employing the method used in AUFFRAY, BOUCHET, AND BRECHET (2010) and originally proposed in MEHRABADI AND COWIN (1991). This method rests on the idea to transform a tensor of n-th order of a three-dimensional vector space $\mathcal{V}^3$ into a second order tensor of a m-dimensional vector space $\mathcal{V}^m$. For the problem considered here, the sixth-order tensor $\boldsymbol{D}$

$$\boldsymbol{D} = D_{ijouvw}\boldsymbol{e}_i\boldsymbol{e}_j\boldsymbol{e}_o\boldsymbol{e}_u\boldsymbol{e}_v\boldsymbol{e}_w \tag{59}$$

has to be transformed into a second order tensor $\hat{\boldsymbol{D}}$ of an eighteen-dimensional vector space

$$\hat{\boldsymbol{D}} = \hat{D}_{\alpha\beta}\hat{\boldsymbol{e}}_\alpha\hat{\boldsymbol{e}}_\beta \,. \tag{60}$$

The latter is defined by the following base vectors

$$\begin{aligned}
&\hat{\boldsymbol{e}}_1 = \boldsymbol{e}_1\boldsymbol{e}_1\boldsymbol{e}_1 && \hat{\boldsymbol{e}}_7 = \boldsymbol{e}_3\boldsymbol{e}_3\boldsymbol{e}_2 && \hat{\boldsymbol{e}}_{13} = \boldsymbol{e}_1\boldsymbol{e}_1\boldsymbol{e}_3 \\
&\hat{\boldsymbol{e}}_2 = \boldsymbol{e}_2\boldsymbol{e}_2\boldsymbol{e}_1 && \hat{\boldsymbol{e}}_8 = \boldsymbol{e}_1\boldsymbol{e}_1\boldsymbol{e}_2 && \hat{\boldsymbol{e}}_{14} = \frac{1}{\sqrt{2}}[\boldsymbol{e}_1\boldsymbol{e}_3 + \boldsymbol{e}_3\boldsymbol{e}_1]\boldsymbol{e}_1 \\
&\hat{\boldsymbol{e}}_3 = \boldsymbol{e}_3\boldsymbol{e}_3\boldsymbol{e}_1 && \hat{\boldsymbol{e}}_9 = \frac{1}{\sqrt{2}}[\boldsymbol{e}_1\boldsymbol{e}_2 + \boldsymbol{e}_2\boldsymbol{e}_1]\boldsymbol{e}_1 && \hat{\boldsymbol{e}}_{15} = \frac{1}{\sqrt{2}}[\boldsymbol{e}_2\boldsymbol{e}_3 + \boldsymbol{e}_3\boldsymbol{e}_2]\boldsymbol{e}_2 \\
&\hat{\boldsymbol{e}}_4 = \frac{1}{\sqrt{2}}[\boldsymbol{e}_1\boldsymbol{e}_3 + \boldsymbol{e}_3\boldsymbol{e}_1]\boldsymbol{e}_3 && \hat{\boldsymbol{e}}_{10} = \frac{1}{\sqrt{2}}[\boldsymbol{e}_2\boldsymbol{e}_3 + \boldsymbol{e}_3\boldsymbol{e}_2]\boldsymbol{e}_3 && \hat{\boldsymbol{e}}_{16} = \frac{1}{\sqrt{2}}[\boldsymbol{e}_1\boldsymbol{e}_2 + \boldsymbol{e}_2\boldsymbol{e}_1]\boldsymbol{e}_3 \\
&\hat{\boldsymbol{e}}_5 = \frac{1}{\sqrt{2}}[\boldsymbol{e}_1\boldsymbol{e}_2 + \boldsymbol{e}_2\boldsymbol{e}_1]\boldsymbol{e}_2 && \hat{\boldsymbol{e}}_{11} = \boldsymbol{e}_3\boldsymbol{e}_3\boldsymbol{e}_3 && \hat{\boldsymbol{e}}_{17} = \frac{1}{\sqrt{2}}[\boldsymbol{e}_1\boldsymbol{e}_3 + \boldsymbol{e}_3\boldsymbol{e}_1]\boldsymbol{e}_2 \\
&\hat{\boldsymbol{e}}_6 = \boldsymbol{e}_2\boldsymbol{e}_2\boldsymbol{e}_2 && \hat{\boldsymbol{e}}_{12} = \boldsymbol{e}_2\boldsymbol{e}_2\boldsymbol{e}_3 && \hat{\boldsymbol{e}}_{18} = \frac{1}{\sqrt{2}}[\boldsymbol{e}_2\boldsymbol{e}_3 + \boldsymbol{e}_3\boldsymbol{e}_2]\boldsymbol{e}_1
\end{aligned} \tag{61}$$

where $\boldsymbol{e}_i\boldsymbol{e}_k\boldsymbol{e}_j$ $(i,j,k = 1,2,3)$ denotes the dyadic product of the orthonormal base vectors of the three-dimensional vector space. The $\hat{\boldsymbol{e}}_\alpha$ are orthonormal base vectors

$$\hat{\boldsymbol{e}}_\alpha \odot \hat{\boldsymbol{e}}_\beta = \delta_{\alpha\beta} \tag{62}$$

where the scalar product has to be evaluated according to

$$(\boldsymbol{e}_i\boldsymbol{e}_j\boldsymbol{e}_k) \odot (\boldsymbol{e}_u\boldsymbol{e}_v\boldsymbol{e}_w) = (\boldsymbol{e}_i \cdot \boldsymbol{e}_u)(\boldsymbol{e}_j \cdot \boldsymbol{e}_v)(\boldsymbol{e}_k \cdot \boldsymbol{e}_w)\,. \tag{63}$$

First, the transformation of the third-order tensor $\boldsymbol{H}$ into a first order tensor $\hat{\boldsymbol{H}}$ in $\mathcal{V}^{18}$ is discussed. Setting

$$\boldsymbol{H} = \hat{\boldsymbol{H}} \tag{64}$$

and employing the orthogonality relation (62) the coordinates of $\hat{\boldsymbol{H}}$ can be calculated according to

$$\hat{H}_\alpha = H_{ijk}(\boldsymbol{e}_i\boldsymbol{e}_j\boldsymbol{e}_k) \odot \hat{\boldsymbol{e}}_\alpha\,. \tag{65}$$

The resulting coordinates are

$$\begin{aligned}
\hat{H}_1 ... \hat{H}_5 :&\quad H_{111}, H_{221}, H_{331}, \sqrt{2}H_{133}, \sqrt{2}H_{122} \\
\hat{H}_5 ... \hat{H}_{10} :&\quad H_{222}, H_{332}, H_{112}, \sqrt{2}H_{121}, \sqrt{2}H_{233} \qquad (66)\\
\hat{H}_{11} ... \hat{H}_{15} :&\quad H_{333}, H_{223}, H_{113}, \sqrt{2}H_{131}, \sqrt{2}H_{232} \\
\hat{H}_{16} ... \hat{H}_{18} :&\quad \sqrt{2}H_{123}, \sqrt{2}H_{132}, \sqrt{2}H_{231} \qquad (67)
\end{aligned}$$

Analogously, setting

$$\boldsymbol{D} = \hat{\boldsymbol{D}} \tag{68}$$

the coordinates of $\hat{\boldsymbol{D}}$ can be calculated using (62). Furthermore, the coordinates of $\hat{\boldsymbol{H}}$ and $\hat{\boldsymbol{D}}$ can be arranged as elements of an algebraic vector $\underline{\hat{\boldsymbol{H}}}$ and an algebraic quadratic matrix $\underline{\underline{\hat{\boldsymbol{D}}}}$, respectively. The transformation ensures that the matrix operation $\underline{\hat{\boldsymbol{H}}}^{\mathrm{T}} \cdot \underline{\underline{\hat{\boldsymbol{D}}}} \cdot \underline{\hat{\boldsymbol{H}}}$ is a proper representation of the tensorial operation $\boldsymbol{H}\vdots\boldsymbol{D}\vdots\boldsymbol{H}$. Therefore, the matrix representation of $\hat{\boldsymbol{D}}$ can be used in order to determine the eigenvalues of $\boldsymbol{D}$ as well as to calculate its inverse. The matrix representation of $\hat{\boldsymbol{D}}$ reads

$$\underline{\underline{\hat{\boldsymbol{D}}}}_{[18\times18]} = \begin{bmatrix} \underline{\underline{\boldsymbol{A}}}_{[5\times5]} & & & & \\ & \underline{\underline{\boldsymbol{A}}}_{[5\times5]} & & & \\ & & \underline{\underline{\boldsymbol{A}}}_{[5\times5]} & & \\ & & & \underline{\underline{\boldsymbol{B}}}_{[3\times3]} & \end{bmatrix} \tag{69}$$

with

$$\underline{\underline{\boldsymbol{A}}} = \begin{bmatrix} \eta_{12}+4(\eta_3+\eta_4+\eta_5) & \eta_1+2\eta_3 & \eta_1+2\eta_3 & (\eta_3+2\eta_4)\sqrt{2} & (\eta_3+2\eta_4)\sqrt{2} \\ & \eta_{12} & \eta_1 & \eta_3\sqrt{2} & (\eta_3+2\eta_5)\sqrt{2} \\ \text{symm.} & & \eta_{12} & (\eta_3+2\eta_5)\sqrt{2} & \eta_3\sqrt{2} \\ & & & (\eta_2+\eta_4+\eta_5)2 & \eta_4 2 \\ & & & & (\eta_2+\eta_4+\eta_5)2 \end{bmatrix} \tag{70}$$

and

$$\underline{\underline{\boldsymbol{B}}} = \begin{bmatrix} 2\eta_2 & 2\eta_5 & 2\eta_5 \\ & 2\eta_2 & 2\eta_5 \\ \text{symm.} & & 2\eta_2 \end{bmatrix} \tag{71}$$

where

$$\eta_{12} = \eta_1 + 2\eta_2 \,. \tag{72}$$

The following eigenvalues are obtained

$$\begin{aligned} \omega_1 &= \frac{3}{2}\eta_1 + 2\eta_2 + 2\eta_3 + 4\eta_4 + \eta_5 - \frac{1}{2}\sqrt{P} & \omega_5 &= \omega_4 \\ \omega_2 &= \frac{3}{2}\eta_1 + 2\eta_2 + 2\eta_3 + 4\eta_4 + \eta_5 + \frac{1}{2}\sqrt{P} & \omega_6 &= \omega_3 \\ \omega_3 &= 2(\eta_2 - \eta_5) & \omega_7 &= \omega_4 \\ \omega_4 &= 2\eta_2 + 4\eta_5 & \omega_8 &= \omega_4 \end{aligned} \tag{73}$$

with

$$P := 9(\eta_1^2 + 4\eta_5^2) + 4\eta_1(6\eta_3 + \eta_5) + 64\eta_4(-\frac{1}{2}\eta_1 + \eta_3 + \eta_4 + \eta_5) + 16\eta_3(6\eta_3 + 7\eta_5) \,. \tag{74}$$

The ω_1 to ω_5 belong to $\underline{\underline{\boldsymbol{A}}}$ and are therefore of multiplicity three, whereas ω_6, ω_7 and ω_8 are the eigenvalues of $\underline{\underline{\boldsymbol{B}}}$.

If a spherical volume element is considered, then the η_k are not completely independent of each other. The reason for this is that in this case $\boldsymbol{H}$ includes a rigid body motion as already shown in GOLOGANU, LEBLOND, ET AL. (1997). For the sake of clarity, parts of the argumentation will be repeated here. The strain gradient tensor $\boldsymbol{H}$ can be splitted into two parts

$$H_{ijk} = H'_{ijk} + \breve{H}_{ijk} \tag{75}$$

with

$$\breve{H}_{ijk} = \frac{1}{4}\left[\delta_{ik}H_{jmm} + \delta_{jk}H_{imm}\right] \tag{76}$$

and

$$H'_{ijk} = H_{ijk} - \breve{H}_{ijk} \,. \tag{77}$$

Evaluating (43 a) setting $\boldsymbol{H} = \breve{\boldsymbol{H}}$, reveals that for this case

$$u_i = \frac{1}{4}H_{imm}\xi_k\xi_k + \left[\frac{1}{4}H_{imm}X_k - \frac{1}{4}H_{kmm}X_i + E_{ik}\right]\xi_k - \frac{1}{4}H_{jmm}X_iX_j \qquad \boldsymbol{x} \in \partial\mathcal{B} \tag{78}$$

if $\boldsymbol{x} = \boldsymbol{X} + \boldsymbol{\xi}$ is taken into account. The first term reads e.g. for a spherical volume element with outer radius R

$$u_i = \frac{1}{4} H_{imm} R^2 \qquad \boldsymbol{\xi} \in \partial\mathcal{B} \tag{79}$$

because of $\xi_k^2 = R^2$ if $\xi_k \in \partial\mathcal{B}$. Therefore, this is a rigid body motion at least for a spherical volume element. Obviously, the last term in (78) is a rigid body motion too, while the second term corresponds to a linear displacement at $\partial\mathcal{B}$ which should be covered completely by the material tensor $\boldsymbol{C}$. Because (78) contains only rigid body motions and linear boundary displacements, $\breve{\boldsymbol{H}}$ must not generate any higher order stresses, i.e.

$$\boldsymbol{D} \vdots \breve{\boldsymbol{H}} = \boldsymbol{0}\,. \tag{80}$$

Taking into account the symmetry properties of $\boldsymbol{D}$, it follows from (80) and (76) that

$$D_{ijklvv} = D_{ivvjkl} = D_{vivjkl} = D_{ijkvlv} = 0_{ijkl} \tag{81}$$

must hold. Evaluating (81) for (57) leads to

$$\eta_4 = \frac{1}{8}\eta_1 - \frac{1}{4}\eta_2 + \frac{1}{4}\eta_3 \tag{82}$$

$$\eta_5 = -\frac{1}{2}\eta_1 - 2\eta_3 \tag{83}$$

and the following eigenvalues result from (73)

$$\omega_1 = \frac{3}{2}\eta_1 + \eta_2 + \eta_3 - \left|\frac{3}{2}\eta_1 + \eta_2 + \eta_3\right| \tag{84}$$

$$\omega_2 = \frac{3}{2}\eta_1 + \eta_2 + \eta_3 + \left|\frac{3}{2}\eta_1 + \eta_2 + \eta_3\right| \tag{85}$$

$$\omega_3 = \eta_1 + 2\eta_2 + 4\eta_3 \tag{86}$$

$$\omega_4 = 2(-\eta_1 + \eta_2 - 4\eta_3) \tag{87}$$

where $|a|$ indicates the absolute value of a. Whether $\frac{3}{2}\eta_1 + \eta_2 + \eta_3$ is positive or negative, either ω_1 or ω_2 is zero. The conclusion is that if $\boldsymbol{D}$ is determined using a spherical volume element it cannot be positive definite but only positive semi-definite. This was observed numerically already in AUFFRAY, BOUCHET, AND BRECHET (2010) for the two-dimensional case.

Finally, in order to ensure that the remaining eigenvalues of $\boldsymbol{D}$ are strictly positive, one of the following conditions has to be fulfilled

$$\eta_1 > 0 \qquad \eta_2 > 0 \qquad -\frac{1}{4}\eta_1 - \frac{1}{2}\eta_2 < \eta_3 < -\frac{1}{4}\eta_1 + \frac{1}{4}\eta_2 \tag{88}$$

$$\eta_1 \leq 0 \qquad \eta_2 > -\frac{5}{2}\eta_1 \qquad -\frac{1}{4}\eta_1 - \frac{1}{2}\eta_2 < \eta_3 < -\frac{1}{4}\eta_1 + \frac{1}{4}\eta_2 \tag{89}$$

$$\eta_1 < 0 \qquad -\eta_1 < \eta_2 \leq -\frac{5}{2}\eta_1 \qquad -\frac{3}{2}\eta_1 - \eta_2 < \eta_3 < -\frac{1}{4}\eta_1 + \frac{1}{4}\eta_2 \tag{90}$$

The estimates obtained within this contribution will be discussed with respect to the above relations in section 6.

4.4. Voigt-estimates for strain gradient effective media

As it can be seen e.g. from (43) and (51), the strain gradient part can be discussed isolated by setting $\boldsymbol{E} = \boldsymbol{0}$. The whole set of equations can be derived by superimposing the results with the corresponding counterparts of the theory of simple continua discussed above.

Following the general idea of the Voigt-estimate, we evaluate Π for a kinematically admissible strain field by setting

$$\hat{u}_i = \frac{1}{2}\left[H_{ijk} - H_{jki} + H_{kij}\right] x_j x_k - H_{ijk} X_k x_j \quad , \quad \boldsymbol{x} \in \mathcal{B} \tag{91}$$

which means that we assume that the displacements (43 a) are not only prescribed at the outer boundary but also inside the volume element. The corresponding strains are

$$\hat{\varepsilon}_{kl} = \frac{1}{2}(H_{klp} + H_{lkp})\xi_p \tag{92}$$

and we obtain for $\Pi(\hat{\boldsymbol{u}})$

$$\Pi(\hat{\boldsymbol{u}}) = \frac{1}{2} H_{ijo} D^*_{ijoklp} H_{klp} \tag{93}$$

with

$$D^*_{ijoklp} = < L_{ijkl}\xi_o\xi_p > \ . \tag{94}$$

It follows from (17) together with (53) and (51) that

$$\boldsymbol{H} \vdots \boldsymbol{D} \vdots \boldsymbol{H} \leq \boldsymbol{H} \vdots \boldsymbol{D}^* \vdots \boldsymbol{H} \, . \tag{95}$$

However, (94) doesn't fulfill the requirements (81). Therefore, it cannot be used as an approximation for $\boldsymbol{D}$. In fact, e.g.

$$D^*_{ijjklp} = < L_{ijkl}\xi_p\xi_j > \tag{96}$$

does not vanish in general. Though, $\boldsymbol{D}^*$ can be modified properly in order to obtain a useful approximation. To do so we express $\boldsymbol{H}'$ as follows

$$H'_{ijk} = G_{ijkuvw} H_{uvw} \tag{97}$$

with

$$G_{ijkuvw} = \delta_{iu}\delta_{jv}\delta_{kw} - \frac{1}{4}\left[\delta_{ik}\delta_{uw}\delta_{jv} + \delta_{iu}\delta_{jk}\delta_{vw}\right] \tag{98}$$

where the sixth order tensor $\boldsymbol{G}$ possesses the symmetries

$$G_{ijkuvw} = G_{uvwijk} = G_{jikuvw} = G_{ijkvuw} \, . \tag{99}$$

We introduce a new constitutive tensor $\bar{\boldsymbol{D}}$, defined by

$$\bar{\boldsymbol{D}} = \boldsymbol{G} \vdots \boldsymbol{D}^* \vdots \boldsymbol{G} \tag{100}$$

whose coordinates are given as follows

$$\begin{aligned}\bar{D}_{ijkxyz} = D^*_{ijkxyz} - \frac{1}{4}\left[D^*_{ijktyt}\delta_{xz} + D^*_{ijkxtt}\delta_{yz}\right] - \frac{1}{4}\left[D^*_{tjtxyz}\delta_{ik} + D^*_{ittxyz}\delta_{jk}\right] \\ + \frac{1}{16}\left[\delta_{ik}\left(D^*_{vjvtyt}\delta_{xz} + D^*_{vjvxtt}\delta_{yz}\right) + \delta_{jk}\left(D^*_{ivvtyt}\delta_{xz} + D^*_{ivvxtt}\delta_{yz}\right)\right] .\end{aligned} \tag{101}$$

However, $\bar{\boldsymbol{D}}$ is no bound. In order to derive an upper bound which fulfills (81), an isotropic sixth-order tensor $\bar{\boldsymbol{D}}^{\mathrm{V}}$ is introduced. $\bar{\boldsymbol{D}}^{\mathrm{V}}$ is completely defined by its coefficients

$$\begin{aligned}\bar{\eta}_1^{\mathrm{V}} &= \bar{\eta}_1 + \Delta\bar{\eta}_1 & \bar{\eta}_2^{\mathrm{V}} &= \bar{\eta}_2 + \Delta\bar{\eta}_2 & \bar{\eta}_3^{\mathrm{V}} &= \bar{\eta}_3 + \Delta\bar{\eta}_3 \\ \bar{\eta}_4^{\mathrm{V}} &= \bar{\eta}_4 + \Delta\bar{\eta}_4 & \bar{\eta}_5^{\mathrm{V}} &= \bar{\eta}_5 + \Delta\bar{\eta}_5\end{aligned} \tag{102}$$

where the $\Delta\bar{\eta}_k$ have to be determined by means of the following conditions. First,

$$\Delta\bar{\eta}_4 = \frac{1}{8}\Delta\bar{\eta}_1 - \frac{1}{4}\Delta\bar{\eta}_2 + \frac{1}{4}\Delta\bar{\eta}_3 \tag{103}$$

$$\Delta\bar{\eta}_5 = -\frac{1}{2}\Delta\bar{\eta}_1 - 2\Delta\bar{\eta}_3 \tag{104}$$

must hold to ensure that $\bar{\boldsymbol{D}}^{\mathrm{V}}$ fulfills (81). Furthermore, demanding

$$\boldsymbol{H} \vdots \boldsymbol{D}^* \vdots \boldsymbol{H} = \boldsymbol{H} \vdots \bar{\boldsymbol{D}}^{\mathrm{V}} \vdots \boldsymbol{H} \tag{105}$$

ensures that

$$\boldsymbol{H} \vdots \boldsymbol{D} \vdots \boldsymbol{H} \leq \boldsymbol{H} \vdots \bar{\boldsymbol{D}}^{\mathrm{V}} \vdots \boldsymbol{H} \tag{106}$$

holds. Therefore, the coefficients $\Delta\bar{\eta}_1$, $\Delta\bar{\eta}_3$ and $\Delta\bar{\eta}_2$ can be determined by setting the eigenvalues of the tensor $\bar{\boldsymbol{D}}^{\mathrm{V}} - \boldsymbol{D}^*$ equal to zero and taking into account (103) and (104). The solution reads in general

$$\Delta\bar{\eta}_1 = \frac{8\,\bar{\eta}_3^2}{\bar{\eta}_1 + 6\bar{\eta}_3 - \bar{\eta}_2} \qquad \Delta\bar{\eta}_2 = 0 \qquad \Delta\bar{\eta}_3 = -\frac{1}{4}\Delta\bar{\eta}_1 \tag{107}$$

This will be discussed for porous elastic micro-structures in section 6.

4.5. Reuss estimates for strain gradient effective media

In order to derive a Reuss estimate we start from the complementary potential Π^{c} for prescribed displacements given by (43). Setting $\boldsymbol{X} = \boldsymbol{0}$ does not change the final

result but it makes the calculations more transparent. Doing so, we have $\boldsymbol{x} = \boldsymbol{\xi}$. Then Π^{c} reads

$$\Pi^{\mathrm{c}}(\hat{\boldsymbol{\sigma}}) = \frac{1}{2}\int\limits_{\mathcal{B}} \hat{\sigma}_{ij} L^{-1}_{ijkl} \hat{\sigma}_{kl}\,\mathrm{d}V - \frac{1}{2}\int\limits_{\partial\mathcal{B}} \hat{\sigma}_{iv}(H_{ijk} - H_{jki} + H_{kij})\xi_j \xi_k n_v\,\mathrm{d}A \tag{108}$$

for any statically admissible stress field $\hat{\boldsymbol{\sigma}}$. Applying Gauss's integral theorem for the surface integral and taking into account the symmetries of $\hat{\boldsymbol{\sigma}}$ and $\boldsymbol{H}$ leads to

$$\Pi^{\mathrm{c}}(\hat{\boldsymbol{\sigma}}) = \frac{1}{2}\int\limits_{\mathcal{B}} \hat{\sigma}_{ij} L^{-1}_{ijkl} \hat{\sigma}_{kl}\,\mathrm{d}V - \int\limits_{\mathcal{B}} \hat{\sigma}_{ij} H_{ijk}\xi_k\,\mathrm{d}V\,. \tag{109}$$

We choose a linear stress field which fulfills the equilibrium conditions (3) by setting

$$\hat{\sigma}_{ij} = \left(\alpha_{ijp} - \frac{1}{4}\left[\delta_{ip}\alpha_{jkk} + \delta_{jp}\alpha_{ikk}\right]\right)\xi_p \tag{110}$$

with constant coefficients α_{ijk}. This can be written more concisely as

$$\hat{\sigma}_{ij} = G_{ijpuvw}\alpha_{uvw}\xi_p \tag{111}$$

where $\boldsymbol{G}$ is already given by (98). Substituting (111) into (109) and normalizing by the volume B of the VE gives

$$\frac{1}{B}\Pi^{\mathrm{c}}(\hat{\boldsymbol{\sigma}}) = \frac{1}{2}\alpha_{uvw}G_{uvwijp} < L^{-1}_{ijkl}\xi_p\xi_q > G_{klqrst}\alpha_{rst} - G_{ijpuvw}\alpha_{uvw}H_{ijk} < \xi_p\xi_k > \,. \tag{112}$$

Using (32) as provided within Section 4.1 we obtain

$$\frac{1}{B}\Pi^{\mathrm{c}}(\hat{\boldsymbol{\sigma}}) = \frac{1}{2}\alpha_{uvw}G_{uvwijp} < L^{-1}_{ijkl}\xi_p\xi_q > G_{klqrst}\alpha_{rst} - G_{ijkuvw}\alpha_{uvw}H_{ijk}\kappa\,, \tag{113}$$

where κ is some number which depends on the geometry of the VE. For instance, for a spherical VE with a spherical void located in its center $\kappa = (1-f)\kappa^{\mathrm{M}}$ has to be used with κ^{M} as given in Table 1.

The optimal choice for $\boldsymbol{\alpha}$ in order to minimize (113) is

$$\alpha_{ijq} = G^{-1}_{ijquvw} < L^{-1}_{uvkl}\xi_w\xi_p >^{-1} H_{klp} \tag{114}$$

which results in

$$\frac{1}{B}\Pi^{\mathrm{c}}(\hat{\boldsymbol{\sigma}}) = -\frac{1}{2}H_{ijo}\widetilde{D}^{*}_{ijoklp}H_{klp} \tag{115}$$

with

$$\widetilde{D}^{*}_{ijoklp} = \kappa^2 < L^{-1}_{ijkl}\xi_o\xi_p >^{-1}\,. \tag{116}$$

It follows from (19) together with (53) and (51) that

$$\boldsymbol{H} \vdots \widetilde{\boldsymbol{D}}^{*} \vdots \boldsymbol{H} \leq \boldsymbol{H} \vdots \boldsymbol{D} \vdots \boldsymbol{H} \tag{117}$$

holds, but, similar to the upper bound problem, $\widetilde{\boldsymbol{D}}^*$ does not fulfill the conditions (81). The same strategy used before in section 4.4 will be applied to overcome this problem. First, the tensor

$$\widetilde{\boldsymbol{D}} = \boldsymbol{G} \vdots \widetilde{\boldsymbol{D}}^* \vdots \boldsymbol{G} \tag{118}$$

is defined, which fulfills (81). Because $\widetilde{\boldsymbol{D}}$ is an isotropic tensor, it is completely defined by the coefficients $\widetilde{\eta}_1, ..., \widetilde{\eta}_5$. Furthermore, an isotropic sixth-order tensor $\bar{\boldsymbol{D}}^{\mathrm{R}}$ is introduced, whose coefficients are defined by

$$\begin{aligned} \bar{\eta}_1^{\mathrm{R}} &= \widetilde{\eta}_1 + \Delta\widetilde{\eta}_1 & \bar{\eta}_2^{\mathrm{R}} &= \widetilde{\eta}_2 + \Delta\widetilde{\eta}_2 & \bar{\eta}_3^{\mathrm{R}} &= \widetilde{\eta}_3 + \Delta\widetilde{\eta}_3 \\ \bar{\eta}_4^{\mathrm{R}} &= \widetilde{\eta}_4 + \Delta\widetilde{\eta}_4 & \bar{\eta}_5^{\mathrm{R}} &= \widetilde{\eta}_5 + \Delta\widetilde{\eta}_5 \end{aligned} \tag{119}$$

where the $\Delta\widetilde{\eta}_k$ have to be determined by means of the following conditions. First,

$$\Delta\widetilde{\eta}_4 = \frac{1}{8}\Delta\widetilde{\eta}_1 - \frac{1}{4}\Delta\widetilde{\eta}_2 + \frac{1}{4}\Delta\widetilde{\eta}_3 \tag{120}$$

$$\Delta\widetilde{\eta}_5 = -\frac{1}{2}\Delta\widetilde{\eta}_1 - 2\Delta\widetilde{\eta}_3 \tag{121}$$

must hold to ensure that $\bar{\boldsymbol{D}}^{\mathrm{R}}$ fulfills (81). Furthermore, demanding

$$\boldsymbol{H} \vdots \widetilde{\boldsymbol{D}}^* \vdots \boldsymbol{H} = \boldsymbol{H} \vdots \bar{\boldsymbol{D}}^{\mathrm{R}} \vdots \boldsymbol{H} \tag{122}$$

ensures that

$$\boldsymbol{H} \vdots \bar{\boldsymbol{D}}^{\mathrm{R}} \vdots \boldsymbol{H} \leq \boldsymbol{H} \vdots \boldsymbol{D} \vdots \boldsymbol{H} \tag{123}$$

holds. The coefficients $\Delta\widetilde{\eta}_1$, $\Delta\widetilde{\eta}_2$ and $\Delta\widetilde{\eta}_3$ can be determined by setting the eigenvalues of the tensor $\bar{\boldsymbol{D}}^{\mathrm{R}} - \widetilde{\boldsymbol{D}}^*$ equal to zero and taking into account (120) and (121). The solution of the problem is given analogously to (107).

5. Alternative approximation scheme

If linear strains according to (91) are assumed inside the VE, the equilibrium conditions cannot be fulfilled. Therefore, a second strain field $\widetilde{\boldsymbol{\varepsilon}}(\boldsymbol{x})$ is superposed. For $\widetilde{\boldsymbol{\varepsilon}}(\boldsymbol{x})$ a third order polynomial is chosen here

$$\widetilde{\varepsilon}_{kl} = a_{kl} + b_{klp}\xi_p + c_{klpq}\xi_p\xi_p + d_{klpqr}\xi_p\xi_q\xi_r \,. \tag{124}$$

We demand that the mean values of $\widetilde{\varepsilon}_{kl}$ vanish

$$< \widetilde{\varepsilon}_{kl} > = a_{kl} + b_{klp} < \xi_p > + c_{klpq} < \xi_p\xi_q > + d_{klpqr} < \xi_p\xi_q\xi_r > = 0_{kl}. \tag{125}$$

The mean values of the odd functions in (124) vanish automatically and with respect to the even functions

$$a_{kl} = -\kappa\, c_{klpp} \tag{126}$$

must hold. However, it turns out that a polynomial of second order taking into account (126) leads to the trivial result

$$b_{ijk} = -H_{ijk} \qquad , \qquad c_{ijkl} = 0_{ijkl} \,. \tag{127}$$

Therefore, we limit ourself to the ansatz

$$\widetilde{\varepsilon}_{kl} = d_{klpqr}\xi_p\xi_q\xi_r \,. \tag{128}$$

In what follows, we use the abbreviation

$$\bar{H}_{ijk} = \frac{1}{2}(H_{ijk} + H_{jik}) \tag{129}$$

in order to deal with shorter equations. At the end, we will incorporate the symmetries into the constitutive equations. The corresponding stresses according to (5) read

$$\sigma_{ij} = L_{ijkl}\left[\bar{H}_{klp}\xi_p + d_{klpqr}\xi_p\xi_q\xi_r\right] \,. \tag{130}$$

For an arbitrary spatial dependence of $\boldsymbol{L}$, the equilibrium conditions cannot be fulfilled in general,

$$\sigma_{ij,j} = L_{ijkl,j}\left[\bar{H}_{klp}\xi_p + d_{klpqr}\xi_p\xi_q\xi_r\right] + L_{ijkl}\left[\bar{H}_{klj} + 3d_{klpqj}\xi_p\xi_q\right] \neq 0_i \,. \tag{131}$$

There are various way to proceed in order to calculate the coefficients d_{klpqr} properly. Here, we will discuss two of them:

- Demanding that the equilibrium conditions are fulfilled in a least square sense

$$\Omega_1 = < \sigma_{ij,j}\sigma_{iv,v} > \Rightarrow \text{ Min} \tag{132}$$

or

- demanding that the strain energy density reaches a mimimal value,

$$\Omega_2 = \frac{1}{2} < \sigma_{ij}\varepsilon_{ij} > \Rightarrow \text{ Min} \,. \tag{133}$$

While the second choice works without problems for every reasonable spatial variation of the material properties at the microlevel, the first strategy will obviously fail for discontinuities with respect to these properties. This can be seen by the following example. Imagine a two-phase composite where every phase can be described by isotropic linear elasticity with constant elastic properties denoted by Lame's constants λ and μ. Furthermore, we assume a spherical VE, where the spatial variation of the material properties depend only on the distance from the origin, meassured by the radius r. If e.g. λ is expressed now by means of a Heaviside-function, integrals over squared Dirac-delta functions will appear in (132) which causes infinite effective properties. It is worth noting, that none of these two concepts mentioned above gives a result which automatically fulfills (81).

In the sequel, we restrict ourself to microstructures with spherical voids surrounded by an isotropic linear elastic matrix material. The matrix material has constant elastic properties given by

$$L_{ijkl} = \begin{cases} \lambda\delta_{ij}\delta_{kl} + \mu(\delta_{ik}\delta_{jl} + \delta_{il}\delta_{jk}) & \boldsymbol{\xi} \in \mathcal{B}^{\mathrm{M}} \\ 0 & \boldsymbol{\xi} \in \mathcal{B}^{\mathrm{I}} \end{cases} \tag{134}$$

with the Lame's constants λ and μ.

Evaluating (80) for (130) yields the constraint

$$M_{ijj} = < \sigma_{ij}\xi_j > = (1-f)\left[\alpha^{\mathrm{M}} L_{ijkl}\bar{H}_{klj} + L_{ijkl}\, d_{klvvj}\right] = 0_i \tag{135}$$

with

$$\alpha^{\mathrm{M}} = \frac{\kappa^{\mathrm{M}}}{3\phi^{\mathrm{M}}} \tag{136}$$

if (38) is taken into account. Equation (135) will be satisfied via Lagrange's technique using the multipliers Λ_i. This will be discussed in the following only for the energetic criterion (133). The constraint extreme value problem reads

$$\begin{aligned} \Omega_2 := \quad & \frac{1}{2}(1-f) < L_{ijkl}\left[\bar{H}_{klp}\xi_p + d_{klpqr}\xi_p\xi_q\xi_r\right]\left[\bar{H}_{ijs}\xi_s + d_{ijstv}\xi_s\xi_t\xi_v\right] >_{\mathcal{B}^{\mathrm{M}}} \\ + \quad & (1-f)\,\Lambda_i\left[\alpha^{\mathrm{M}} L_{ijkl}\bar{H}_{klj} + L_{ijkl}\, d_{klvvj}\right] \quad \Rightarrow \quad \mathsf{Min}\,. \end{aligned} \tag{137}$$

Derivation of (137) with respect to the coefficients d_{abxyz} and Λ_v, respectively, gives

$$\frac{\partial\Omega_2}{\partial\, d_{abxyz}} = (1-f)\left\{L_{abkl}\left[\bar{H}_{klp}A_{pxyz} + d_{klpqr}\, B_{pqrxyz}\right] + \Lambda_i L_{izab}\delta_{xy}\right\} \quad = 0_{abxyz} \tag{138}$$

$$\frac{\partial\Omega_2}{\partial\Lambda_v} = (1-f)\left\{\alpha^{\mathrm{M}} L_{vjkl}\bar{H}_{klj} + L_{vjkl}\, d_{klwwj}\right\} \qquad = 0_v\,. \tag{139}$$

For arbitrary void volume fractions f, $f \in (0,1)$, these conditions can only be satisfied if the terms within the curly brackets vanish. The geometrical moment tensors $\boldsymbol{A}$ and $\boldsymbol{B}$ have to be evaluated by integrating only over the matrix volume. In the following we omit indicating this explicitely by the superindex M, in order to avoid overloaded equations.

Equation (138) can be used to express the d_{klvwj} as functions of the Λ_i

$$d_{klvwj} = -\bar{H}_{klp}A_{pxyz}B^{-1}_{xyzvwj} - \Lambda_i I_{kliz}\delta_{xy}B^{-1}_{xyzvwj} \tag{140}$$

where $\boldsymbol{I}$ is the fourth-order unit tensor

$$I_{kliz} = \frac{1}{2}[\delta_{ik}\delta_{lz} + \delta_{kz}\delta_{il}]\,. \tag{141}$$

Putting (140) and (139) together leads to

$$\Lambda_m = \left[\alpha^{\mathrm{M}} L_{vjkl}\bar{H}_{klj} - L_{vjkl}\bar{H}_{klp}A_{pxyz}B^{-1}_{xyzwwj}\right]\gamma^{-1}_{vm} \tag{142}$$

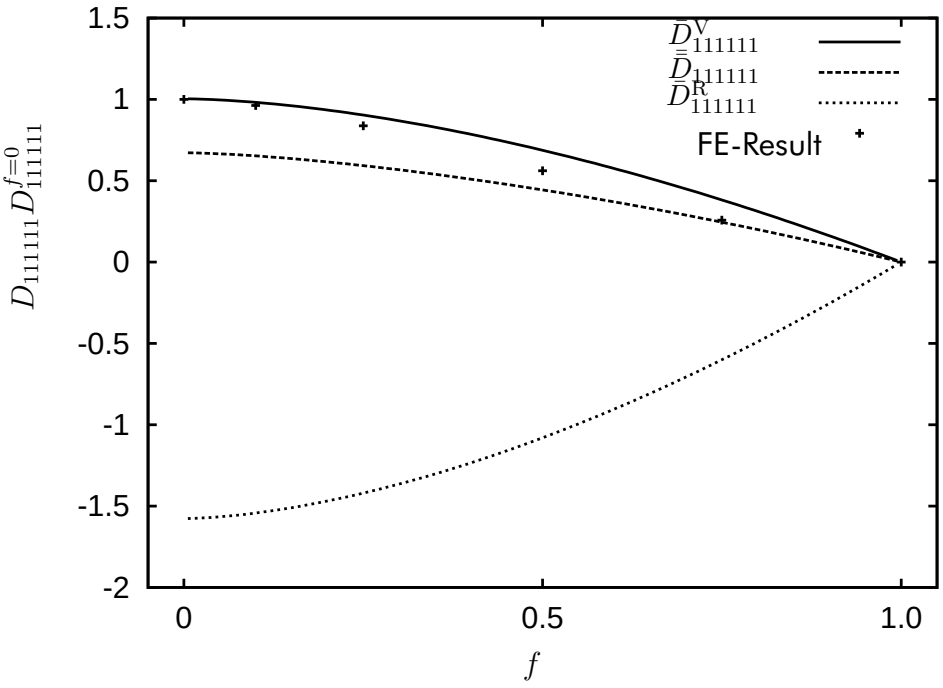

Fig. 2: Comparision between numerically determined coefficients D_{111111} and the corresponding estimations for $\nu = 0.3$ and varying porosity f. All results have been normalized by the value obtained for D_{111111} from the numerical solution of the boundary value problem for $f = 0$.

with

$$\gamma_{iv} = L_{izvj} B^{-1}_{jzwwyy} \,. \tag{143}$$

Using the relations for isotropic and fully symmetric tensors provided in C, γ_{iv} can be expressed by

$$\gamma_{iv} = \frac{1}{\theta^{\mathrm{M}}} L_{ijvj} \,. \tag{144}$$

Using the elasticity tensor (134), the γ_{iv} can be written as

$$\gamma_{iv} = \frac{\lambda + 4\mu}{\theta^{\mathrm{M}}} \, \delta_{iv} \,. \tag{145}$$

Furthermore, the Λ_m can be simplified as follows

$$\begin{aligned}
\Lambda_m &= L_{vjkl} \frac{\theta^{\mathrm{M}}}{\lambda + 4\mu} \delta_{vm} \left[\alpha^{\mathrm{M}} \delta_{jp} - \phi^{\mathrm{M}} (\delta_{px}\delta_{yz} + \delta_{py}\delta_{xz} + \delta_{pz}\delta_{xy}) B^{-1}_{xyzwwj} \right] \bar{H}_{klp} \\
&= \frac{\theta^{\mathrm{M}}}{\lambda + 4\mu} L_{mjkl} \left[\alpha^{\mathrm{M}} \delta_{jp} - 3\phi^{\mathrm{M}} \frac{1}{\theta^{\mathrm{M}}} \delta_{pj} \right] \bar{H}_{klp} \\
&= \Gamma L_{mklp} \bar{H}_{klp}
\end{aligned} \tag{146}$$

with

$$\Gamma = \frac{\alpha^{\mathrm{M}}\theta^{\mathrm{M}} - 3\phi^{\mathrm{M}}}{\lambda + 4\mu}\,. \tag{147}$$

Using the result (146) for the Λ_i, the coefficients d_{klvwj} can be derived from (140)

$$\begin{aligned} d_{klpqr} =& -\bar{H}_{klv}A_{vxyz}B^{-1}_{xyzpqr} - \Gamma L_{iuvw}\bar{H}_{uvw}\, I_{kliz}\delta_{xy}B^{-1}_{xyzpqr} \\ =& -\bar{H}_{klv}A_{vxyz}B^{-1}_{xyzpqr} - \Gamma L_{kuvw}H_{uvw}\, B^{-1}_{lzzpqr} \\ =& -3\phi^{\mathrm{M}}\bar{H}_{klv}B^{-1}_{vzzpqr} - \Gamma L_{kuvw}\bar{H}_{uvw}\, B^{-1}_{lzzpqr}\,. \end{aligned} \tag{148}$$

The stress field within the matrix material is now completely determined by (130) while the stresses within the void vanish. According to (50), the corresponding higher order stresses have to be calculated in order to derive the approximation $\bar{\bar{\boldsymbol{D}}}$ for the higher order elasticity tensor $\boldsymbol{D}$. From the definition of the M_{ijk} (46) together with (38), (146) and (148), we obtain

$$\begin{aligned} <\sigma_{ij}\xi_o> =& (1-f)L_{ijkl}\left[\kappa^{\mathrm{M}}\bar{H}_{klo} - 3\phi^{\mathrm{M}}H_{klv}B^{-1}_{vzzpqr}A_{qpro} - \Gamma L_{kuvw}\bar{H}_{uvw}B^{-1}_{lzzpqr}A_{pqro}\right] \\ =& (1-f)L_{ijkl}\left[\kappa^{\mathrm{M}}\bar{H}_{klo} - 9(\phi^{\mathrm{M}})^2\bar{H}_{klv}B^{-1}_{vzzppo} - \Gamma L_{kuvw}\bar{H}_{uvw}B^{-1}_{lzzppo}3\phi^{\mathrm{M}}\right] \\ =& (1-f)L_{ijkl}\left[\left(\kappa^{\mathrm{M}} - \frac{9(\phi^{\mathrm{M}})^2}{\theta^{\mathrm{M}}}\right)\delta_{ku}\delta_{vl}\delta_{ow} - \Gamma\frac{3\phi^{\mathrm{M}}}{\theta^{\mathrm{M}}}L_{kuvw}\delta_{lo}\right]\bar{H}_{uvw} \end{aligned} \tag{149}$$

where again the relations given in C have been used. It can be show that $<\sigma_{ij}\xi_j> = 0_i$ holds. Finally, the sixth order constitutive tensor $\bar{\bar{\boldsymbol{D}}}$ can be directly deduced from (149)

$$\begin{aligned} \bar{\bar{D}}_{ijouvw} =& \bar{\bar{\eta}}_1\delta_{ij}\delta_{uv}\delta_{ow} + \bar{\bar{\eta}}_2(\delta_{iu}\delta_{jv} + \delta_{iv}\delta_{ju})\delta_{ow} \\ &+ \bar{\bar{\eta}}_3[\delta_{ij}(\delta_{ou}\delta_{vw} + \delta_{ov}\delta_{uw}) + \delta_{uv}(\delta_{iw}\delta_{jo} + \delta_{io}\delta_{jw})] \\ &+ \bar{\bar{\eta}}_4[\delta_{io}(\delta_{ju}\delta_{vw} + \delta_{jv}\delta_{uw}) + \delta_{jo}(\delta_{iu}\delta_{vw} + \delta_{iv}\delta_{uw})] \end{aligned} \tag{150}$$

with

$$\bar{\bar{\eta}}_1 = \lambda\beta_1 + \lambda^2\beta_2 \qquad \bar{\bar{\eta}}_2 = \mu\beta_1 \tag{151}$$

$$\bar{\bar{\eta}}_3 = \lambda\mu\beta_2 \qquad \bar{\bar{\eta}}_4 = \mu^2\beta_2 \tag{152}$$

and

$$\beta_1 = (1-f)\left(\kappa^{\mathrm{M}} - \frac{9(\phi^{\mathrm{M}})^2}{\theta^{\mathrm{M}}}\right) \qquad \beta_2 = -\frac{\beta_1}{\lambda + 4\mu} \tag{153}$$

if $\boldsymbol{H}$ is replaced by (129). The approximation $\bar{\bar{\boldsymbol{D}}}$ is no bound at all because the displacement field which corresponds to the employed strain field does not fulfill the boundary conditions (43 a).

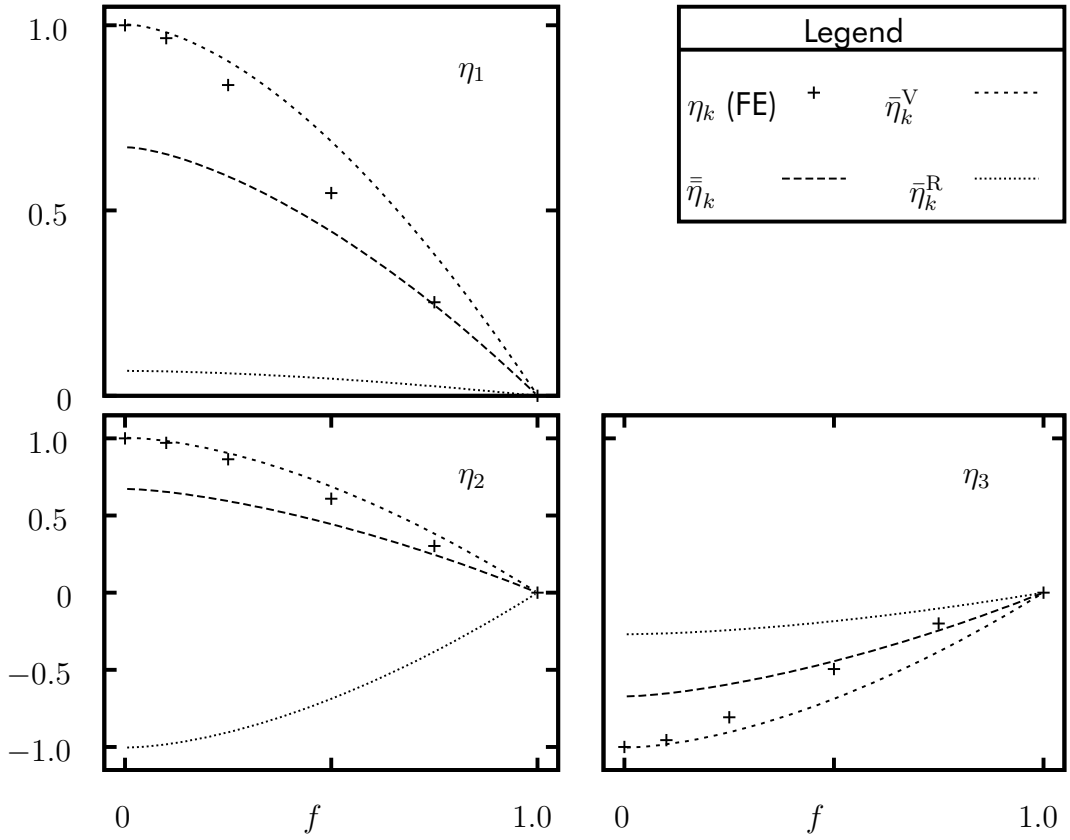

Fig. 3: Numerically obtained results for the independent coefficients η_1, η_2 and η_3, together with the corresponding analytical approximations for $\nu = 0.3$ and varying porosity f. All results have been normalized by the values obtained for the corresponding η_k from the numerical solution of the boundary value problem for $f = 0$.

	Voigt-estimate			Reuss-estimate		
k	$\boldsymbol{D}^*$	$\bar{\boldsymbol{D}}$	$\bar{\boldsymbol{D}}^{\mathrm{V}}$	$\widetilde{\boldsymbol{D}}^*$	$\widetilde{\boldsymbol{D}}$	$\bar{\boldsymbol{D}}^{\mathrm{R}}$
1	λ	λ	$\frac{4\lambda\mu}{\lambda+4\mu}$	$-\frac{\lambda\mu}{3\lambda+\mu}$	$-\frac{\lambda\mu}{3\lambda+\mu}$	$-\frac{4\lambda\mu}{11\lambda+4\mu}$
2	μ	μ	μ	μ	μ	μ
3	0	$-\frac{1}{4}\lambda$	$-\frac{\lambda\mu}{\lambda+4\mu}$	0	$\frac{1}{4}\frac{\lambda\mu}{3\lambda+\mu}$	$\frac{\lambda\mu}{11\lambda+4\mu}$
4	0	$\frac{1}{16}(\lambda-4\mu)$	$-\frac{\mu^2}{\lambda+4\mu}$	0	$-\frac{1}{16}\frac{\mu(13\lambda+4\mu)}{3\lambda+4\mu}$	$-\frac{\mu(3\lambda+\mu)}{11\lambda+4\mu}$
5	0	0	0	0	0	0

Tab. 2: Coefficients η_k, $k=1,...,5$ of the different isotropic sixth-order elasticity tensors involved in the calculations of the Voigt and Reuss bounds for porous elastic microstructures normalized by $\bar{\beta}$.

6. Discussion of the results for porous elastic microstructures

In order to evaluate the quality of the analytical approximations, the boundary value problem has been solved numerically for a spherical VE with a spherical void in its center. Different values of the void volume fraction f have been considered and the multi-purpose finite element program Abaqus ABAQUS (2005) was used.

The matrix material was supposed to be characterized by (134) and $E=200000$MPa and $\nu=0.3$ have been chosen for the Young's modulus E and the Poisson's ratio ν, respectively. All simulations were performed using 10-node bi-quadratic terahedral elements.

Taking into account (38) together with the other relations discussed within the previous section, the material tensor $\boldsymbol{D}^*$ (94) is given by

$$D^*_{ijouvw} = \eta^*_1\delta_{ij}\delta_{uv}\delta_{ow} + \eta^*_2(\delta_{iu}\delta_{jv}+\delta_{iv}\delta_{ju})\delta_{ow} \tag{154}$$

with the two material parameters

$$\eta^*_1 = \bar{\beta}\lambda \qquad\qquad \eta^*_2 = \bar{\beta}\mu \tag{155}$$

where

$$\bar{\beta} = \frac{R^2}{5}(1-\sqrt[3]{f^5})\,. \tag{156}$$

The material tensor $\bar{\boldsymbol{D}}$ was already given by (101) for the general case. Based on (154), $\bar{\boldsymbol{D}}$ can be calculated for a spherical VE with a spherical void in its center. The

final result reads

$$\begin{aligned}\bar{D}_{ijouvw} = \; & \bar{\eta}_1\delta_{ij}\delta_{uv}\delta_{ow} + \bar{\eta}_2(\delta_{iu}\delta_{jv} + \delta_{iv}\delta_{ju})\delta_{ow} \\ & + \bar{\eta}_3[\delta_{ij}(\delta_{ou}\delta_{vw} + \delta_{ov}\delta_{uw}) + \delta_{uv}(\delta_{iw}\delta_{jo} + \delta_{io}\delta_{jw})] \\ & + \bar{\eta}_4[\delta_{io}(\delta_{ju}\delta_{vw} + \delta_{jv}\delta_{uw}) + \delta_{jo}(\delta_{iu}\delta_{vw} + \delta_{iv}\delta_{uw})] \end{aligned} \tag{157}$$

with four independent material constants

$$\bar{\eta}_1 = \; \bar{\beta}\lambda \qquad\qquad \bar{\eta}_2 = \; \bar{\beta}\mu \tag{158}$$

$$\bar{\eta}_3 = -\frac{1}{4}\bar{\beta}\lambda \qquad\qquad \bar{\eta}_4 = \frac{1}{16}\bar{\beta}(\lambda - 4\mu) \tag{159}$$

where $\bar{\beta}$ is given by (156). From (154) and (157) it can be seen that $\eta_1^* = \bar{\eta}_1$ and $\eta_2^* = \bar{\eta}_2$. The Voigt estimate was determined as proposed at the end of section 4.4. Also the Reuss-estimate has been calculated, where the scheme outlined in section 4.3 was used in order to perform the involved calculation of the inverse of a sixth-order tensor. Both estimates have the very same structure as $\bar{\boldsymbol{D}}$. Therefore, $\bar{\boldsymbol{D}}^{\mathrm{V}}$ and $\bar{\boldsymbol{D}}^{\mathrm{R}}$ can be obtained from (157) just by replacing the $\bar{\eta}_k$ by $\bar{\eta}_k^{\mathrm{V}}$ and $\bar{\eta}_k^{\mathrm{R}}$, respectively. The coefficients of $\bar{\boldsymbol{D}}^{\mathrm{V}}$ and $\bar{\boldsymbol{D}}^{\mathrm{R}}$ are given by

$$\bar{\eta}_1^{\mathrm{V}} = \; 4\bar{\beta}\frac{\lambda\mu}{\lambda + 4\mu} \qquad\qquad \bar{\eta}_2^{\mathrm{V}} = \; \bar{\beta}\mu \tag{160}$$

$$\bar{\eta}_3^{\mathrm{V}} = -\bar{\beta}\frac{\lambda\mu}{\lambda + 4\mu} \qquad\qquad \bar{\eta}_4^{\mathrm{V}} = -\bar{\beta}\frac{\mu^2}{\lambda + 4\mu} \tag{161}$$

and

$$\bar{\eta}_1^{\mathrm{R}} = -\bar{\beta}\frac{4\lambda\mu}{11\lambda + 4\mu} \qquad\qquad \bar{\eta}_2^{\mathrm{R}} = \; \bar{\beta}\mu \tag{162}$$

$$\bar{\eta}_3^{\mathrm{R}} = \; \bar{\beta}\frac{\lambda\mu}{11\lambda + 4\mu} \qquad\qquad \bar{\eta}_4^{\mathrm{R}} = -\bar{\beta}\frac{\mu(3\lambda + \mu)}{11\lambda + 4\mu}\,, \tag{163}$$

respectively. The $\bar{\eta}_k^{\mathrm{R}}$ fulfill (88) while the $\bar{\eta}_k^{\mathrm{R}}$ met the condition (89). Therefore, $\bar{\boldsymbol{D}}^{\mathrm{V}}$ and $\bar{\boldsymbol{D}}^{\mathrm{R}}$ are positive semi-definit with no more than three zero eigenvalues. The coefficients of all tensors involved in the calculation of $\bar{\boldsymbol{D}}^{\mathrm{V}}$ and $\bar{\boldsymbol{D}}^{\mathrm{R}}$ are summarized in Table 2. A somewhat surprising result is the fact that $\bar{\eta}_2^{\mathrm{V}}$ and $\bar{\eta}_2^{\mathrm{R}}$ are identical. The approximation $\bar{\bar{\boldsymbol{D}}}$ was already obtained only for porous elastic materials within the previous section, see (150) and it can be proven that $\bar{\bar{\boldsymbol{D}}}$ fulfills (88).

Exemplarily, $\bar{D}^{\mathrm{V}}_{111111}$, $\bar{D}^{\mathrm{R}}_{111111}$ and $\bar{\bar{D}}_{111111}$ are compared with the corresponding numerical results for different values of the porosity f what is shown in Figure 2. These components contain all coefficients $\bar{\eta}_k^{\mathrm{V}}$, $\bar{\eta}_k^{\mathrm{R}}$ and $\bar{\bar{\eta}}_k$, respectively. That's why they have been chosen for the discussion of the results. The numerical values for D_{111111} were obtained by prescribing the boundary displacements according to (43a) setting all coefficients equal to zero except H_{111} for which $H_{111} = 0.1$ was used. The corresponding higher order stresses M_{111} were determined by a postprocessing routine according to its definition (46), where the value 1952N/mm was obtained for example for M_{111} in the case of $f = 0$. Then

$$D_{111111} = \frac{M_{111}}{H_{111}} \tag{164}$$

has been determined for all considered void volume fractions. An example for the finite element meshes used for the numerical calculations is shown in Figure 4.

The Voigt-estimate $\bar{D}^{\mathrm{V}}_{111111}$ is almost exact for $f = 0$ and approximates well the true material parameter D_{111111} for small values of f. On the other hand, the alternative approximation $\bar{\bar{D}}_{111111}$ underestimates the behaviour of the VE especially for small void volume fractions, while the approximation gets better as the void volume fraction increases. However, constitutive relations for strain gradient elasticity obtained by prescribing quadratic displacements make the material in general too stiff. Therefore, an underestimation of the material properties is not necessarily a disadvantage.

Solving the boundary value problem for more eloborated choices with respect to the H_{ijk} allows to extract the particular η_k separately. The results are shown together with the corresponding analytical approximations in Figure 3. Again, the Voigt-estimates are almost exact for $f = 0$ and approximate well the corresponding numerical results for small void volume fractions while the alternative approximations are closer to the numerical results for large values of f. Although the importance of the Reuss-estimate $\bar{D}^{\mathrm{R}}_{111111}$ is undoubted because of its lower bound property, the results plotted in Figure 3 show that it does not provide a useful approximation.

The fifth coefficient is zero for all approximations but the numerical results reveal that the true η_5 does not vanish. However, η_5 is small compared with all other coefficients, e.g $\frac{|\eta_5|}{|\eta_1|} < 0.05$.

It can be seen from (46) that the components of $\boldsymbol{D}$ have to be proportional to the Young's modulus of the matrix material. Furthermore, all geometrical quantites included in $\boldsymbol{D}$ can be expressed by R^2 and the void volume fraction f. Hence, the D_{ijouvw} can be written as follows

$$D_{ijouvw} = ER^2\, h_{ijouvw}(\nu, f)\,, \tag{165}$$

where the h_{ijouvw} are some functions of ν and f. It follows from (154) and (157) that the estimates $\boldsymbol{D}^*$ and $\bar{\boldsymbol{D}}$ are proportional to ER^2 as well. Therefore, all results shown in Figure 2 and Figure 3 are independent of E and R because they are normalized with respect to the corresponding values from the numerical solution of the boundary value problem for $f = 0$.

One might argue that for vanishing porosity a Cauchy continuum should be recovered which would imply that all coefficients of the strain gradient elasticity tensor must vanish for $f = 0$. However, the porosity in the constitutive equations refers to the porosity at a given macroscopic point. Therefore, vanishing f means that the porosity vanishes only locally at this very point of the continuum. Of course, a Cauchy continuum has to be obtained if f approaches zero everywhere in the body but this cannot be decided by a local meassure. Thatswhy, the strain gradient constants must not vanish only because f goes to zero locally. This is different compared with the approach developed by DRUGAN AND WILLIS (1996). Here, a statistical homogenization procedure has been developed, assuming a statistical spatial distribution of the porosity. Vanishing porosity in DRUGAN AND WILLIS (1996) is tantamount to a vanishing spatial distribution which implies that the porosity vanishes everywhere.

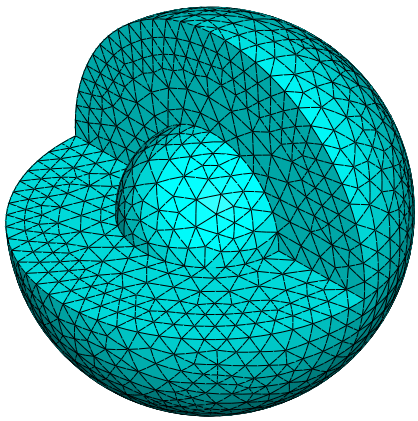

Fig. 4: Example for the finite element mesh of the sphere model used for the numerical verification of the analytical results. The void has been modeled as inclusion with vanishing Young's modulus and a quarter of the matrix material has been clipped in the drawing in order to get a better visualization of the mesh.

7. Concluding remarks

The methods to derive approximations for strain gradient effective continua have been discussed focusing especially on porous elastic microstructures. However, the presented concepts can be applied straight forward to the case of elastic inclusions which enables us to approximate the higher order material tensors analytically at least for two important types of idealized microstructures. The restriction with respect to isotropic volume elements is a clear disadvantage because it provides only positive semi-definite higher order elasticity tensors. However, it allows for much more concise notations by employing the tensor concept compared with the calculations necessary for non-isotropic volume elements as e.g. performed in FOREST AND SAB (1998). The approximations obtained within the work are based on a fundamental concept introduced in GOLOGANU, LEBLOND, ET AL. (1997) which consists in the considerion of a volume element under so-called higher order boundary conditions in order to derive contitutive relations for generalized continua. This has been sketched here for strain gradient elasticity in Section 4.2. Although this concept is quite compelling at a first glance, it provokes most naturally conceptual problems when discussing it together with the origins of estimates. Estimates have been discussed especially within the context of materials with statistically varying properties, see e.g. KROENER (1967) in order to derive a corresponding effective medium, ensemble averages are employed. This concept is also known as mean-field approach. A key point of this aproach is the Principle of Macrohomogeneity also known as non-correlation postulate, which is valid if fluctuations of energetic ensemble averages can be neglected. It can be shown that if this principle holds then the effective medium is a simple con-

tinuum as long as the underlying microstructure can be fully described by a simple continua. Assuming now ergodicity, which means replacing the ensemble averages by volume averages, leads to the alternative consideration of representative volume element under defined boundary conditions. Then the statement which corresponds to the Principle of Macrohomogeneity is the Hill condition and simple estimates can be derived as outlined in Section 3. Arguing in the reverse sense with respect to the concept outlined in Section 4.2 would mean that in this case at least a certain kind of fluctuations in the energetic ensemble averages is taken into account. By applying the ergodicity assumption the flucation should correspond to e.g. quadratic boundary displacements. However, this link is still missing what is seen here as an open question which should be discussed thoroughly in the future. The same argumentation holds of course for micromorphic continua and deeper insight can be expected by comparing the approach used here with the nonlocal mean field concept employed e.g. in DRUGAN AND WILLIS (1996).

A. Traction boundary conditions for homogenization relation to strain gradient elasticity

In the following a centrosymmetric volume element with prescribed linear tractions

$$t_i = R_{ik} n_k + T_{ikl} n_k x_l \quad \boldsymbol{x} \in \partial\mathcal{B} \tag{166}$$

at the outer boundary $\partial\mathcal{B}$ is considered. From the balance of momentum for the volume element

$$\int_{\partial\mathcal{B}} t_i \,\mathrm{d}A = R_{ik} \int_{\partial\mathcal{B}} n_k \,\mathrm{d}A + T_{ikl} \int_{\partial\mathcal{B}} x_l n_k \,\mathrm{d}A = 0 \tag{167}$$

it follows

$$T_{ikk} = 0_i \tag{168}$$

because of

$$\int_{\partial\mathcal{B}} n_k \,\mathrm{d}A = 0_k \qquad \text{and} \qquad \int_{\partial\mathcal{B}} x_l n_k \,\mathrm{d}A = \delta_{kl} B \,. \tag{169}$$

The balance of momentum of momentum

$$\int_{\partial\mathcal{B}} \epsilon_{ijk} x_j t_k \mathrm{d}A = 0_i \tag{170}$$

reads using (166) after some algebra

$$\epsilon_{ijk}(R_{kj} + T_{ijq} X_q) = 0_i \,. \tag{171}$$

where ϵ_{ijk} stands for the Levi-Cevita-tensor. It follows from (171) that

$$R_{kj} = R_{jk} \qquad \text{and} \qquad T_{kjq} = T_{jkq}\,. \tag{172}$$

From the definition of the macro-stresses Σ_{ij} it can be seen that

$$\Sigma_{ij} = \frac{1}{B}\int\limits_{\partial\mathcal{B}} \sigma_{ik} x_j n_k \,\mathrm{d}A = \frac{1}{B}\int\limits_{\partial\mathcal{B}} t_i x_j \,\mathrm{d}A = R_{ij} + T_{ijl} X_l \tag{173}$$

and therefore

$$\partial_m \Sigma_{ij} := \frac{\partial \Sigma_{ij}}{\partial X_m} = T_{ijm} \tag{174}$$

by which we can identify the T_{ijk} with the gradients of the macroscopic stresses. In order to be consistent with the notation used throughout the paper, we define

$$\widetilde{M}_{ijk} := \partial_m \Sigma_{ij}\,. \tag{175}$$

The coefficients A_{ij} can be calculated from (173)

$$R_{ij} = \Sigma_{ij} - \widetilde{M}_{ijl} X_l\,. \tag{176}$$

Therefore, (166) finally reads

$$t_i = \Sigma_{ik} n_k + \widetilde{M}_{ikl} n_k (x_l - X_l) \qquad \boldsymbol{x} \in \partial\mathcal{B}\,. \tag{177}$$

Using this result in order to evaluate the Hill-Mandel lemma

$$\frac{1}{2B}\int\limits_{\mathcal{B}} \sigma_{ij}\varepsilon_{ij}\,\mathrm{d}V = \frac{1}{2}\Sigma_{ij}E_{ij} + \frac{1}{2B}\int\limits_{\partial\mathcal{B}} (u_i - E_{ip}\xi_p)(t_i - \Sigma_{ij} n_j)\,\mathrm{d}A \tag{178}$$

gives an extended Hill-condition

$$\frac{1}{2B}\int\limits_{\mathcal{B}} \sigma_{ij}\varepsilon_{ij}\,\mathrm{d}V = \frac{1}{2}\Sigma_{ij}E_{ij} + \frac{1}{2}\widetilde{M}_{ikl}\widetilde{H}_{ikl} \tag{179}$$

with

$$\widetilde{H}_{ikl} = \frac{1}{B}\int\limits_{\mathcal{B}} \varepsilon_{ik}\xi_l\,\mathrm{d}V \tag{180}$$

where

$$\xi_l = x_l - X_l\,. \tag{181}$$

B. Calculating the higher order stress tensor M from boundary data

The higher order stresses M_{ijk} given by (46) can be written as

$$M_{ijk} = \frac{1}{B}\int_{\mathcal{B}} \sigma_{ij}\xi_k \,\mathrm{d}V = \frac{1}{B}\int_{\mathcal{B}} (\sigma_{ip}\xi_j)_{,p}\,\xi_k \,\mathrm{d}V = \frac{1}{B}\int_{\partial\mathcal{B}} \sigma_{ip}\xi_j\xi_k \, n_p \mathrm{d}A - \frac{1}{B}\int_{\mathcal{B}} \sigma_{ik}\xi_j \,\mathrm{d}V \,. \tag{182}$$

Defining

$$N_{ijk} = \frac{1}{B}\int_{\partial\mathcal{B}} \sigma_{ip}\xi_j\xi_k \, n_p \mathrm{d}A \tag{183}$$

equation (182) can be written as

$$M_{ijk} + M_{ikj} = N_{ijk} \tag{184}$$

By cyclic permutation of the indices we obtain three linear equations with the result that

$$M_{ijk} = \frac{1}{2}(N_{ikj} + N_{jik} - N_{kji}) \tag{185}$$

because of the symmetry properties of $\boldsymbol{M}$. This shows that the M_{ijk} can be obtained completely from the boundary data.

C. Relations for isotropic and symmetric sixth-order tensors

In the following, some standard relation with respect to isotropic and fully symmetric sixth-order tensors are provided. For further details see e.g. MOAKHER (2007). Every fully symmetric and isotropic sixth-order tensor $\boldsymbol{B}$ can be written as

$$B_{ijklmn} = c_1 J_{ijklmn} + c_2 K_{ijklmn} + c_3 P_{ijklmn} \tag{186}$$

with

$$J_{ijklmn} = \delta_{ij}\delta_{kl}\delta_{mn} \tag{187}$$

$$K_{ijklmn} = \delta_{ij}\delta_{km}\delta_{ln} + \delta_{ij}\delta_{kn}\delta_{lm} + \delta_{kl}\delta_{im}\delta_{jn} + \delta_{kl}\delta_{in}\delta_{jm} + \delta_{mn}\delta_{ik}\delta_{jl} + \delta_{mn}\delta_{il}\delta_{jk} \tag{188}$$

$$\begin{aligned} P_{ijklmn} = \quad & \delta_{ik}\delta_{jm}\delta_{ln} + \delta_{ik}\delta_{jn}\delta_{lm} + \delta_{il}\delta_{km}\delta_{jn} + \delta_{il}\delta_{kn}\delta_{jm} \\ & + \delta_{im}\delta_{kj}\delta_{ln} + \delta_{im}\delta_{kn}\delta_{lj} + \delta_{in}\delta_{kj}\delta_{lm} + \delta_{in}\delta_{km}\delta_{lj} \,. \end{aligned} \tag{189}$$

Here, especially the contracted tensors B_{ijklmm} and B_{ijkkmm} and their reciprocal tensors are needed. Contracting B_{ijklmn} with respect to the indices m and n gives

$$B_{ijklmm} = c_1 J_{ijklmm} + c_2 K_{ijklmm} + c_3 P_{ijklmm} \tag{190}$$

with

$$J_{ijklmm} = 3\delta_{ij}\delta_{kl} \tag{191}$$
$$K_{ijklmm} = 4\delta_{ij}\delta_{kl} + 3(\delta_{ik}\delta_{jl} + \delta_{il}\delta_{jk}) \tag{192}$$
$$P_{ijklmm} = 4\left(\delta_{ik}\delta_{jl} + \delta_{il}\delta_{jk}\right) . \tag{193}$$

This can be expressed as follows

$$B_{ijklmm} = g_1\delta_{ij}\delta_{kl} + g_2(\delta_{il}\delta_{jk} + \delta_{ik}\delta_{jl}) \tag{194}$$

with

$$g_1 = 3c_1 + 4c_2 \qquad\qquad g_2 = 3c_2 + 4c_3 . \tag{195}$$

Further contraction with respect to the indices k and l leads to

$$B_{ijkkmm} = c_1 J_{ijkkmm} + c_2 K_{ijkkmm} + c_3 P_{ijkkmm} \tag{196}$$

with

$$J_{ijkkmm} = 9\delta_{ij} \tag{197}$$
$$K_{ijkkmm} = 18\delta_{ij} \tag{198}$$
$$P_{ijkkmm} = 8\delta_{ij} . \tag{199}$$

This can be written more concisely as

$$B_{ijkkmm} = \theta\delta_{ij} \tag{200}$$

with

$$\theta = 9c_1 + 18c_2 + 8c_3 . \tag{201}$$

The reciprocal tensors needed here can be written as follows

$$B^{-1}_{ijkkmm} = \frac{1}{\theta}\delta_{ij} \tag{202}$$
$$B^{-1}_{ijklmm} = \frac{1}{4g_2}(\delta_{ik}\delta_{jl} + \delta_{il}\delta_{jk}) - \frac{g_1}{2g_2(3g_1 + 2g_2)}\delta_{ij}\delta_{kl} \tag{203}$$

References

ABAQUS (2005): *Version 6.7 Documentation*. Hibbit, Karlsson and Sorensen (HKS) Inc., Pawtuchek.

AUFFRAY, N., BOUCHET, R., AND BRECHET, Y. (2010): "Strain gradient elastic homogenization of bidimensional cellular media". In: *International Journal of Solids and Structures* 47, pp. 1698–1710.

BACIGALUPO, A. AND GAMBAROTTA L. (2010): "Second-order computational homogenization of heterogeneous materials with periodic microstructure". In: *Zeitschrift für Angewandte Mathematik und Mechanik (ZAMM)* 90. 10-11, pp. 796–811.

BERAN, MJ (1971): "Application of statistical theories to heterogeneous materials". In: *Physica Status Solidi (a)* 6. 2.

BIGONI, D. AND DRUGAN, WJ (2007): "Analytical derivation of Cosserat moduli via homogenization of heterogeneous elastic materials". In: *Journal of Applied Mechanics* 74, pp. 741–753.

CHEN, HUAN, LIU, XIAONING, ET AL. (2009): "Identification of material parameters of micropolar theory for composites by homogenization method". In: *Computational Materials Science* 46, pp. 733–737.

DRUGAN, W.J. AND WILLIS, J.R. (1996): "A micromechanics-based nonlocal constitutive equation and estimates of representative volume element size for elastic composites". In: *Journal of the Mechanics and Physics of Solids* 44. 4, pp. 497–524.

ERINGEN, A. CEMAL (2002): *Nonlocal Continuum Field Theories*. Springer.

ERINGEN, C. (1999): *Microcontinuum Field Theories, Vol. I: Foundations and Solids*. Springer Verlag New York.

FOREST, S. (2002): "Homogenization methods and the mechanics of generalized continua-part 2". In: *Theoretical and Applied Mechanics* 28. 29, pp. 113–144.

– (1998): "Mechanics of generalized continua: construction by homogenization". In: *Journal de Physique-Colloques* 8. 4, pp. 39–48.

FOREST, S., DENDIEVEL, R., AND CANOVA, GR (1999): "Estimating the overall properties of heterogeneous Cosserat materials". In: *Modelling and Simulation in Materials Science and Engineering* 7. 5, pp. 829–840.

FOREST, S. AND SAB, K. (1998): "Cosserat overall modeling of heterogeneous materials". In: *Mechanics Research Communications* 25. 4, pp. 449–454.

GOLOGANU, M., LEBLOND, J.B., ET AL. (1997): "Recent extensions of Gurson's model for porous ductile metals". In: *Springer-Verlag Cism Courses And Lectures: International Centre For Mechanical Sciences Series*, pp. 61–130.

KACZMARCYK, LUKASZ, PEARCE, CHRIS J., AND BICANIC, NENAD (2008): "Scale transition and enforcement of RVE boundary conditions in second order computational homogenization". In: *International Journal for Numerical Methods in Engineering* 74, pp. 506–522.

KOUZNETSOVA, V.G. (2002): "Computational homogenization for the multi-scale analysis of multi-phase materials". PhD thesis. Technische Universiteit Eindhoven.

KROENER, E. (1967): "Elastic moduli of perfectly disordered composite materials". In: *Journal of the Mechanics and Physics of Solids* 15, pp. 319–329.

MAYE, R. (1969): *On the determination of micromorhic material constants from properties of the constituents*. Nasa Contractor Report CR 132. Nasa.

MEHRABADI, M. M. AND COWIN, S. C. (1991): "Eigentensors of linear anisotropic elasticity". In: *Quaterly Journal of Mechanics and Applied Mathematics* 43, pp. 15–42.

MINDLIN, RD (1965): "Second gradient of strain and surface-tension in linear elasticity (Linear deformation of elastic solid in which potential energy-density is function of strain and first and second gradients)". In: *International Journal of Solids and Structures* 1, pp. 417–438.

MINDLIN, RD AND ESHEL, NN (1968): "On first strain-gradient theories in linear elasticity". In: *International Journal of Solids and Structures* 4, pp. 109–124.

MOAKHER, MAHER (2007): "Fourth-order cartesian tensors: old and new facts, notion and applications". In: *The Quarterly Journal of Mechanics and Applied Mathematics* 61. 2, pp. 181–203.

NEMAT-NASSER, SIA AND HORI, MUNEO (1999): *Micromechanics: Overall Properties of Heterogeneous Materials*. 2nd ed. North-Holland, Elsevier.

PEERLINGS, RHJ AND FLECK, NA (2004): "Computational evaluation of strain gradient elasticity constants". In: *International Journal for Multiscale Computational Engineering* 2, pp. 599–619.

QU, JIANMIN AND CHERKAOUI, MOHAMMED (2006): *Fundamentals of Micromechanics of Solids*. John Wiley & Sons, Inc.

TEKOĞLU, CIHAN AND ONCK, PATRICK R. (2008): "Size effects in two-dimensional Voronoi foams: Acomparison between generalized continua and discrete models". In: *Journal of the Mechanics and Physics of Solids* 56, pp. 3541–3564.

TRUESDELL, C. AND NOLL, W. (2004): *The nonlinear field theories of mechanics*. Ed. by Antman, Stuart S. 3rd ed. Springer.

WILLIS, J.R. (1987): "Randomly homogeneous media". In: *Homogenization techniques for composite media*. Ed. by Sanchez-Palencia, E. and Zaoui, A. Vol. 272. Lecture Notes in Physics. Springer. Chap. V, pp. 281–337.

ZYBELL, L., MÜHLICH, U., AND KUNA, M. (2008): "Constitutive equations for porous plane-strain gradient elasticity obtained by homogenization". In: *Archive of Applied Mechanics* 79, pp. 359–357.

A first order strain gradient damage model for simulating quasi-brittle failure in porous elastic solids
In: *Archive of Applied Mechanics* DOI: 10.1007/s00419-013-0729-6

A first order strain gradient damage model for simulating quasi-brittle failure in porous elastic solids

Uwe Mühlich Lutz Zybell Geralf Hütter Meinhard Kuna

In order to simulate quasi-brittle failure in porous elastic solids, a continuum damage model has been developed within the framework of strain gradient elasticity. An essential ingredient of the continuum damage model is the local strain energy density for pure elastic response as a function of the void volume fraction, the local strains and the strain gradients, respectively. The model adopts Griffith's approach, widely used in linear elastic fracture mechanics, for predicting the onset and the evolution of damage due to evolving micro-cracks. The effect of those micro-cracks on the local material stiffness is taken into account by defining an effective void volume fraction. Thermodynamic considerations are used to specify the evolution of the latter.
The principal features of the model are demonstrated by means of a one-dimensional example. Key aspects are discussed using analytical results and numerical simulations. Contrary to other continuum damage models with similar objectives, the model proposed here includes the effect of the internal length parameter on the onset of damage evolution. Furthermore, it is able to account for boundary layer effects.

1 Introduction

One important feature of quasi-brittle rupture is the accumulation of damage prior to final failure, see e.g. [2]. Furthermore, considering specimens of different sizes but with self-similar geometry and made of the same material, different nominal failure

stresses are observed in general. This phenomenon is known as size effect and a widely accepted explanation for it is the following: The size of the damage zone is mainly controlled by intrinsic length properties of the considered material like e.g. the initial defect spacing. Applying the same nominal load to specimens of different sizes, the damage zones within the different specimens will have similar geometrical extensions. However, the smaller the specimen the higher the proportion of damaged material. Therefore, contrary to the weakest link theory, smaller specimens may break at lower nominal loads if quasi-brittle failure occurs as reported e.g. for porous concrete in [21].

Moreover, size effects in structural components made of brittle or quasi-brittle materials such as concrete, ceramics, etc. are in general the result of an interplay of deterministic and statistical effects, as pointed out e.g. in [20]. Hence, numerical investigations were performed e.g. in [19, 10, 6] incorporating the details of the microstructure of the material to a certain account by using beam networks, the discrete element method or similar techniques. This approach has the advantage to reflect a priori the ratio of the microstructural length properties like defect spacing, cell size, etc. to the macroscopic dimensions of the considered problem. Furthermore, random variations of microstructural properties can be incorporated rather intuitively. Although important information can be gathered by this approach, its applicability is limited by the simulation time and the amount of data to be processed. Because the model size increases rapidly with increasing overall dimensions, simulations may become hardly feasible even for relatively moderate macroscopic dimensions. Furthermore, statistical investigations require always a considerable number of simulations. Hence, model size becomes an important issue.

Therefore, an effective continuum description is desirable not only for practical reasons but also to supplement the discrete approach. However, continuum models formulated within the theory of simple materials cannot account for deterministic size effects because the influence of the microstructure on the macroscopic behaviour can only be incorporated by means of specific values like void volume fraction, microcrack density, etc. as extensively discussed in the literature. For porous materials which are considered here this means that the aforementioned models cannot distinguish between a material whose microstructure consists of many small voids surrounded by linear elastic matrix material and another material with less but bigger voids as long as the void volume fraction is the same in both cases.

Furthermore, if quasi-brittle failure is attempted to be described by a continuum approach, the softening behaviour due to the evolution of damage causes particular difficulties. In general, rupture is supposed to be initiated by local softening accompanied by localization of damage and deformation in narrow zones. Nowadays, it is well understood that continuum theories belonging to the class of simple continua are not suitable to describe this phenomenon properly. This becomes apparent e.g. by the spurious dependence of the numerical results obtained with those models on the spatial discretization after the onset of localization of the deformation.

From the preliminary discussion above it becomes evident that a continuum approach which aims to describe properly quasi-brittle failure must meet the following minimum requirements:

- It has to account for the evolution of damage.
- It must incorporate at least one length scale which correlates to a genuine material length scale associated with the damage process.
- The numerical results must not show any spurious dependence on the spatial discretization.

All three topics, continuum damage mechanics, size effects and the proper modeling of localization behaviour are subjects of intensive research since various decades now. The reader is referred to the following review articles and text books: [9], [2], [3], [5] which provide most of the needed information. However, due to the huge amount of literature regarding the topics under consideration, such a selection is mostly a matter of convenience and equally valuable references from other authors could be given.

Spurious mesh dependence of the numerical results after the onset of localization can be avoided if so-called generalized continuum theories, like non-local continua, gradient enhanced continua, micromorphic continua, etc., are employed. A feature common to all these approaches is the presence of at least one internal length scale. On the other hand, an internal length scale is needed as well to take into account size effects. However, the mere existence of such a length parameter does not automatically ensure that a considered model is suitable for localization phenomena and captures well the observed size effects at the same time as shown e.g. in [7]. According to the investigation reported in [7], strain gradient elasticity as developed in [14] and [15] is a good candidate to handle both problems simultaneously.

The constitutive relations of linear strain gradient elasticity can be expressed by means of the conventional fourth order elasticity tensor and an additional tensor of order six. Considering an isotropic material, the fourth order tensor is given completely by two independent constants, e.g. Young's modulus and Poisson's number. The higher order elasticity tensor however, involves already five independent material constants in this case as shown for example in [15]. Hence, the effort to determine the material parameters is considerably higher compared to classical elasticity and the whole procedure can be a rather challenging task. However, key insight with respect to the correlations between material parameters and quantities measurable with reasonable effort can be gained by homogenization methods. Here, we focus on porous elastic solids with only four genuine material characteristics: Young's modulus and Poisson's ratio of the elastic matrix, the void volume fraction and the mean spacing between adjacent voids. The material parameters for plane porous strain gradient elasticity without damage have been already estimated in [23], where the generalized homogenization concept proposed in [8] was used. Based on these constitutive relations a continuum damage model is derived in the present paper, which rests on an energetic criterion for the onset of damage evolution. It should be noted that the methodology proposed here is by no means limited to plane problems. What matters is that a strain energy density of Mindlin-type is available for the pure elastic response. The plane case is chosen here because an analytical solution for the strain energy density exists. Furthermore, it is easier to illustrate certain points in two dimensions which seems advantageous The passage from two dimensions to three-dimensional problems is rather straight forward and estimates for the strain energy

density considering micro-structures characterised by spherical voids surrounded by linear elastic matrix material were already derived in [16]

The paper is organized as follows. Within the next two sections, strain gradient elasticity and the corresponding generalized homogenization concept are briefly reviewed. Furthermore, the continuum damage model is derived. After that, particular aspects of the implementation into a finite element framework are discussed. Finally, the general behaviour of the model is discussed by means of a numerical example.

In the sequel, symbolic notation as well as index notation together with the summation convention are used simultaneously for tensorial quantites. With respect to the symbolic notation, boldface symbols indicate tensors whose rank is given by the context. Capital letters refer to macroscopic variables. Macroscopic and microscopic variables depend on the macroscopic coordinates $\boldsymbol{X}$ and the microscopic coordinates $\boldsymbol{x}$, respectively. The abbreviation $()_{,i}$ indicates the partial derivative of the considered quantity () with respect to the corresponding spatial coordinate. For the numerical implementation, tensors are converted into algebraic forms, where underlined and double underlined bold symbols indicate algebraic vectors and matrices, respectively.

2 First order strain gradient elasticity

Strain gradient elasticity was first introduced in [14] based on an earlier work of [18]. It rests on the idea to extend the strain energy density W, which depends in the case of linear elasticity only on the strains $\boldsymbol{E}$, either by the strain gradients $\breve{\boldsymbol{H}}$ or the second gradients of the displacements $\boldsymbol{H}$. There exists also a third possibilitiy. However, all three approaches lead to equivalent formulations, see e.g. [15] or [1]. The second gradients of the displacements are used in this work, because this provides some advantages with respect to the numerical implementation.

Based on the extended strain energy density the following set of equations holds for a body which occupies the region $\mathcal{B}$ with boundary $\partial\mathcal{B}$ if the cartesian coordinate vector $\boldsymbol{X}$ is used for the spatial description:

Equilibrium conditions:

$$\left(\Sigma_{ij} - M_{kji,k}\right)_{,j} = 0_i \qquad \boldsymbol{X} \in \mathcal{B} \tag{1}$$

Kinematic relations:

$$E_{ij} = \frac{1}{2}\left[U_{i,j} + U_{j,i}\right] \qquad \boldsymbol{X} \in \mathcal{B} \tag{2}$$

$$H_{ijk} = U_{k,ij} \qquad \boldsymbol{X} \in \mathcal{B} \tag{3}$$

Constitutive equations:

$$\Sigma_{ij} = C_{ijkl} E_{kl} \qquad \boldsymbol{X} \in \mathcal{B} \tag{4}$$

$$M_{ijk} = D_{ijklmn} H_{lmn} \qquad \boldsymbol{X} \in \mathcal{B} \tag{5}$$

Natural boundary conditions:

$$T_i = \overline{T}_i \qquad \boldsymbol{X} \in \partial\mathcal{B}_T \tag{6}$$

$$R_i = \overline{R}_i \qquad \boldsymbol{X} \in \partial\mathcal{B}_R \tag{7}$$

Essential boundary conditions:

$$U_i = \overline{U}_i \qquad \boldsymbol{X} \in \partial\mathcal{B}_U \tag{8}$$

$$N_p U_{i,p} = \overline{V}_i \qquad \boldsymbol{X} \in \partial\mathcal{B}_{DU} \tag{9}$$

In the equations above, the U_i are the components of the displacement vector. The macroscopic stress tensor $\boldsymbol{\Sigma}$ and the higher order stress tensor $\boldsymbol{M}$ are related to their work conjugate kinematic variables, namely the strain tensor $\boldsymbol{E}$ and the strain gradient tensor $\boldsymbol{H}$, by the fourth and sixth order tensors $\boldsymbol{C}$ and $\boldsymbol{D}$, respectively.

The surface tractions T_i and the higher order surface tractions R_i in (6) and (7) read

$$T_i = N_j(\Sigma_{ij} - M_{kji,k}) - \mathcal{D}_j(N_k \breve{M}_{kji}) + (\mathcal{D}_l N_l) N_j N_k M_{kji} \tag{10}$$

$$R_i = N_k N_j M_{kji} \tag{11}$$

where N_i are the components of the unit normal vector. The components $\mathcal{D}_j$ of the surface gradient operator are given by

$$\mathcal{D}_j(.) = (\delta_{jp} - N_j N_p)(.)_{,p}\,. \tag{12}$$

Overlined quantities denote prescribed values.

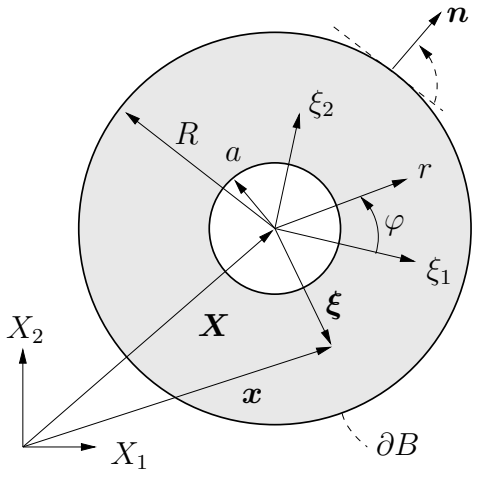

Fig. 1: Cylindrical volume element (VE) containing a cylindrical void used for the homogenization

3 Constitutive relations

3.1 Plane porous strain gradient elasticity

Constitutive equations for plane porous strain gradient elasticity were derived in [23] using a generalized homogenization procedure as proposed in [8]. A cylindrical volume element (VE) with a cylindrical void in its center surrounded by linear elastic matrix material as shown in Figure 1 was considered by the authors.

Plane strain respectively plane stress conditions were assumed and quadratic displacements

$$u_i|_{\partial B} = E_{ij}x_j + \frac{1}{2}H_{ijk}x_jx_k - \frac{1}{2}[H_{ijk} - H_{jki}]X_kx_j \tag{13}$$

were prescribed at the outer boundary of the volume element. The homogenization in [23] was carried out using the strain gradients $\breve{H} = E_{ij,k}$ instead of the second gradients of the displacements. However, the results can be converted into one another in a straightforward manner.

The macroscopic stresses and higher order stresses were defined as mean values with respect to the corresponding microscopic fields

$$\Sigma_{ij} = \frac{1}{B}\int_B \sigma_{ij}\,\mathrm{d}V \tag{14}$$

$$M_{ijk} = \left[\frac{1}{B}\int_B \sigma_{ki}(x_j - X_j)\,\mathrm{d}V + \frac{1}{B}\int_B \sigma_{kj}(x_i - X_i)\,\mathrm{d}V\right] \tag{15}$$

where B is the total volume of the volume element. Solving the boundary value problem for the VE leads to the material tensors $\boldsymbol{C}$ and $\boldsymbol{D}$. The material tensor $\boldsymbol{C}$ depends on the void volume fraction

$$f = \frac{a^2}{R^2} \tag{16}$$

and the properties of the matrix material, whereas the material tensor $\boldsymbol{D}$ hinges, in addition, on the outer radius R of the VE, where R is interpreted as the half mean spacing between adjacent microvoids. The solution was derived analytically. However, the final results obtained in [23] support the use of the following approximation for the elasticity tensor $\boldsymbol{C}$

$$\boldsymbol{C} = (1-f)^2\,\bar{\boldsymbol{C}} \tag{17}$$

where $\bar{C}$ denotes the well-known elasticity tensor for an elastic bulk material without voids.

The higher order elasticity tensor $\boldsymbol{D}$ is given in matrix form in Table 1. The coefficients b_1 and b_3 are rather complex functions of the void volume fraction f, Young's modulus and Poisson's ratio whose derivatives, needed for the finite element approximation scheme, become even more complex and lengthy. Therefore, b_1 and b_3 are

approximated as follows

$$b_1 = \frac{\hat{E}R^2}{16(3-\hat{\nu})}\frac{1}{2}\left[1.0+\cos\left(\pi f\right)\right] \tag{18}$$

$$b_3 = \frac{\hat{E}R^2}{16(1+\hat{\nu})}\frac{1}{2}\left[1.0+\cos\left(\pi f\right)\right] \tag{19}$$

where the terms including $\hat{E}$, $\hat{\nu}$ and R^2 are the respective limits for $f \to 0$ of the corresponding exact solutions. The parameters $\hat{E}$ and $\hat{\nu}$ have to be chosen according to

$$\hat{E},\ \hat{\nu} \quad = \quad \begin{cases} E, \nu & \text{plane stress} \\ E/(1-\nu^2),\ \nu/(1-\nu) & \text{plane strain} \end{cases} . \tag{20}$$

For the problem considered later on, plane strain conditons are assumed.

Finally, the overall elastic strain energy density of the volume element is given by

$$W = \frac{1}{2}\left[\boldsymbol{E} : \boldsymbol{C} : \boldsymbol{E} + \boldsymbol{H} \vdots \boldsymbol{D} \vdots \boldsymbol{H}\right]. \tag{21}$$

which is one of the basic ingredients in the derivation of the continuum damage model within the next section. The triple scalar product used in (21) is defined here as

$$\boldsymbol{\alpha} \vdots \boldsymbol{\beta} = \alpha_{ijk}\beta_{lmn}(\boldsymbol{e}_i \cdot \boldsymbol{e}_l)(\boldsymbol{e}_j \cdot \boldsymbol{e}_m)(\boldsymbol{e}_k \cdot \boldsymbol{e}_n) = \alpha_{ijk}\beta_{ijk}\,. \tag{22}$$

	111	221	112	222	121	211	122	212
111	h_1	$-h_1$	0	0	0	0	h	h
221	$-h_1$	h_1	0	0	0	0	$-h$	$-h$
112	0	0	h_1	$-h_1$	$-h$	$-h$	0	0
222	0	0	$-h_1$	h_1	h	h	0	0
121	0	0	$-h$	h	h_1	h_1	0	0
211	0	0	$-h$	h	h_1	h_1	0	0
122	h	$-h$	0	0	0	0	h_1	h_1
212	h	$-h$	0	0	0	0	h_1	h_1

$$\begin{aligned} h &= b_1 - b_3 \\ h_1 &= b_1 + b_3 \end{aligned}$$

Tab. 1: Components of the material tensor ${}^6\boldsymbol{D}$ written in matrix form ($[D]_{(ijk)(lmn)}$).

3.2 Continuum damage model

The constitutive model outlined within the previous subsection does not account for damage evolution. In order to derive a continuum damage model, it is assumed that under certain loading conditions, material degradation starts at the void surface, e.g. due to the evolution of micro-cracks as illustrated in Figure 2. After reaching a certain

degradation level, the affected material loses its load bearing capacity. Here, this is accounted for by interpreting f as an effective void volume fraction whose value can increase. The volume element is seen as a system in thermodynamic equilibrium, where for the moment it is supposed that any thermodynamic equilibrium state is completely defined by the strain tensor $\boldsymbol{E}$, the second gradient of the displacements $\boldsymbol{H}$ and the effective void volume fraction f. The total elastic strain energy of the volume element can be expressed by

$$\mathcal{W} = W\, B \tag{23}$$

with the total volume B of the volume element and the strain energy density W given by (21). Following the general idea of Griffith's criterion used in linear elastic fracture mechanics, it is assumed that the volume element can relax its actual state but only by void growth. Neglecting the dynamics of such a process, the actual equilibrium state is compared with the equilibrium state after the process of effective void growth has been completed. The energy balance for the transition from f to $f + \Delta f$ reads for fixed $\boldsymbol{E}$ and $\boldsymbol{H}$

$$\Delta W\, B + \Delta\Gamma = 0 \tag{24}$$

with $\Delta W = W(f + \Delta f) - W(f)$. The right hand side of the balance (24) is zero because the work of external loads vanishes due to the fact that the displacements are prescribed at the outer surface of the volume element, see as well (13).

In order to specify the amount of energy $\Delta\Gamma$ needed to let the void grow, the mechanism already mentioned above and illustrated in Figure 2 is envisaged. Starting from the actual void surface, geometrically described by the radius a, n microcracks evolve up to an average crack length of Δa. The zone affected by these microcracks is supposed to be completely damaged after a critical microcrack density

$$\varrho_{\mathrm{cr}} = \frac{n_{\mathrm{cr}}}{2\pi a} \tag{25}$$

is reached. The damaged volume is no longer taken into account and the void is replaced by a larger void with radius $a + \Delta a$. The energy $\Delta\Gamma$ consumed by this process is therefore given by

$$\Delta\Gamma = n_{\mathrm{cr}}\, \beta\, 2\Delta a\, h = 2\varrho_{\mathrm{cr}}\beta\, 2\pi a\, \Delta a\, h \tag{26}$$

where h is the height of the volume element and β is the amount of energy needed in order to generate a unit surface. From the definition of the void volume fraction f (16)

$$\Delta a = \frac{R^2}{2a}\Delta f + \mathcal{O}\left((\Delta f)^2\right) \tag{27}$$

results and defining $\bar{\gamma} := 2\varrho_{\mathrm{cr}}\beta$ the energy $\Delta\Gamma$ can finally be expressed as

$$\Delta\Gamma = \bar{\gamma} B \Delta f\,. \tag{28}$$

Using (28), it follows from (24) that

$$-\Delta W = \bar{\gamma}\Delta f \tag{29}$$

holds. The left hand side of (29) can be associated with the energy supply whereas the right hand side is equal to the amount of energy needed in order to increase the void volume fraction by Δf.

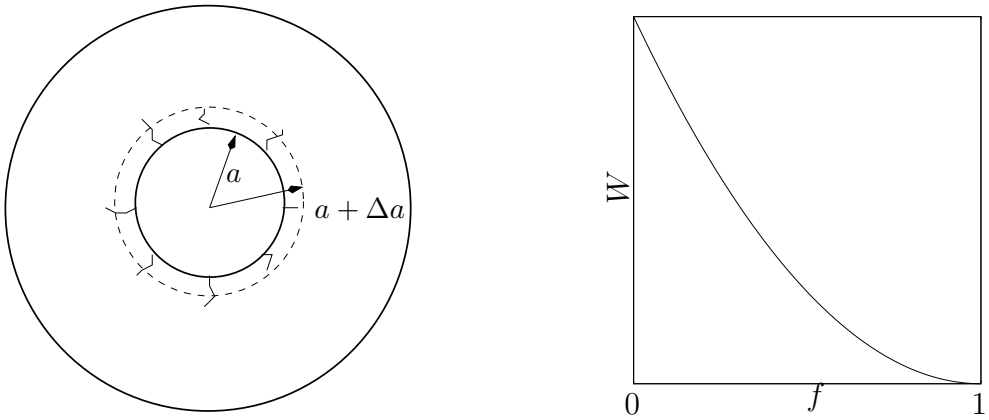

Fig. 2: Interpretation of the damage process for the volume element (lhs) and the qualitative behavior of the strain energy density W of the volume element for increasing void volume fraction f and fixed overall strains $\boldsymbol{E}$ and overall second gradients $\boldsymbol{H}$, respectively.

The constitutive relations given in Section 3.1 show that for constant $\boldsymbol{E}$ and $\boldsymbol{H}$ the strain energy density decreases monotoneously with increasing void volume fraction, see as well Figure 2. Therefore, two cases can be distinguished

$$\Delta W < 0 \Longleftrightarrow \Delta f > 0 \tag{30}$$

$$\Delta W > 0 \Longleftrightarrow \Delta f < 0 \tag{31}$$

where (31) must be excluded on physical grounds because a "healing" of the material is unreasonable.

Dividing both sides of (29) by Δf and taking the limit $\Delta f \to 0$ finally gives

$$Y - \bar{\gamma} = 0 \tag{32}$$

where the Y is defined by

$$Y = -W' \tag{33}$$

and the prime indicates the differentiation with respect to f ($()' := \frac{\partial}{\partial f}()|_{\boldsymbol{E},\boldsymbol{H}}$) for fixed strains and second gradients of the displacements. If (32) holds, then the state characterised by $\boldsymbol{E}$, $\boldsymbol{H}$ and f is a thermodynamic equilibrium state which means that there is no change in the void volume fraction f. A left hand side of (32) greater than zero indicates a non-equilibrium state because of the surplus in the energy supply. However, if the left hand side of (32) turns out to be lower than zero, the volume

element just maintains its actual equilibrium state because the energy supply is not sufficient to initiate any change of the void volume fraction. Therefore,

$$\Phi := Y - \bar{\gamma} \leq 0 \tag{34}$$

holds for any equilibrium state.

For the following discussion thermodynamics of internal variables is adopted, where $\boldsymbol{E}$ and $\boldsymbol{H}$ are defined as the observable quantities and the actual void volume fraction f is treated as internal variable. Following [17], a second internal variable θ is introduced in order to account for hardening behaviour as well. It is supposed that the free energy Ψ of the volume element can be split into an elastic part and a second part related to the hardening during the damage process

$$\Psi = \Psi^{\mathrm{el}}(\boldsymbol{E}, \boldsymbol{H}, f) + \Psi^{\mathrm{D}}(\theta) = \frac{1}{\varrho} W + \Psi^{\mathrm{D}}(\theta) \tag{35}$$

where ϱ is the density related to the volume element given by $\varrho = (1 - f_0)\varrho^{\mathrm{M}}$ with the initial void volume fraction f_0 and the density of the matrix material ϱ^{M}. It should be noted that due to the damage mechanism envisaged here, the density of the material does not correlate at all with the void volume fraction f but only with its initial value. This is because f is an effective quantity which only accounts for the portion of degraded material whereas the material itself does not vanish (see also Figure 2).

The Clausius-Duhem inequality can be obtained by the usual procedure similar to the case of ordinary elasticity with damage. Here, it reads

$$\left[\Sigma_{ij} - \varrho \frac{\partial \Psi}{\partial E_{ij}}\right] \dot{E}_{ij} + \left[M_{ijk} - \varrho \frac{\partial \Psi}{\partial H_{ijk}}\right] \dot{H}_{ijk} - \varrho \frac{\partial \Psi}{\partial f} \dot{f} - \varrho \frac{\partial \Psi}{\partial \theta} \dot{\theta} \geq 0 \tag{36}$$

and the first two terms can be canceled out by the classical argumentation, that (36) must hold as well for pure elastic response ($\dot{f} = 0 \wedge \dot{\theta} = 0$), which gives simultaneously the constitutive equations for $\boldsymbol{\Sigma}$ and $\boldsymbol{M}$ already reported in Section 3.1. Using (33) and defining in addition

$$Z := -\varrho \frac{\partial \Psi}{\partial \theta} = -\varrho \frac{\partial \Psi^{\mathrm{D}}}{\partial \theta} \tag{37}$$

the inequality (36) can be written as

$$Y \dot{f} + Z \dot{\theta} \geq 0 \,. \tag{38}$$

In order to separate hardening behaviour from the onset of damage evolution, $\bar{\gamma}$ in (34) is replaced by $\gamma + \gamma_0$, and Z is set to

$$Z = -\gamma \,. \tag{39}$$

The modified damage potential reads

$$\Phi = Y + Z - \gamma_0 \leq 0 \tag{40}$$

with the material constant γ_0. Postulating the principal of maximum dissipation implies to maximize the left hand side of (38) for given fluxes $\dot{f}$ and $\dot{\theta}$ under the constraint imposed by (40) in the case of the equality sign. Incorporating the constraint is equivalent to demand that the system passes continuously through equilibrium states. The corresponding Lagrangian reads

$$L(Y, Z, \lambda) = Y\,\dot{f} + Z\,\dot{\theta} - \lambda\,\Phi \tag{41}$$

with the Lagrange-multiplier λ and Φ given by (40) together with (39). Two particular cases have to be distinguished. If the constraint is not active ($\lambda = 0$) then

$$\dot{f} = 0 \quad \wedge \quad \dot{\theta} = 0 \tag{42}$$

must hold. However, if the constraint is active it follows from (41) that

$$\dot{f} = \lambda \frac{\partial \Phi}{\partial Y} = \lambda \tag{43}$$

$$\dot{\theta} = \lambda \frac{\partial \Phi}{\partial Z} = \lambda \tag{44}$$

and hence

$$\theta = \theta_0 + f \tag{45}$$

with some constant θ_0. Therefore, only one internal variable remains. This is mainly due to the choice (39).

Using (37) and (39) together with the information that the hardening variable and f are equal up to some constant as given by (45), Ψ^{D} can be put into concrete terms as follows

$$\Psi^{\mathrm{D}} = \frac{1}{\varrho} \int_{f_0}^{f} \gamma(\bar{f}) \mathrm{d}\bar{f} \tag{46}$$

with $\gamma(f) > 0$. The function $\gamma(f)$ is seen as an R-curve for the matrix material during the growth of micro-cracks. In addition it accounts heuristically for the rather complex interaction between micro-cracks during the degradation process.

Finally, the dissipation rate can be expressed in terms of γ_0 and $\dot{f}$ by re-writing the Clausius-Duhem inequality (36) incorporating (43), (44) and $\gamma_0 = Y + Z$ where the latter results from (40) for active constraint. The result reads

$$\dot{\mathcal{D}} = \gamma_0 \dot{f} > 0\,. \tag{47}$$

A summary of the model is given in Table 2.

It should be noted that the general structure of damage model derived within this section is similar to that of Marigo, see e.g [11] or [12]. It differs from the latter by the choice of the strain energy density which has been obtained here by means of a homogenization procedure. The use of homogenization techniques not only provides a deeper insight into the model itself but it also facilitates a micromechanical

Free energy density:

$$\Psi(\boldsymbol{E},\boldsymbol{H},f)=\frac{1}{\varrho}W+\frac{1}{\varrho}\int_{f_0}^{f}\gamma(\bar{f})\mathrm{d}\bar{f}=\frac{1}{2\rho}\left[\boldsymbol{E}:\boldsymbol{C}:\boldsymbol{E}+\boldsymbol{H}\vdots\boldsymbol{D}\vdots\boldsymbol{H}\right]+\frac{1}{\varrho}\int_{f_0}^{f}\gamma(\bar{f})\mathrm{d}\bar{f}$$

Damage potential:

$$\Phi=-W'-\gamma(f)-\gamma_0$$

Case differentiation (loading - unloading):

$$\begin{aligned}\text{elastic response:}\quad &\Phi<0\rightarrow\dot{f}=0\\ \text{damage:}\quad &\Phi=0\wedge\dot{f}>0\end{aligned}$$

Tab. 2: Summary of the continuum damage model within the framework of thermodynamics of internal variables. The prime indicates the differentiation with respect to the effective void volume fraction f.

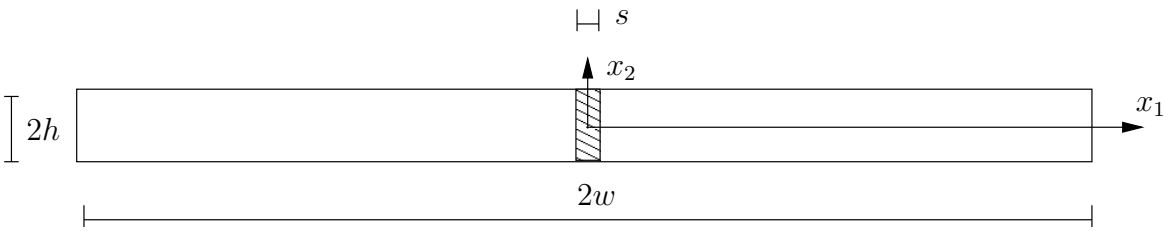

Fig. 3: Geometry of the strip with a zone of reduced damage initiation resistance.

interpretation of the results obtained from them. Furthermore, the formulation of elastic damage models by means of the strain energy density provides the advantage that this quantity can be estimated much easier by homogenization techniques than other quantites like the distributions of micro-stresses or micro-strains.

It is clear from the applied homogenisation procedure that f corresponds to a perfectly cylindrical void, at least for the constitutive equations used here. This does not mean that the model predicts damage evolution only for macroscopic strain or stress states, respectively, which induce certain symmetries at the micro-scale. On the contrary, the strain energy density (21) and, hence the damage potential is meaningful for any finite macroscopic stress / strain state. It just means that isotropic as well as anisotropic micro-crack evolution are associated with a rotational symmetric growth of the corresponding effective void. In other words, the model does not account for the evolution of anisotropy at the macro-scale due to anisotropic micro-crack evolution. However, since such anisotropy effects can be incorporated by means of analytical solutions or proper estimates for the strain energy density of a volume element with an elliptical void, this is not a conceptual problem.

4 Example with forced damage localisation

4.1 Objectives, geometry, boundary conditions and material parameters

M	N_s	l_e	$R=\frac{s}{2}$	$R=s$	$R=\frac{3}{2}s$	$R=2s$	$R=3s$
1	1	s	2	1	$\frac{2}{3}$	$\frac{1}{2}$	$\frac{1}{3}$
2	3	$\frac{s}{3}$	$\frac{2}{3}$	$\frac{1}{3}$	$\frac{2}{9}$	$\frac{1}{6}$	$\frac{1}{9}$
3	5	$\frac{s}{5}$	$\frac{2}{5}$	$\frac{1}{5}$	$\frac{2}{15}$	$\frac{1}{10}$	$\frac{1}{15}$
4	7	$\frac{s}{7}$	$\frac{2}{7}$	$\frac{1}{7}$	$\frac{2}{21}$	$\frac{1}{14}$	$\frac{1}{21}$
5	9	$\frac{s}{9}$	$\frac{2}{9}$	$\frac{1}{9}$	$\frac{2}{27}$	$\frac{1}{18}$	$\frac{1}{27}$

Tab. 3: Overview of the performed simulations varying the mesh density for different values of the internal length R. The table shows the ratios between the element width l_e and the internal length R for the respective simulations. N_s denotes the number of elements over the width of the zone with reduced initial initiation resistance.

Some general features of the continuum damage model are demonstrated within this section by means of a standard example with forced damage localization. A strip of width $2w$ and height $2h$ is considered as sketched in Figure 3 together with the denominations used in the following and the chosen coordinate system. The following displacement boundary conditions are applied

$$u_1(x_1=-w,x_2)=-\bar{u}, \qquad u_1(x_1=w,x_2)=\bar{u}\,. \tag{48}$$

Furthermore, $u_2 = \psi_{11} = \psi_{12} = \psi_{21} = \psi_{22} = 0$ is prescribed at the outer left hand side and the outer right hand side of the strip. In addition $u_2 = \psi_{21} = \psi_{12} = \psi_{22} = 0$ is enforced at the bottom and the top of the stripe, where $\psi_{ij} = u_{j,i}$.

All computations were performed with Poisson's ratio $\nu = 0.3$. An initial void volume fraction $f_0 = 0.1$ was chosen The resistance curve $\gamma(f)$ was assumed to be a linear function of f with $\gamma(f = f_0) = \gamma_0$ and $\gamma(f = 1) = \hat{\gamma}$

$$\gamma(f) = \frac{1}{1 - f_0} \left[(\hat{\gamma} - \gamma_0) f + \gamma_0 - f_0 \hat{\gamma} \right] \tag{49}$$

with $f \in [f_0, 1)$, $\gamma_0/E = 10^{-5}$ and $\hat{\gamma}/E = 8.3\,10^{-3}$, where E denotes Young's modulus. The material parameters have been chosen more or less arbitrarily.

Localization of damage is enforced by reducing the resistance to damage initiation in the center part of the strip ($x_1 \in [-s/2, s/2]$) while in the remaining part γ_0 is used. A value of $0.1\gamma_0$ is used for $x_1 \in [-s/2, s/2]$ and the hardening parameter $\hat{\gamma}$ is adapted in order to assure the same hardening behaviour everywhere in the strip. The following values, given in length units, were employed for the geometrical quantities: $w = 1.0$, $s = 0.05$.

Due to the geometry and the boundary conditions the considered problem is in fact one-dimensional. As long as the problem remains purely elastic, i.e. before damage evolution initiates, and if the material properties do not vary with respect to the spatial position, an analytic solution exists. Using the constitutive relations given in section 3.1, the solution for the displacement u_1 as a function of the spatial coordinate x_1 reads

$$\frac{u_1(x_1)}{\bar{u}} = a x_1 - b \sinh\left(\sqrt{\kappa} \frac{w}{R} x_1 \right) \tag{50}$$

with

$$\kappa = \frac{(1 - f)^2}{1 + \cos(\pi f)} \frac{8(3 - \hat{\nu})}{1 - \hat{\nu}} \tag{51}$$

and

$$a = \frac{\cosh\left(\sqrt{\kappa}\frac{w}{R}\right) \sqrt{\kappa}\frac{1}{R}}{\cosh\left(\sqrt{\kappa}\frac{w}{R}\right) \sqrt{\kappa}\frac{w}{R} - \sinh\left(\sqrt{\kappa}\frac{w}{R}\right)} \qquad b = \frac{1}{\cosh\left(\sqrt{\kappa}\frac{w}{R}\right) \sqrt{\kappa}\frac{w}{R} - \sinh\left(\sqrt{\kappa}\frac{w}{R}\right)}, \tag{52}$$

where f is equal to the initial void volume fraction f_0. The solution for the displacement which corresponds to a prescribed displacement $\bar{u}/w = 0.001$ is shown in Figure 4 (lhs) for three different ratios between the internal length R and the half width of the strip w. Because of the boundary conditions used here, a boundary layer effect due to the presence of the internal length parameter R can be observed. Of course, this boundary layer effect becomes apparent as well in the related damage potentials shown in Figure 4 (rhs). Figure 4 reveals in addition that the model predicts the onset of damage evolution at lower prescribed displacements as R/w increases. Furthermore, it can be shown that the analytical solution predicts an increase in the overall stiffness of the strip with increasing R/w.

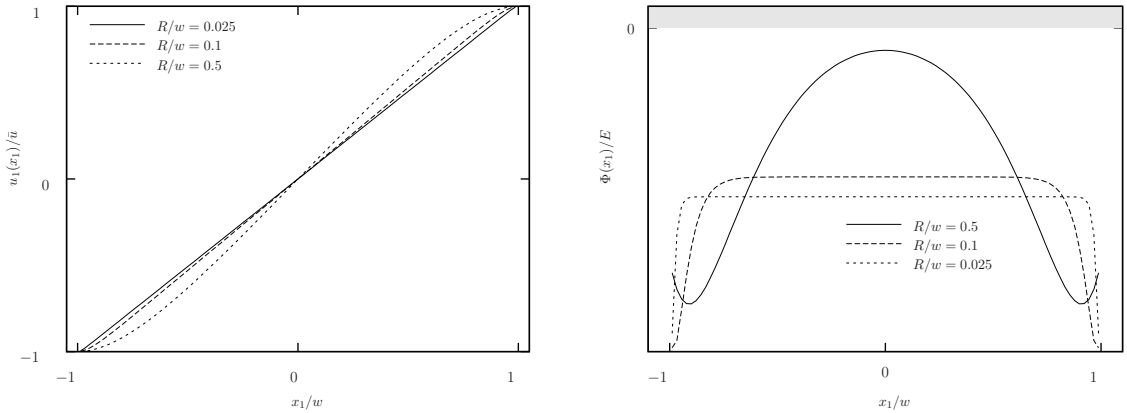

Fig. 4: Exact solution for the one-dimensional example considered here in terms of the displacement prior to the initiation of damage evolution (lhs) and the corresponding damage potentials $\Phi(x)$ as given in Table 2 normalized by the Young's modulus for a fixed prescribed displacement $\bar{u}/w = 0.0005$. The damage potentials evolve for the different R/w ratios with increasing $\bar{u}/w$ and damage starts when the respective Φ hits the shaded area. The solution for the displacement has been normalized by the prescribed boundary displacement $\bar{u}$ (see (48)). The results correspond to three different values for the ratio between internal length R and the half width of the strip w (see also Figure 3).

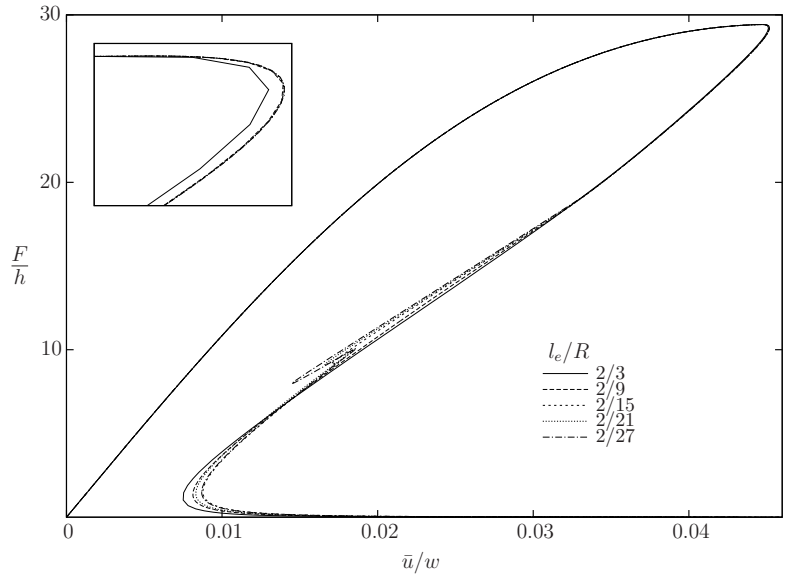

Fig. 5: Illustration of the global convergence behaviour for $R = \frac{3}{2}s$ by means of the load normalised by the height of the strip versus normalised displacement for different mesh densities. The box in the upper left corner shows a zoom of the primary snap-back.

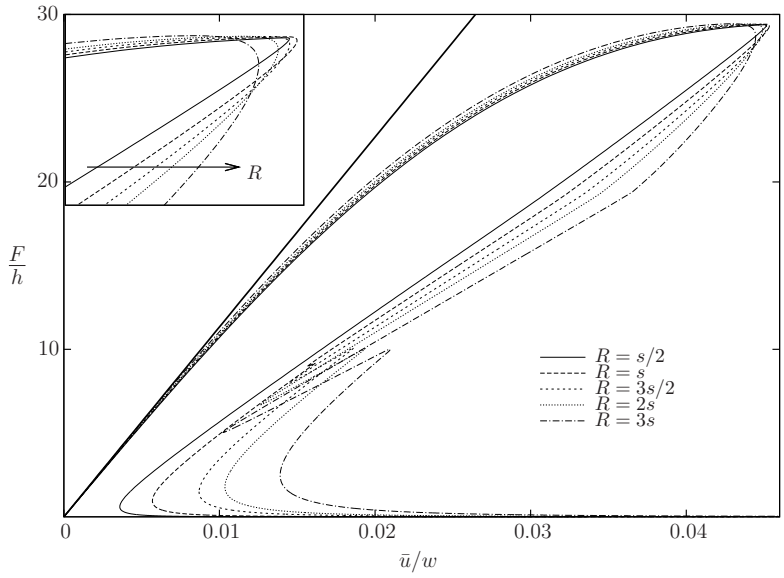

Fig. 6: Load normalised by the height of the strip versus normalised displacement for different values of the internal length R. In addition, the pure elastic response for $R = 3s$ (bold solid line) is plotted. The box in the upper left corner shows a zoom of the first snap-back.

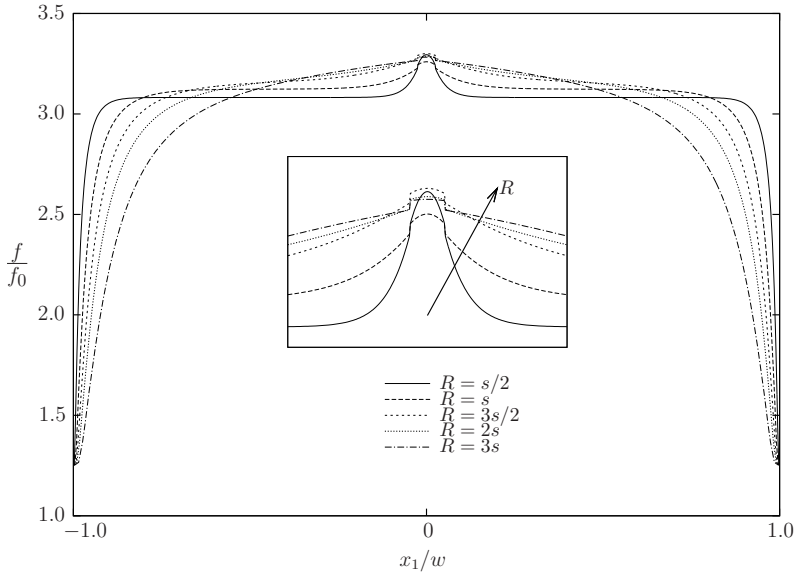

Fig. 7: Distribution of the normalised void volume fraction $\frac{f}{f_0}$ along the strip at maximum load for different values of the internal length R.

4.2 Finite-Element implementation, spatial discretization and numerical studies

A finite-element scheme has been implemented for the numerical solution of the problem described within the previous section using MATLAB [13]. One-dimensional elements based on Hermite shape functions have been used in order to assure $C^{(1)}$-continuity of the global displacement field. The implementation incorporates an arc-length method with quadratic constrained as discussed e.g. in [4] and [22].

The mesh density was varied in order to obtain N_s elements within the zone of reduced damage initiation resistance. In total five different finite element meshes have been used, each of it characterized by the length l_e of the finite elements within the zone of reduced damage initiation implied directly by the choice for N_s, $l_e = s/N_s$. In addition, the internal length R can be varied independently on the finite element discretization giving different ratios l_e/R as listed in Table 3.

The global convergence behaviour is illustrated in Figure 5 by means of the load displacement response for $R = \frac{3}{2}s$. Up to the primary snap-back, a converged solution is obtained already for $l_e/R = 2/9$. This mesh density is sufficient even for the initial part after the first snap-back. However, a significant change in the slope can be observed at a certain arc-length of the curve. After reaching this point, a much higher mesh density is necessary in order to get converged results. This behaviour is characteristic for all cases investigated here.

The effect of the internal length R on the mechanical response is examined next. The following discussion is based on the results obtained with the finest mesh for each particular value of R as listed in Table 3. All load displacement curves shown in Figure 6 start with a linear part followed by a nonlinear behaviour and a significant snap-back after reaching the maximum load. Furthermore, the model predicts changes in the post-peak behaviour with increasing R. While for smaller ratios R/w the final failure is preceded by a single snap-back, the breakdown is accompanied by multiple snap-backs for higher R/w ratios. In addition, R effects significantly the slope of the load displacement curve after the initial snap-back.

Finally, the regularisation capabilities of the model become apparent from the distribution of the normalised void volume fraction along the strip at maximum load which are depicted in Figure 7. The results show the expected smoothing of the damage distribution with increasing internal length R. Furthermore, the expected boundary layer effect can be observed. The regularization capability of the model becomes also apparent by the symmetry of the obtained numerical solutions because symmetry was not enforced here a priori but it is a result of the simulations.

5 Concluding remarks

A continuum damage model within the framework of generalized continua has been derived for porous elastic materials. The model has been developed by combining micro-mechanical arguments and thermodynamical considerations. It has been shown by means of a numerical example that the continuum damage model presented in Section 3.2 gives meaningfull results. It provides the necessary regulariza-

tion capabilities for the simulation of quasi-brittle failure. Furthermore, it is able to capture boundary layer effects prior to the initiation of the damage evolution as well as in the course of the latter. This is a clear advantage over models developed within the framework of simple continua and heuristically modified by means of a non-local evolution equation for the damage variable. The model presented here involves a manageable number of material parameters. In addition, the inital void volume fraction f_0 and the mean distance between adjacent voids have a transparent meaning. More difficulties have to be expected with regard to the determination of the elastic constants of the matrix material. The most challenging material property in the model is certainly the resistance curve of the matrix material $\gamma(f)$.

Acknowledgements

The authors highly appreciate the contribution of Andreas Seupel, who implemented the one-dimensional model in combination with the arc-length method as part of his ongoing Master's thesis at the Institute of Mechanics and Fluid Dynamics of the Technical University Freiberg.

References

[1] E. Amanatidou and N. Aravas. Mixed finite element formulations of strain-gradient elasticity problems. *Computational Methods in Applied Mechanics and Engineering*, 191:1723–1751, 2002.

[2] Z.P. Bažant. *Scaling of structural strength*. Elsevier, 2005.

[3] Z.P. Bažant and M. Jirasek. Nonlocal integral formulations of plasticity and damage: survey of progress. *Journal of Engineering Mechanics*, 128:1119, 2002.

[4] M Crisfield. A fast incremental / iterative solution procedure that handles snap through. *Computers and Structures*, 13:55–62, 1981.

[5] R. de Borst, L.J. Slyus, H.-B. Mühlhaus, and J. Pamin. Funamental issues in finite element analysis of localization of deformation. *Engineering Computations*, 10(2):99–121, 1993.

[6] J. Elias and M. Vorochevsky. Discrete numerical simulation of fracture propagation in disordered materials: mesh dependency. In *ECF 17*, pages 2599–2606, 2008.

[7] RAB Engelen, NA Fleck, RHJ Peerlings, and MGD Geers. An evaluation of higher-order plasticity theories for predicting size effects and localisation. *International journal of solids and structures*, 43(7-8):1857–1877, 2006.

[8] M. Gologanu, J.B. Leblond, G. Perrin, and J. Devaux. Recent extensions of Gurson's model for porous ductile metals. *Springer-Verlag Cism Courses And Lectures: International Centre For Mechanical Sciences Series*, pages 61–130, 1997.

[9] L. Kachanov. *Introduction to Continuum Damage Mechanics*. Springer, 1986.

[10] I. Kadashevich and D. Stoyan. A beam-network model for autoclaved aerated concrete and its use for the investigation of relationships between youngs modulus and microstructure. *Computational Materials Science*, 43(2):293–300, 2008.

[11] J. Lemaitre and R. Desmorat. *Engineering Damage Mechanics*. Springer, 2005.

[12] J.J. Marigo. Constitutive relations in plasticity, damage and fracture mechanics based on a work property. *Nuclear Engineering and Design*, (114):249–272, 1989.

[13] The MathWorks Inc, Natick, Massachusetts. *MATLAB*.

[14] RD Mindlin. Micro-structure in linear elasticity. *Archive for Rational Mechanics and Analysis*, 16(1):51–78, 1964.

[15] RD Mindlin and NN Eshel. On first strain-gradient theories in linear elasticity. *International Journal of Solids and Structures*, 4:109–124, 1968.

[16] U Mühlich, L Zybell, and M Kuna. Estimation of material properties for linear elastic strain gradient effective media. *European Journal of Mechanics, A/Solids*, 31(1):117–130, 2012.

[17] S. Murakami and K. Kamiya. Constitutive and damage evolution equations of elastic-brittle materials based on irreversible thermodynamics. *International Journal of the Mechanics and Physics of Solids*, 39(4):473 – 486, 1997.

[18] R.A. Toupin. Elastic materials with couple-stresses. *Archive for Rational Mechanics and Analysis*, 11(1):385–414, 1962.

[19] J.G.M. Van Mier and M.R.A. Van Vliet. Influence of microstructure of concrete on size/scale effects in tensile fracture. *Engineering fracture mechanics*, 70(16):2281–2306, 2003.

[20] M.R.A. van Vliet and J.G.M. van Mier. Experimental investigation of size effect in concrete and sandstone under uniaxial tension. *Engineering Fracture Mechanics*, 65(2-3):165–188, 2000.

[21] S. Wolf, H. Walther, P. Langer, and D. Stoyan. Statistische Untersuchungen der Druckfestigkeit von Porenbeton - Größeneffekt und Umrechnungsfaktoren. *Mauerwerk*, 12(1):19–24, 2008.

[22] P Wriggers. *Nichtlineare Finite-Element-Methoden*. Springer, 2001.

[23] L. Zybell, U. Mühlich, and M. Kuna. Constitutive equations for porous plane-strain gradient elasticity obtained by homogenization. *Archive of Applied Mechanics*, 79(4):359–375, 2008.